

UCSF

UC San Francisco Electronic Theses and Dissertations

Title

Dynamics of Single Human Notch1 Receptors at the Surface of Live Mammalian Cells

Permalink

<https://escholarship.org/uc/item/3dt8n4pg>

Author

Farlow, Justin

Publication Date

2014

Peer reviewed|Thesis/dissertation

Dynamics of Single Human Notch1 Receptors
at the Surface of Live Mammalian Cells

by

Justin Thomas Farlow

DISSERTATION

Submitted in partial satisfaction of the requirements for the degree of

DOCTOR OF PHILOSOPHY

in

Biochemistry and Molecular Biology

in the

GRADUATE DIVISION

of the

UNIVERSITY OF CALIFORNIA, SAN FRANCISCO

Copyright (2014)

By

Justin Farlow

Acknowledgements

I owe much to my family. The encouragement, freedom, and support provided by my parents, Thomas & Lorelei Farlow, and their parents, Thomas N. & Marinelle Farlow and Robert & Lee Pokral, enabled this long reach. My brother, Colin Farlow drove significant and continued motivation. I thank them.

Zev Gartner provided a first-class scientific environment to investigate these challenging and interesting questions. I thank him for his insight, engagement and outstanding character. I could not have done this work without his guidance. Further, the cultivation of his entire lab has been a significant source of pride. Every one in the Gartner lab has worked with me, helped me, and inspired me. I thank them all.

I thank Professors Bo Huang, Young-wook Jun & Orion Weiner for their scientific support, expertise and time. Professors Stephen Blacklow, Ron Vale, & Valerie Weaver generously supplied biological reagents used in my studies. Professors Jack Taunton, Kevan Shokat, Bo Huang, and Pam England kindly shared facilities and equipment required for this research. The Nikon Imaging Center, the CVRI Microscopy core, the Laboratory for Cell Analysis, and the Viracore provided instrumentation and materials required for this research. I would also like to specifically thank the postdocs, Robert Kasper, Marcus Taylor, & Daeha Seo for their assistance, training, and patience.

Part of this dissertation is a reproduction of material previously published and contains contributions from collaborators listed therein. Chapter 3 and parts of Chapter 2 are reproduced in part with permission from Farlow JF, Seo D, Broaders KE, Taylor M, Gartner ZJ & Jun YW. 2013. Formation of targeted monovalent quantum dots by steric exclusion. *Nature*

Methods **10**, 1203-1205, and Seo D, Farlow J, Southard K , Jun YW, Gartner ZJ. "Production & Targeting of Monovalent Quantum Dots." JOVE (2014).

Parts of Chapter 4 are reproduced with permission from Liu, J.S.; Farlow, J.T.; Paulson, A.; LaBarge, M.A.; Gartner, Z.J., 2012. Programmed Cell-to-Cell Variability in Ras Activity Triggers Emergent Behaviors during Mammary Epithelial Morphogenesis. *Cell Reports* 2, 1461- 1470.

Dynamics of Single Human Notch1 Receptors at the Surface of Live Mammalian Cells

Justin Farlow

Abstract

The Notch signaling pathway is required in sensing the local cellular environment during multicellular development. Because Notch utilizes juxtacrine contact between two cells and relies upon a set of protease cleavage events, understanding the distribution and dynamics of the receptor during activation are of particular importance in order to understand its regulation. Notch must not just be expressed and present at the cell surface, but must be at the right place at the right time for proper activation to occur. Here we invent and then use monovalent Quantum Dots (mQDs) to target and monitor human Notch1 on the surface of live mammalian cells. We track and observe the dynamics of the receptor and compare the diffusion and distribution of Notch with other structural features at the surface of the cell. We find Notch to be slow and confined in its diffusion at the cell surface. In comparing temporal dynamics with static high-resolution static microscopy of the receptor we find Notch to be excluded from particular regions on the surface. These regions of exclusion include focal adhesions as

determined by co-imaging Paxillin and Notch. In an attempt to determine the mechanism of exclusion we systematically pared domains from the receptor and identify the extracellular Notch regulatory region (NRR) as playing a significant role in distributing the receptor at the cell surface.

Additional work tries to quantitate the emergent behaviors observed in intercellular interactions taking place in heterogeneous collections of tissues. We repurpose single molecule tracking techniques used to track single molecules in order to track and identify the distribution and dynamics of cells to arrive at quantitative descriptions of multicellular interactions. We find two emergent behaviors in mosaic microtissues: cells with activated H-Ras are basally extruded or lead motile multicellular protrusions that direct the collective motility of their wild-type neighbors. Our results directly demonstrate that cell-to-cell variability in pathway activation within local populations of epithelial cells can drive emergent behaviors during epithelial morphogenesis.

Contents

1. Introduction	1
1.1. Notch Signaling	3
1.2. Notch Structure	4
1.3. Notch Activation	5
1.4. Single Molecule Imaging	6
1.5. Single Particle Analysis Software	7
1.6. References	7
2. Monitoring Human Notch1 in Mammalian Cells	10
2.1. Notch cell lines	10
2.1.1. <i>Validation of Notch-expressing cell lines</i>	11
2.1.2. <i>Validation of Notch-reporting cell lines</i>	12
2.2. Notch fusions with synthetic tags	14
2.3. Notch Truncations	19
2.4. Localization of Notch	19
2.4.1. <i>using STORM</i>	20
2.4.2. <i>relative to focal adhesions</i>	22
2.4.3. <i>in time</i>	23
2.5. Measuring the diffusion of Notch	25
2.6. Analysis of Notch dynamics	26
2.7. Discussion	27
2.8. References	29
3. Production & Targeting of Monovalent Quantum Dots.....	31
3.1. mQDs produced by Steric Exclusion	32
3.2. Targeting mQDs by hybridization	33
3.3. Production of Benzylguanine-DNA	36
3.4. Confirming Monovalency	37
3.5. Passivation for <i>in vivo</i> imaging	40

3.6.	Discussion	41
3.7.	References	42
4.	Multicellular Interactions	45
4.1.	Emergent behaviors in communicative microtissues	46
4.1.1.	<i>Variable Ras activation as a trigger for cell-to-cell variability in epithelial microtissues</i>	<i>46</i>
4.1.2.	<i>Development of reproducible 3D epithelial microtissues using chemically programmed assembly</i>	<i>47</i>
4.1.3.	<i>Observation of emergent behaviors in heterogeneous microtissues</i>	<i>48</i>
4.1.4.	<i>Quantitation of observed emergent behaviors in heterogeneous microtissues</i>	<i>50</i>
4.1.5.	<i>Conclusion</i>	<i>52</i>
4.2.	Synthetically programmed polarization	53
4.2.1.	<i>Surface adhesion of cells via a synthetic protein via a DNA-mediated linkage</i>	<i>54</i>
4.2.2.	<i>Cell-cell mediated adhesion enriches junctions with the synthetic adhesion protein.....</i>	<i>55</i>
4.2.3.	<i>Attempt to activate a synthetic EGFR-like receptor via clustering at cell-cell junctions.....</i>	<i>56</i>
4.2.4.	<i>SENSYR - a synthetic protein sensor based on the Notch regulatory region</i>	<i>57</i>
4.2.5.	<i>Conclusion</i>	<i>57</i>
4.3.	Statistical spatial analysis.....	58
4.3.1.	<i>Evaluating the uniformity of nucleic-acid scaffolding between proteins</i>	<i>59</i>
4.3.2.	<i>Measuring the intensity of a fluorescent reporter at the surface of a bead</i>	<i>59</i>
4.3.3.	<i>Quantifying spatial distribution of ER-active cells in mammary tissue</i>	<i>60</i>

4.3.4. Determining the 'spatial error' introduced during the gel transfer step of Chemically Programmed Assembly.....	61
4.4. References.....	62
5. Software	64
5.1. Track analysis - Tracker	65
5.2. Time-lapse annotation - NEP	65
5.3. References	66
A. Appendices	67
A.1. Genetic Constructs	67
A.1.1. flag-hNotch1-Gal4	67
A.1.2. flag-hNotch1-HALO-mCherry	68
A.1.3. flag-SNAP-hNotch1-Gal4	70
A.1.4. flag-SNAP-dEGF.hNotch1-Gal4	71
A.1.5. SNAP-NRR	72
A.1.6. SNAP-TM	73
A.1.7. SNAP-NICD-GFP	73
A.1.8. NICD-GFP	74
A.1.9. SENSYR	75
A.2. Code & Software	76
A.2.1. Random Difusion	76
A.2.2. Spatial Analysis of Nuclei Distribution	80
A.2.3. Kinase Bead Assay Analysis	82
A.2.4. Spatial Error	87
A.2.5. 3D Nuclei Counter	89
A.3. List of Publications	94
A.3.1. <i>Nature Methods (2013)</i>	94
A.3.2. <i>JOVE (2014)</i>	94
A.3.3. <i>Cell Reports (2013)</i>	94
A.3.4. <i>Submitted (2014)</i>	94

A.4. Publishing Agreement95

Figures

1. Introduction

- 1.1. The Notch Signaling Pathway3
- 1.2. Structure of Human Notch14

2. Monitoring Human Notch1 in Mammalian Cells

- 2.1. Presence of Notch1 in various mammalian cell lines as measured by FACS.....11
- 2.2. Doxycycline dependent induction of Notch expression.....12
- 2.3. Silencing of background activity in CHO cells using DAPT.....13
- 2.4. Measuring the Activation of Notch using various ligands13
- 2.5. Exclusive staining of hN1-Halo-mCherry with Halo Ligands.....15
- 2.6. Exclusive surface labeling of SNAP-tagged hN1 with various probes.....16
- 2.7. Activation of both SNAP-tagged and untagged hN1 using plated Dll118
- 2.8. Schematics of various SNAP-tagged Notch truncations.....19
- 2.9. STORM image of SNAP-hN1 on CHO cells show areas of exclusion & enrichment.....21
- 2.10. Confocal images of Notch & Paxillin.....22
- 2.11. Quantitative Analysis of the colocalization of SNAP-tagged proteins & Paxillin23
- 2.12. Quantitative Analysis of the colocalization of SNAP-tagged Notch Truncations & Paxillin.....24
- 2.13. Single particle tracking of SNAP-Notch tagged with BG-AF647 & BG-targeted mQDs.....25
- 2.14. Diffusion of Notch on a live U2OS cell as measured with mQDs26
- 2.15. Confinement of SNAP-tagged Notch on live U2OS cells as measured with mQDs26

3. Production & Targeting of Monovalent Quantum Dots

- 3.1. Monovalent QDs produced by steric exclusion.....33

3.2.	mQDs produced with various sized/colored QDs.....	34
3.3.	Schematic of the Modularity of mQDs targeted by hybridization.....	34
3.4.	mQDS targeted to the surface of live Jurkat cells using Lipid-DNA.....	35
3.5.	mQDS targeted to SNAP & CLIP tags by BG- & BC-DNA, respectively	36
3.6.	Characterizing the monovalency of mQDs.....	37
3.7.	Characterizing the size of mQDs.....	38
3.8.	EM Images characterizing the valency of mQDs and streptavidin QDS linked via hybridization to Au-nanoparticles.....	39
3.9.	Diffusion of various concentrations of Streptavidin QDs & mQDs across a supported lipid bilayer.....	40
3.10.	Various Passivation steps in the production of mQDs.....	40
3.11.	Diffusion of Notch measured either by dye or MQDs is similar.....	41

4. Multicellular Interactions

4.1.	Programmed Assembly of Mosaic Epithelial Aggregates.....	48
4.2.	Examples of behaviors exhibited by microtissues of mammary epithelial cells...	49
4.3.	Quantitation of the location, speed & distance of various emergent behaviors found in mammary microtissues.....	51
4.4.	Schematic of mechanism & result of synthetic cell-cell adhesions.....	53
4.5.	Adhesion of Jurkat cells to a surface by hybridization to a synthetic Adhesion protein	54
4.6.	Confocal sectioning of a heterogeneous cluster of cells adhered by the synthetic adhesion protein.....	55
4.7.	Genetic schematic of SENSYR	57
4.8.	General format of observed & calculated data used for spatial analysis	58
4.9.	Quantitative analysis of the Distribution of distances between proteins in scaffolded complexes.....	59
4.10.	Computationally defined Rings outlining a bead and its local background used to measure intensity values.....	60

4.11. The centroids ER-positive and ER-negative cells, and quantitation of the number of positive cells within 1 cell diameter.....61

4.12. Heatmap showing distance between a cell before & after lifting into a gel61

Tables

3. Production & Targeting of Monovalent Quantum Dots

3.1. Comparison of various fluorophores.....32

Introduction

The identity of a biological object is not entirely determined by intrinsic factors. An organism, a tissue, a cell and a system can be significantly influenced by extrinsic factors of the object's local environment. The local environment is determined by a position in space and time. In multicellular tissues, the environment is largely shaped by other cells. Often this influence is carried through diffusible soluble factors, structural extracellular matrix, or direct cell-cell contacts - each capable of eliciting a range of behaviors. The Gartner Lab is generally interested in the range of collective behaviors driven by interactions between a society of heterogeneous cells, for these behaviors underlie the complexity achieved by of organs and organisms. This project in particular is designed to inspect a particular, known, bounded but poorly characterized mechanism of information transfer that is sensitive to changes in a single cell's local environment - the Notch signaling pathway.

Notch signaling is a mechanism by which nearly all cells in a multi-cellular organism make fate-determining decisions - and this is accomplished by sampling their spatial environment. Because Notch signaling requires direct cell-cell contact between sending and receiving cells it is particularly capable of reading sensitive spatial information. This spatial information has been demonstrated at the level of a tissue, as seen in the selective distribution of the receptor and ligand in epithelial tissues, and hinted at in sub-cellular processes such as T-cell activation. Biochemically we understand that Notch activation requires the co-localization of two proteins on separate cells, however observing this "double-molecule" interaction is a significant challenge. Much of this research is an effort to create a system where that challenge can be successfully addressed, and the tools to engage experimentally with the individual components of the multi-component activation process.

CHAPTER 1. INTRODUCTION

Here I present research that focuses on the molecular dynamics of the pre-activation state of a particular signaling molecule responsible for significant identity determination in multicellular organizations, the Notch receptor. I build a live mammalian system capable of expressing variants of Notch with properties that make the receptor amenable to observation. This system is then employed to monitor the dynamics of the receptor at the cell surface with high spatial and temporal resolution. Owing to the requirements of long-term single molecule microscopy, we develop a modular, monovalent quantum dot that is then used to further investigate the temporal dynamics of Notch at the surface of live cells. Finally, the research is put into context by additional investigations into both the mechanism and behavioral outcome of differential signaling in multicellular environments. I use the same mathematical and image processing tools to analyze whole cells rather than individual molecules and find emergent behaviors in their organization. And I repurpose the raw genetic “tools,” initially developed as experimental standards, in an attempt to develop a synthetic signaling platform capable of being used to ask fundamental questions about the capabilities of biological juxtacrine signaling. An additional section is devoted to the computational and mathematical tools used to achieve these ends.

1.1 Notch Signaling

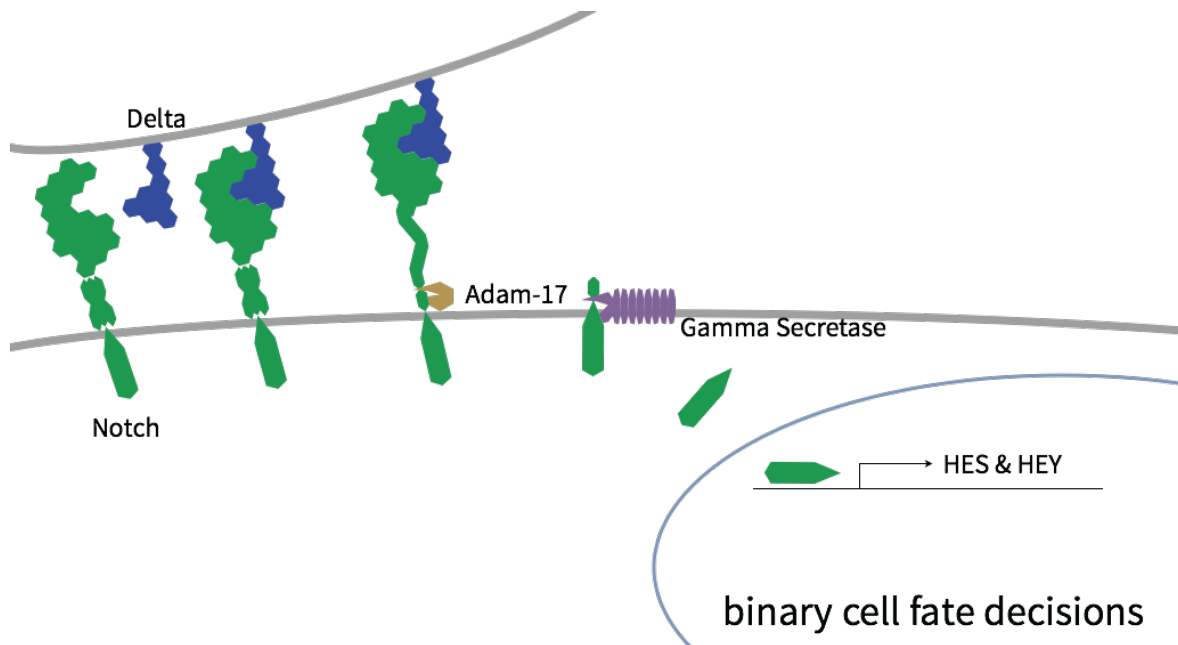


FIGURE 1.1: THE NOTCH SIGNALING PATHWAY

The Notch signaling pathway is present in all metazoans. It operates in a contact-dependent manner thought to be mediated by a force-dependent mechanism of activation¹. The pathway is functionally required for mediating cell fate decisions during early stages of development as well as in the maintenance of adult tissues.²

In the human nervous system Notch is critical for the migration, patterning, and differentiation of neurons³. In the immune system the intensity, and possibly duration of Notch signal directs the differentiation of precursor cells into B-cells and various T-cells⁴. Loss of regulation of this process results in constitutive Notch activity contributing to the pathology of many diseases including in T-cell acute lymphocytic leukemia (T-ALL)⁵. Similarly, Notch has been implicated in regulating differentiation, angiogenesis and apoptosis in cancers of the breast, lung, pancreas, and other organs⁶.

The canonical Notch signaling pathway (**Figure 1.1**) begins with the binding of membrane-bound ligand and receptor in trans. A force-mediated conformational change exposes an otherwise buried metalloprotease cleavage site on the receptor.⁷ Cleavage of the receptor's extracellular domain by the metalloprotease ADAM-17 permits subsequent cleavage by γ -secretase at an intramembrane cleavage site. Despite increased knowledge on these signaling events, little is known about the spatiotemporal dynamics of the receptor at the cell surface immediately before and after activation by ligands.

1.2 Notch Structure

There are four isotypes of the Notch receptor in mammals. Being required, Notch1 and Notch2 are better studied.⁸ Here we deal with human Notch1 (**Figure 1.2**). Human Notch1 is a 2555 amino acid, 272 kDa type-I transmembrane protein. It consists of 36 heavily glycosylated EGF repeats that make up the ligand binding domain; repeats 11, 12 & 13 being essential for binding to Jagged2.⁹ These repeats are attached to a three-part Notch Regulatory Region (NRR) which sterically shield a protease cleavage site until unfolded. This buried cleavage site sits just above the cell membrane while a second cleavage site is embedded within the transmembrane (TM) region. The Notch intracellular domain (NICD) consists of a set of 5 ankyrin repeats which, with RBPJk, form a transcription factor that bind to Notch Responsive Elements (NREs) on the genome. The NICD is terminated with a degradation domain.¹⁰

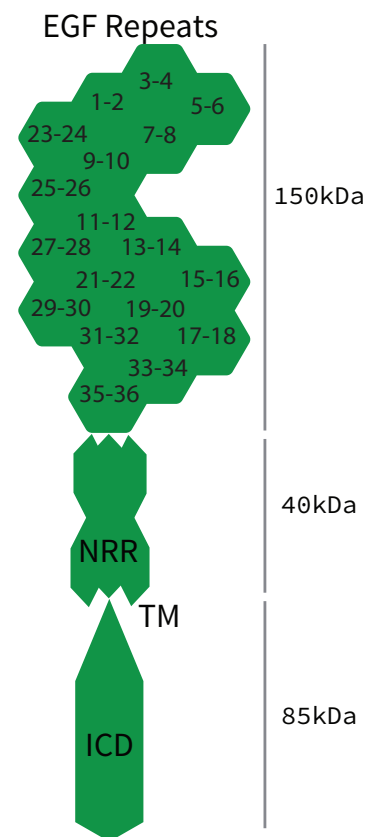


FIGURE 1.2:
STRUCTURE OF HUMAN NOTCH1

Notch1 has 36 EGF repeats numbered from its N-terminus that are bound to the Notch Regulatory Region (NRR) made of three similar LNR domains. The receptor passes through the membrane by a transmembrane domain containing a protease cleavage site, and is terminated with its intracellular domain.

1.3 Notch Activation

The mechanism of Notch activation is much studied for its unique ability to resist activation when presented with ligand in a soluble form, being activated only by an anchored ligand. Most evidence suggests Notch is activated by the mechanical unfolding of the NRR induced by a pulling force applied by a membrane-anchored ligand presented in trans. Ligand presented in cis, on the same cell as the receptor, actually inhibits receptor activation.¹¹

The unfolding of the receptor itself does not seem to constitute activation, but requires two sequential proteases cleavage events after unfolding. First, the receptor is cleaved by a membrane-bound ADAM protease - ADAM-17 has specificity for the S2 cleavage site buried in the NRR.¹² Once cleaved, the receptor is capable of being bound by the gamma-secretase complex, which upon recognition of the S3 site in the transmembrane domain, cleaves Notch once more.¹³ Once released from the membrane, the NICD is directed via nuclear localization signals into the nucleus where it binds to the DNA-binding protein RBP-Jk of the CSL family. Together these factors assemble into a transcriptional activation complex promoting a family of basic Helix Loop Helix (bHLH) repressors, including HES1, HES5 and HEY1. These repressors go on to either repress specific genes, or sequester other repressors via dimerization.¹⁴

Experiments designed to test the necessary components of activation have shown an anchored ligand to be required. By requiring a ligand that is tethered to a much larger object, the Notch signaling pathway is a detector of 'large objects' in contrast to an RTK that detects 'small molecules'. Delta1 non-specifically adhered to a plastic or glass surface can activate Notch.¹⁵ Delta4 bound to a bead can also activate Notch.¹⁶ Blocking of the final cleavage event by inhibiting gamma-secretase with a drug such as DAPT successfully inhibits Notch activation.¹⁷

Completed activation requires contact between at least four separate proteins; Notch, Ligand, ADAM-17 & gamma-secretase. It is reasonable that the cell might spatially regulate the

pathway by segregating these components - necessitating further interactions with the spatial regulation machinery. The dynamics of these interactions have not been studied on a live cell in their endogenous environment. There are a number of hypothetical interaction sites for Notch to interact with other proteins. Notch is significantly glycosylated in its EGF repeats which are known to be sites of interaction with other extracellular components. The NRR has a putative interaction domain wherein a flat face of one of the protective domains is uncharged and conserved. Further, large chunks of NICD do not yet have a known function. It is the goal of this research to elucidate some of these interactions in an effort to better describe the process of Notch activation in its endogenous environment.

1.4 Single Molecule Imaging

To study individual receptors and other protein components at a single molecule level on a live cell surface requires advanced microscopy techniques. The highest spatial resolution technique we will use is STORM - enabling sub-diffraction reconstruction of the localization of single molecules. Generally, TIRF microscopy can be performed on live cells to enable imaging of single molecule dynamics. Confocal microscopy allows us to leave the basal side of the cell in order to image surfaces of the cell that are not in contact with such an artificial environment, however we lose significant spatial resolution and signal to noise. Each of the three techniques complement each other by allowing refinement along different axes of investigation - spatial resolution, time & 3D location.

Techniques alone, however, are often insufficient in obtaining useful data. One needs imaging reagents capable of withstanding the rigors of single molecule imaging. Generally, there are three classes of imaging probes available: organic dyes, fluorescent proteins, & quantum dots. Each have advantages and disadvantages. We found no commercial agent capable of meeting the demands we required: long-term stable, monovalent, and bright probes for imaging surface

receptors. So we invented a process to produce a monovalent quantum dot with such properties.

1.5 State of Analysis Software

In order to obtain enough data for statistical analysis of the movement of particles, one needs hundreds of tracks composed of tens to hundreds of points. Obtaining these points accurately and rapidly requires good software. There are a number of methodologies employed by a number of various pieces of software, however none are ideal. Functionally, there are a number of steps - all of which must be completed to obtain high quality tracking data: 1) identification of particles, 2) linking of particles between time-frames to form a coherent set of tracks, 3) curation of identified tracks by quality, 4) experimental analysis of the tracks.

1.6 References

-
- ¹ Gordon, W. R., Roy, M., Vardar-Ulu, D., Garfinkel, M., Mansour, M. R., Aster, J. C., & Blacklow, S. C. (2009). Structure of the Notch1-negative regulatory region: implications for normal activation and pathogenic signaling in T-ALL. *Blood*, 113(18), 4381–4390. doi:10.1182/blood-2008-08-174748
 - ² Artavanis-Tsakonas, S., Rand, M. D., & Lake, R. J. (1999). Notch signaling: cell fate control and signal integration in development. *Science (New York, N. Y.)*, 284(5415), 770–776.
 - ³ Louvi, A., & Artavanis-Tsakonas, S. (2006). Notch signalling in vertebrate neural development. *Nature Reviews. Neuroscience*, 7(2), 93–102. doi:10.1038/nrn1847
 - ⁴ Doerfler, P., Shearman, M. S., & Perlmutter, R. M. (2001). Presenilin-dependent gamma-secretase activity modulates thymocyte development. *Proceedings of the National Academy of Sciences of the United States of America*, 98(16), 9312–9317. doi:10.1073/pnas.161102498

-
- ⁵ Weng, A. P., Ferrando, A. A., Lee, W., Morris, J. P., Silverman, L. B., Sanchez-Irizarry, C., et al. (2004). Activating mutations of NOTCH1 in human T cell acute lymphoblastic leukemia. *Science (New York, N.Y.)*, *306*(5694), 269–271. doi:10.1126/science.1102160
- ⁶ Yin, L., Velazquez, O. C., & Liu, Z.-J. (2010). Notch signaling: emerging molecular targets for cancer therapy. *Biochemical Pharmacology*, *80*(5), 690–701. doi:10.1016/j.bcp.2010.03.026
- ⁷ Chen, J., & Zolkiewska, A. (2011). Force-induced unfolding simulations of the human Notch1 negative regulatory region: possible roles of the heterodimerization domain in mechanosensing. *PLoS One*, *6*(7), e22837. doi:10.1371/journal.pone.0022837
- ⁸ Kraman, M., & McCright, B. (2005). Functional conservation of Notch1 and Notch2 intracellular domains. *FASEB Journal : Official Publication of the Federation of American Societies for Experimental Biology*, *19*(10), 1311–1313. doi:10.1096/fj.04-3407fje
- ⁹ Wang, N. J., Sanborn, Z., Arnett, K. L., Bayston, L. J., Liao, W., Proby, C. M., et al. (2011). Loss-of-function mutations in Notch receptors in cutaneous and lung squamous cell carcinoma. *Proceedings of the National Academy of Sciences of the United States of America*, *108*(43), 17761–17766. doi:10.1073/pnas.1114669108
- ¹⁰ McGill, M. A., & McGlade, C. J. (2003). Mammalian Numb Proteins Promote Notch1 Receptor Ubiquitination and Degradation of the Notch1 Intracellular Domain. *The Journal of Biological Chemistry*, *278*(25), 23196–23203. doi:10.1074/jbc.M302827200
- ¹¹ Sprinzak, D., Lakhanpal, A., Lebon, L., Santat, L. A., Fontes, M. E., Anderson, G. A., et al. (2010). Cis-interactions between Notch and Delta generate mutually exclusive signalling states. *Nature*, *465*(7294), 86–90. doi:10.1038/nature08959
- ¹² Murthy, A., Shao, Y. W., Narala, S. R., Molyneux, S. D., Zúñiga-Pflücker, J. C., & Khokha, R. (2012). Notch Activation by the Metalloproteinase ADAM17 Regulates Myeloproliferation and Atopic Barrier Immunity by Suppressing Epithelial Cytokine Synthesis. *Immunity*, *36*(1), 105–119. doi:10.1016/j.immuni.2012.01.005

-
- ¹³ Greenwald, I., & Kovall, R. (2013). Notch signaling: genetics and structure. *WormBook : the Online Review of C. Elegans Biology*, 1–28. doi:10.1895/wormbook.1.10.2
- ¹⁴ Iso, T., Kedes, L., & Hamamori, Y. (2003). HES and HERP families: multiple effectors of the Notch signaling pathway. *Journal of Cellular Physiology*, 194(3), 237–255. doi:10.1002/jcp.10208
- ¹⁵ Mazzone, M., Selfors, L. M., Albeck, J., Overholtzer, M., Sale, S., Carroll, D. L., et al. (2010). Dose-dependent induction of distinct phenotypic responses to Notch pathway activation in mammary epithelial cells. *Proceedings of the National Academy of Sciences of the United States of America*, 107(11), 5012–5017. doi:10.1073/pnas.1000896107
- ¹⁶ Taqvi, S., Dixit, L., & Roy, K. (2006). Biomaterial-based notch signaling for the differentiation of hematopoietic stem cells into T cells. *Journal of Biomedical Materials Research. Part A*, 79(3), 689–697. doi:10.1002/jbm.a.30916
- ¹⁷ Geling, A., Steiner, H., Willem, M., Bally Cuif, L., & Haass, C. (2002). A γ -secretase inhibitor blocks Notch signaling in vivo and causes a severe neurogenic phenotype in zebrafish. *EMBO Reports*, 3(7), 688–694. doi:10.1093/embo-reports/kvf124

Monitoring Human Notch1 in Mammalian Cells

The size and mechanical complexity of the Notch receptor make it simultaneously a fantastic protein for biochemical study, and a difficult protein for in-vivo study. The various domains are individually expressible and robust enough to run thorough biochemical and biophysical experiments to tease apart each domain's function. However the size of the overall receptor, the fact that it spans the lipid membrane, the relatively long timescale of single-molecule interactions (minutes¹), and the numerous molecular interactions makes observing Notch on a live surface a daunting task. This chapter focuses on the design, evaluation, and elaboration of tools to relieve many of these challenges. Here we use a robust method for generating cell lines which stably express various forms of Notch. The various tractable Notch constructs are described and evaluated for their functionality. Further, various imaging techniques are explored that are both compatible with the technical requirements to observe single molecules on a live mammalian cell-surface, and the biological requirements to track Notch over an extended period of time, with respect to other relevant markers. Once evaluated, these tools are used to monitor Notch and show how the receptor is excluded from particular regions of the cell surface - namely focal adhesions. This exclusion property is then explored with respect to particular domains of the receptor.

2.1 Notch Cell Lines

In order to perform an investigation of the Notch receptor, cell lines were required that expressed an experimentally tractable version of the receptor. As human Notch1 is a large transmembrane protein, the cloning and production of such constructs, and then inserting them stably into a mammalian cell line posed significant challenges. Fortunately, Professor Stephen Blacklow has generated a system in which Notch was recombined into the genome of

U2OS cells both, containing a FLP site, and expressing the tetracycline repressor. The Notch Receptor's large size prevented it from being stably integrated by a lentivirus, and so the FLP-recombinase system was instead used to generate stable cell lines. Professor Blacklow provided an empty U2OS-FLP-FRT cell line along with U2OS cell lines expressing flag-hN1-GFP or flag-hN1-Gal4 constructs². These cell lines and genetic constructs formed the basis for the materials used throughout this study. CHO cells, like 3T3 cells, are not human, and were initially also used in parallel to U2OS cells for most experiments. However, CHO cells were found to have significant gamma-secretase-dependent background activation and so U2OS cell lines were preferred in most experiments.

2.1.1 Validation of Notch-Expressing cell lines

Notch constructs were all built into the pcDNA6 FLP plasmid so that further truncations and fusions could produce experimentally similar cell lines. Once the construct was created, cell lines were produced by co-expressing the plasmid containing the construct along with the commercial pOG44 plasmid containing the FLP recombinase. After two days of co-expression, cells were selected for over the course of two weeks using Hygromycin. Cells surviving selection were assayed for surface expression of Notch by flow cytometry using either an anti-flag or anti-hN1 antibodies. These cells were then expanded and frozen down at as low passage as possible.

Using FACS, U2OS cells expressing flag-hN1-GFP were compared to other cell lines by means of measuring surface-Notch with anti-hN1 antibodies. Most cell lines tested expressed Notch1 endogenously (**Figure**

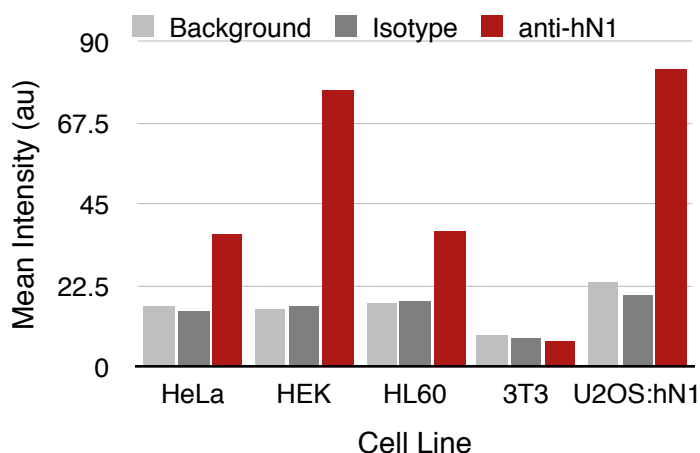


FIGURE 2.1: PRESENCE OF NOTCH1 IN VARIOUS MAMMALIAN CELL LINES AS MEASURED BY FACS

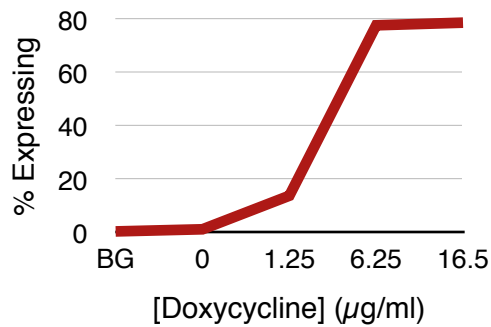


FIGURE 2.2: DOXYCYCLINE DEPENDENT INDUCTION OF NOTCH EXPRESSION

2.1). Mouse 3T3 cells did not express human Notch1 and were used as a control. U2OS cells without the Notch construct had no expression of human Notch1 detectable over background. Once inserted, the expression of Notch was controlled by induction with tetracycline (or the more stable, doxycycline). Maximal expression was obtained after 48 hours in the presence of 10 $\mu\text{g/ml}$ doxycycline (**Figure 2.2**). These conditions

were used for all subsequent experiments requiring the expression of Notch, unless otherwise noted.

2.1.2 Validation of Notch Reporting cell lines

To both monitor Notch activation, and to establish an assay to verify that any Notch constructs created did not disturb endogenous function, we built a live-cell Notch reporter system. Essentially the reporter consists of a genetically encoded fluorophore driven by a promoter engaged by the intracellular domain of the Notch construct. In parallel we developed a fluorophore driven by Gal4 via yeast's Upstream Activation Sequence (UAS)³, and by the endogenous Notch Responsive Element (NRE).⁴

Repeated elements generally confer a tighter regulation of activation, and so 6 NRE doublets (12x repeat) of the NRE were cloned upstream of a minimal CMV promoter. Additional control over activation can be achieved by optimizing the stability and localization of the expressed fluorophore. We created reporters that expressed GFP & mCherry along with destabilized variants by fusing the fluorophore with PEST domains. Additionally we drove localization using either an NLS fusion or an H2B fusion. Coexpression of the reporters along with a GFP tagged truncation of the Notch intracellular domain (GPF-NICD) allowed rapid evaluation of the

efficacy of these reporters. The reporters were all produced in lentiviral backbones so as to be easily inserted into mammalian cells once evaluated.

We found the yeast Gal4 system to be more tightly controlled than the Notch reporter system. The H2B variant was mostly tightly directed to the nucleus where observation could be more quantitatively measured by microscopy. Both CHO & U2OS cell lines expressing either flag-hN1 or flag-hN1-Gal4 were transduced with their respectively driven H2B-mCherry reporting systems. The reporter systems were found to be very leaky in CHO cells in a gamma-secretase dependent manner; cells expressing the receptor and the reporter with no addition of an activating agent expressed significant mCherry which disappeared upon incubation with DAPT (a gamma-secretase inhibitor) (**Figure 2.3**).

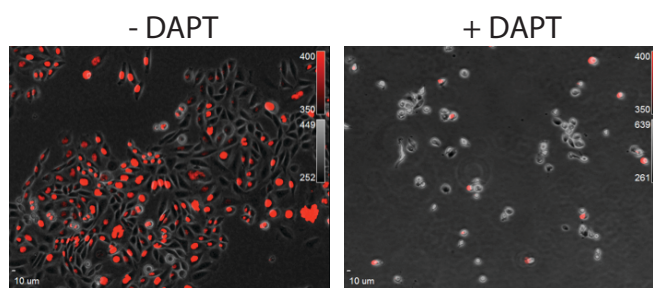


FIGURE 2.3: SILENCING OF BACKGROUND ACTIVITY IN CHO CELLS USING DAPT
CHO cells expressing hN1-Gal4 show autofluorescence of UAS_mCherry that is shut down upon DAPT treatment.

U2OS were preferable for experiments measuring the activation of Notch, as there was little background activation as measured by reporter activity in the absence of activating ligands (**Figure 2.4**). Additionally, U2OS cells showed similar levels of reporter activity in the presence and absence of DAPT, and a significant increase in mCherry expression upon exposure to plastic treated with fc-Delta1, or when cocultured with 3T3

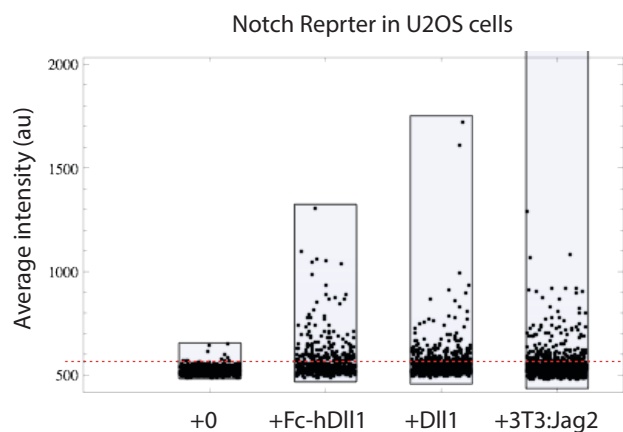


FIGURE 2.4: MEASURING THE ACTIVATION OF NOTCH USING VARIOUS LIGANDS
U2OS cells expressing hN1-Gal4 are plated for 48hrs on plastic with ligands, or in coculture with Jagged2 expressing 3T3 cells. Average mCherry intensity of the cells was measured by microscopy.

cells expressing Jagged2.

U2OS cell lines expressing the flag-Notch-gal4 construct were transduced with lentivirus containing the UAS-driven H2B-mCherry system in order to generate stable cell lines for the monitoring of Notch activation. After selection, the heterogeneous cell culture was activated with *fc-Dll1* plated non-specifically on tissue culture plastic and cells were collected by FACS that had the greatest fluorescence intensity. Cells were then allowed to grow on plastic in the absence of plated ligand and resorted for those cells with the lowest fluorescence intensity. The remaining pool of cells were frozen down as U2OS cells expressing notch that have a high dynamic range of mCherry expression.

2.2 Notch Fusions with Synthetic Tags

The flag-Notch-GFP construct demonstrated Notch could successfully be tagged with a fluorophore, however it quickly became apparent that much of the Notch (and therefore GFP) expressed in a cell was not at the cell surface. The background associated with internalized and nuclear-localized GFP made isolation of surface-localized Notch extraordinarily difficult. Additionally, the fluorescent protein was not stable enough to perform single molecule imaging experiments on live-cells - photobleaching within seconds. In seeking alternative labeling strategies we fused a number of synthetic tags to Notch at locations that had already been utilized, either for the flag-tag at its extracellular terminus, or in the NICD where the Gal4 domain had replaced the ANK repeats.

Initially mCherry replaced the Gal4 protein in the NICD of the flag-Notch-Gal4 construct. This was done to make further analysis significantly more straightforward by being able to easily

FIGURE 2.6: EXCLUSIVE SURFACE LABELING OF SNAP-TAGGED HN1 WITH VARIOUS PROBES
U2OS cells expressing either SNAP-hN1 or hN1-GFP are cocultured and exposed to a BG-probe (**a**). Confocal images (**b**) show exclusive labeling with various probes.

evaluate the expression or disruption thereof of any additional markers fused to Notch. Subsequently we tested a HALO tag fused directly forward of the mCherry domain. Promisingly, when incubated with the cell-permeable Halo-Oregon Green dye, only those cells that expressed mCherry were labeled. Further, those same cells when incubated with a cell-impermeable dye did not label (**Figure 2.5**).

This provided evidence that mCherry (and Notch) were at least folding and being properly produced, and that the HALO enzyme/dye system were robustly labeling live cells expressing the HALO construct.

We then fused a SNAP, CLIP or HALO tag

directly behind the FLAG tag at the N-terminus of the receptor. These extracellular enzymatic tags in particular enabled us to label Notch in a variety of ways depending on the needs of a particular experiment. The SNAP tag was the first construct we successfully cloned and so for practical reasons is the construct most-used in this research. The ability to use a number of different Benzylguanine-linked biomolecules enabled us to label Notch in a variety of ways, from an organic dye, to biotin, to our mQDs via Benzylguanine-linked DNA. The SNAP system proved to specifically label Notch receptors at the cell surface after incubation with $\sim 1\mu\text{M}$ of a benzylguanine molecule at 37C for 20-30 minutes.

We developed a labeling assay to assess the specificity of benzylguanine linked ligands that involved the coculture of Notch-GFP and SNAP-Notch U2OS cells. Those cells expressing GFP should not label in the presence of a SNAP-specific labeling agent, while those without GFP expression should label in its presence. This assay was used to find conditions under which various labels could have either maximal signal, or minimal background to increase the

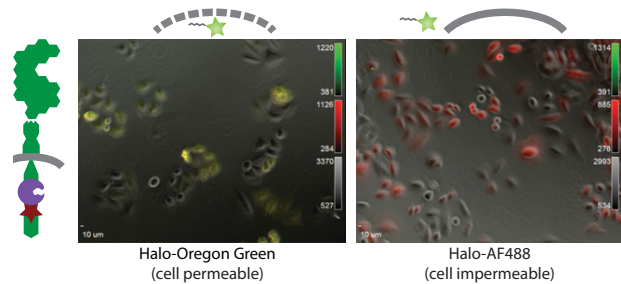
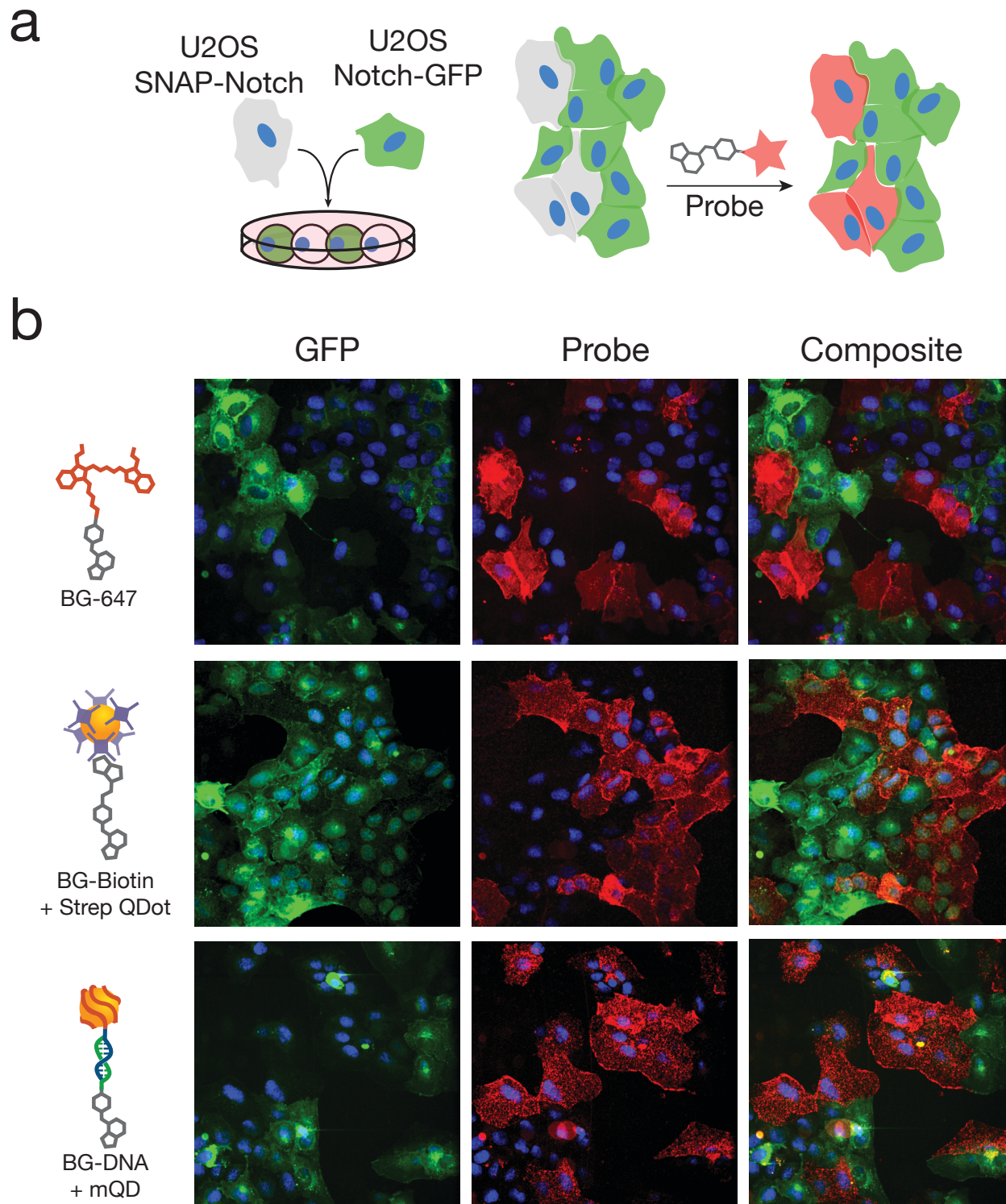


FIGURE 2.5: EXCLUSIVE STAINING OF HN1-HALO-MCHERRY WITH HALO LIGANDS
U2OS cells expressing hN1-HALO-mCherry were treated with cell permeant HALO-OG or cell impermeant HALO-AF488. The permeant dye colocalized with mCherry indicating an intracellular localization of the HALO tag.



robustness of any given experiment. **Figure 2.6** shows the exclusive labeling of SNAP-Notch expressing cells when presented with BG-alexafluor647, BG-biotin coupled with alexafluor647-streptavidin, and BG-DNA when complemented with DNA-bound mQDs (605nm).

In order to determine whether the enzymatic tags were interfering with Notch activation, U2OS cell lines expressing both the Notch reporter (UAS_H2B-mCherry) and either flag-hNotch-Gal4, or flag-SNAP-hNotch-Gal4 constructs were assayed for activation. Both cell lines activated in the presence of surface-bound Dll1 (**Figure 2.7**) and were inactive in its absence (and upon addition of DAPT). Though difficult to judge based upon relative fluorescence intensity, especially considering the heterogeneity of the populations of cells, it did seem as though the SNAP-tagged Notch receptor might have produced more background activation than the receptor lacking the SNAP-tag.

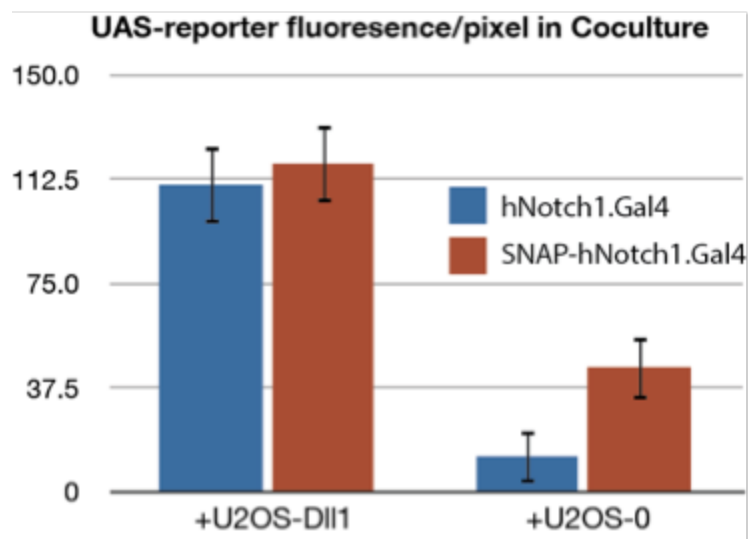


FIGURE 2.7: ACTIVATION OF BOTH SNAP-TAGGED AND UNTAGGED HN1 USING PLATED DLL1

U2OS cells expressing either hN1-Gal4 or SNAP-hN1-Gal4 are cultured on plastic with and without non-specific adhesion of fcDll1. Cells cultured in the presence of Dll1 showed significant increase in average fluorescence via activation of UAS_H2B.mCherry.

2.3 Notch Truncations

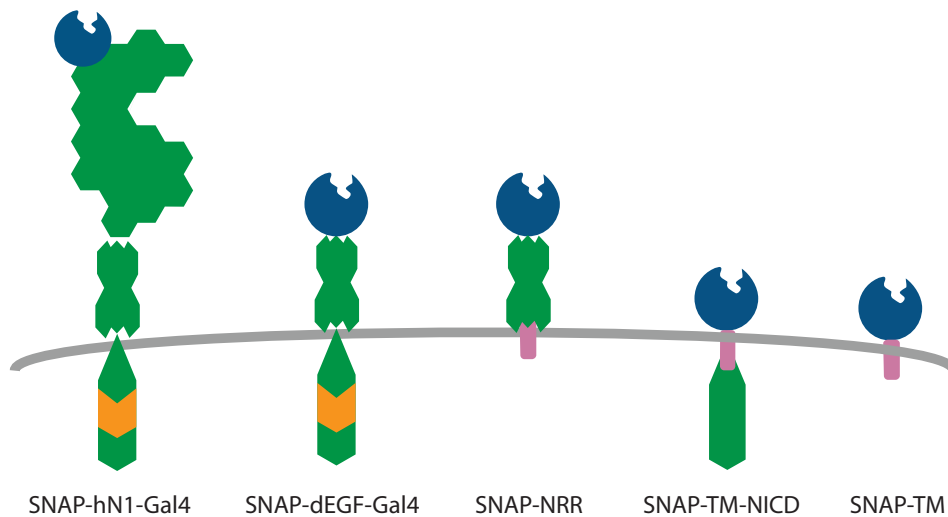


FIGURE 2.8: SCHEMATIC OF VARIOUS SNAP-TAGGED TRUNCATIONS

Notch (green) is tagged with an extracellular SNAP tag (blue) and has part of its NICD replaced with Gal4 (orange). A generic transmembrane domain (pink) replaces the cleavable Notch transmembrane domain.

In order to isolate the functions of the various Notch domains we produced a series of truncation constructs (**Figure 2.8**). Keeping in mind the known biophysical mechanism of Notch so as to produce experimentally tractable proteins, we produced truncations by removing the entire series of EGF repeats (deltaEGF)⁵, a construct containing the entire NICD fused to a bare transmembrane domain (TM-NICD), along with a construct containing the 3 domains of the NRR fused to a bare transmembrane domain (NRR-TM). These truncations were all terminated with an extracellularly displayed SNAP tag to enable their monitoring. In conjunction with a control construct (TM), containing an intracellular GFP fused to an extracellular SNAP by a generic transmembrane domain (from CD86) we are able to break down the necessity of particular domains of the Notch receptor to particular functions of the receptor.

2.4 Localization of Notch

The SNAP-tagged Notch receptors enabled live-cell labeling of just those receptors present on the surface of the cell. Cell lines produced with these constructs were then imaged using a number of different imaging techniques in order to investigate the spatial distribution of the receptor at the cell-surface. STORM was used in order to observe Notch with sub-diffraction spatial resolution. We found Notch to be heterogeneously distributed across the cell surface, though quantitative analysis of the relatively noisy data proved difficult. Some of the heterogeneity was attributed to exclusion from focal adhesions, and made visible by counterstaining the cells by expressing an mCherry-Paxillin fusion. Finally, using the mQDs described in the next chapter we were able to monitor the temporal dynamics of Notch on live cells.

2.4.1 using STORM

Stochastic optical reconstruction microscopy (STORM) is a computational technique applied to a series of microscopy images taken under conditions where the fluorophore blinks, that can reconstruct positional information from a sample with sub-diffraction resolution. It is ideal for determining 2D positional information for a sample imaged in TIRF mode where the object of study is near the glass surface. Particular fluorophores that blink are required to acquire the best reconstructions.⁶ The SNAP tag allowed us to change our fluorophore without need for a new cell line, which allowed us to quickly utilize STORM techniques.

Incubation of SNAP-tagged cells cultured on pre-cleaned No 1.5 glass with 500nM BG-AF647 or BG-AF488 for 20 minutes at 37 C followed by PBS washes stained cells well for STORM imaging. Cells were then fixed with 4% PFA and imaged in STORM imaging buffer.

Strikingly, the Notch receptors stained at the surface of the cell were significantly heterogeneously distributed. Long, wide, linear regions were devoid of Notch, while Notch seemed to be enriched in smaller fibrous lines both at the rim of the cell, and elsewhere in the cell (**Figure 2.9**).

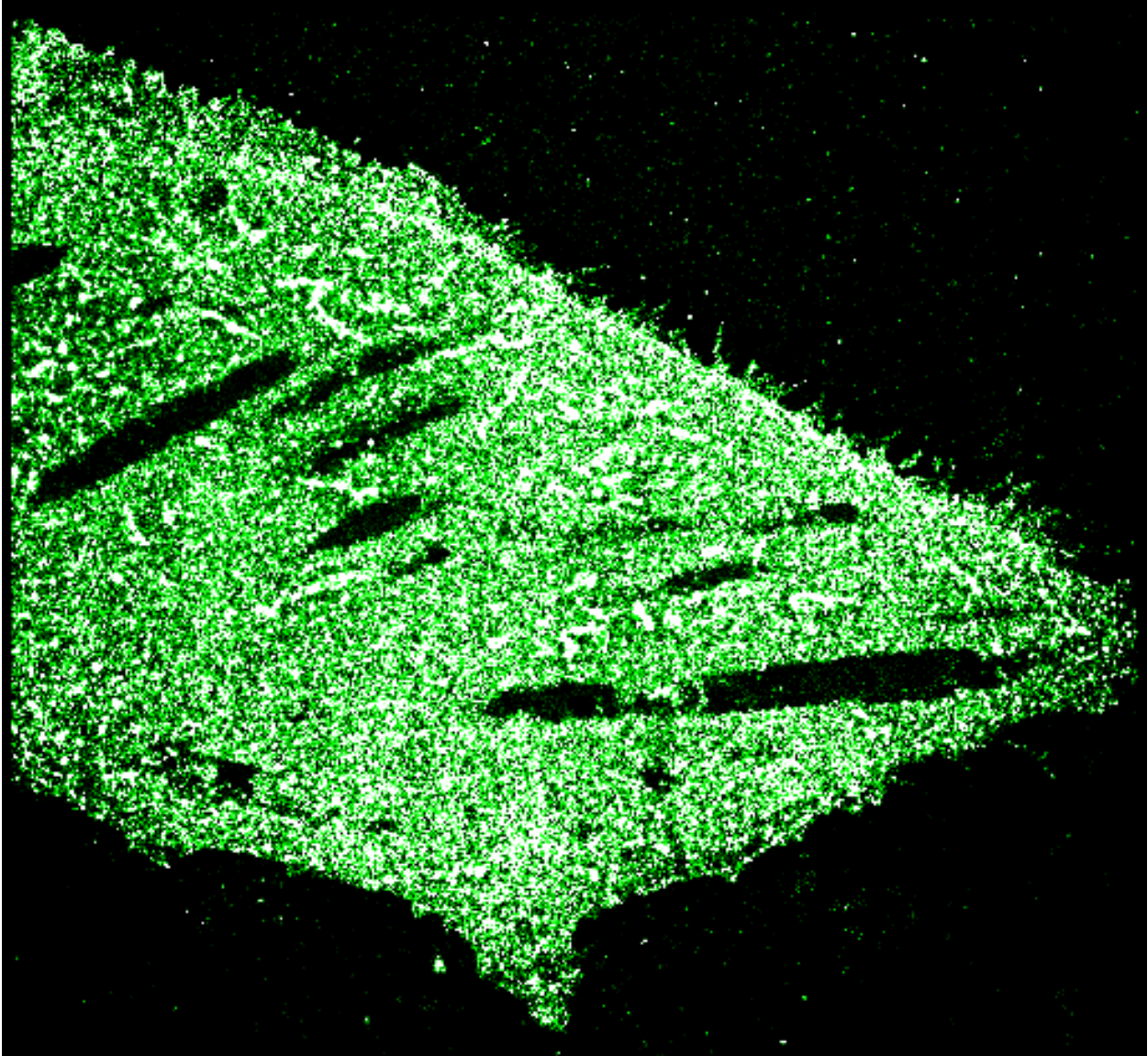


FIGURE 2.9: STORM RECONSTRUCTION OF SNAP-HN1 ON CHO CELLS SHOW AREAS OF EXCLUSION & ENRICHMENT

CHO cells expressing SNAP-hN1 incubated with $1\mu\text{M}$ BG-AF647 are fixed and imaged via TRIF. The reconstruction above comes from post-processing of thousands of consecutive images.

The voids imaged seemed to be focal adhesions. Ideally we'd be able to image both Notch and a protein that was part of a focal adhesion either simultaneously or in sequence. However, the labeling of a focal adhesion with a STORM-capable dye proved to be a challenge. Stress fibers - long actin filaments that are often attached to the membrane at focal adhesions - were more

easily imaged. Dye-conjugated phalloidin added to our fixed samples allowed us to co-image the stress fibers along with Notch. Unfortunately, limitations in drift, signal-to-noise, and time prevented a more quantitative analysis of our results. Ideally a well-calibrated system might have been able to quantitatively characterize the regions of enrichment and Notch clustering, and the voids with respect to other proteins. Ultimately, additional dyes and additional proteins in the Notch pathway tagged with orthogonal enzymatic tags may yet yield quantitative data regarding the steady-state distribution of Notch and its partners at the cell surface.

2.4.2 *relative to focal adhesions*

The initial images produced using STORM showed clear regions of both enrichment and exclusion. The excluded regions appeared similar to the inverse of a focal adhesion. To test whether Notch was being excluded from focal adhesions we obtained an mCherry-Paxillin fusion protein from the Weaver lab and expressed this construct in U2OS cells also expressing SNAP-hN1. When stained with BG-647 a clear mutually exclusive distribution was observed at the surface of the cells (**Figure 2.10**).

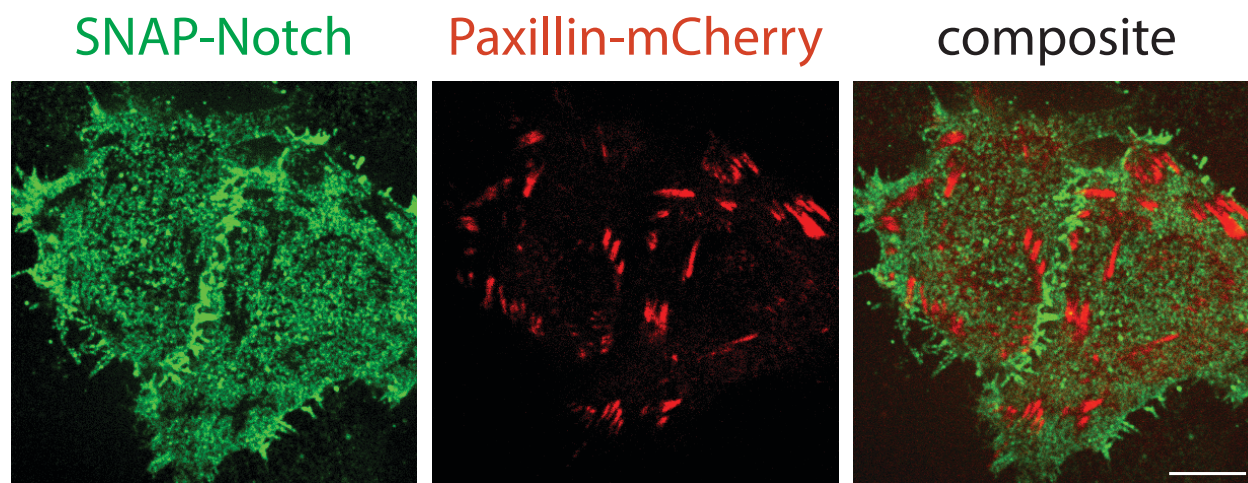


FIGURE 2.10: CONFOCAL IMAGES OF NOTCH & PAXILLIN.

U2OS cells expressing SNAP-hN1 & Paxillin-mCherry are stained with BG-647 and imaged via confocal microscopy. The two markers appear exclusively localized.

At first glance the exclusion of a receptor containing a very large extracellular domain from a tightly-packed focal adhesion due to the steric hindrance seemed a straightforward mechanism. However other large receptors either did not exhibit such exclusion (CD86,

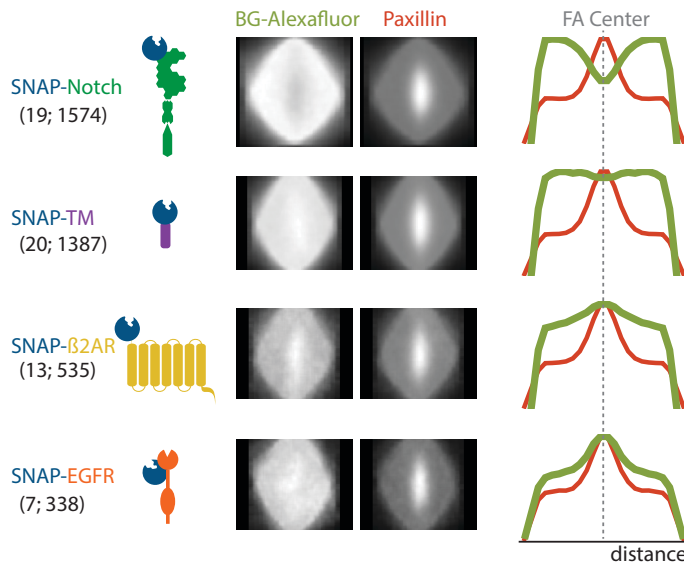


FIGURE 2.11: QUANTITATIVE ANALYSIS OF THE COLOCALIZATION OF SNAP-TAGGED PROTEINS & PAXILLIN

Various SNAP-tagged receptors expressed with Paxillin-mCherry in U2OS cells are stained with BG-AF647. Across a number of cells focal adhesions are isolated (cells;FAs) and averaged in both channels resulting in a graph of their colocalization as a function of the distance to the center of the focal adhesion.

Dopamine1, βAR2, or a bare transmembrane domain) or even seemed to exhibit enrichment within a focal adhesions (EGFR) (Figure 2.11). In order to account for the exclusion not simply being the result of steric hindrance, we took a number of different hypothesis. Notch is heavily glycosylated and it was recently shown that heavily glycosylated proteins, even if small, can be excluded from focal adhesions.⁷ Notch also has a set of significant intracellular domains, not all of which are well characterized, that could interact with intracellular cytoskeletal scaffolding. Further, a putative interaction domain on the NRR might enable intramolecular interactions

with other surface-proteins that mediate exclusion from focal adhesions. To test each of these hypotheses we expressed the SNAP-tagged truncations of Notch along with mCherry-Paxillin.

Cells expressing the full length Notch receptor were exclusively and strongly absent from focal adhesions as measured by colocalization of SNAP-dye with mCherry as imaged by confocal microscopy. Cells expressing the Transmembrane-bound-NICD were found to be evenly

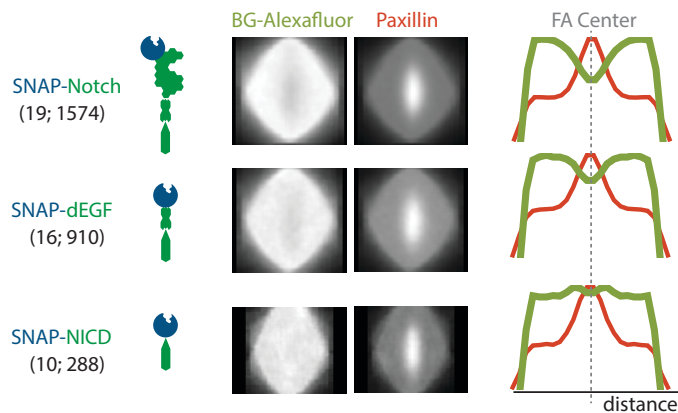


FIGURE 2.12: QUANTITATIVE ANALYSIS OF THE COLOCALIZATION OF SNAP-TAGGED NOTCH TRUNCATIONS & PAXILLIN

Various SNAP-tagged Notch truncations expressed with Paxillin-mCherry in U2OS cells are stained with BG-AF647. Across a number of cells focal adhesions are isolated (cells;FAs) and averaged in both channels resulting in a graph of their colocalization as a function of the distance to the center of the focal adhesion.

2.4.3 *in time*

The monovalent Quantum Dots were designed and produced particularly in order to monitor the temporal dynamics of Notch during its activation at the surface of live cells. Cells expressing each of the SNAP-tagged truncations were incubated with benzylguanine-DNA complementary to our mQDs and then the mQDs themselves at a concentration amenable to single molecule tracking (~500pM). Individual quantum dots were tracked over the course of 30 seconds every 50 ms on a single cell using a 100x objective on a TIRF microscope. Cells expressing both mCherry-Paxillin and SNAP-Notch were also co-imaged; an mCherry image was taken just prior to a time-lapse of the Quantum dots. This co-imaging allowed us to reconstruct how any given particle behaved with respect to its microenvironment (**Figure 2.13**). The mQDs were essential in allowing us to monitor the spatiotemporal dynamics of Notch at a single-molecule level over a long time-period.

distributed both outside of and within mCherry-stained regions of the cell suggesting some part of the extracellular portion of the Notch receptor was responsible for the exclusion (**Figure 2.12**). The NRR-TM construct was not completed at the time of writing, however the truncation missing all of the EGF repeats clearly showed exclusion from focal adhesions, implicating the NRR in the exclusion.

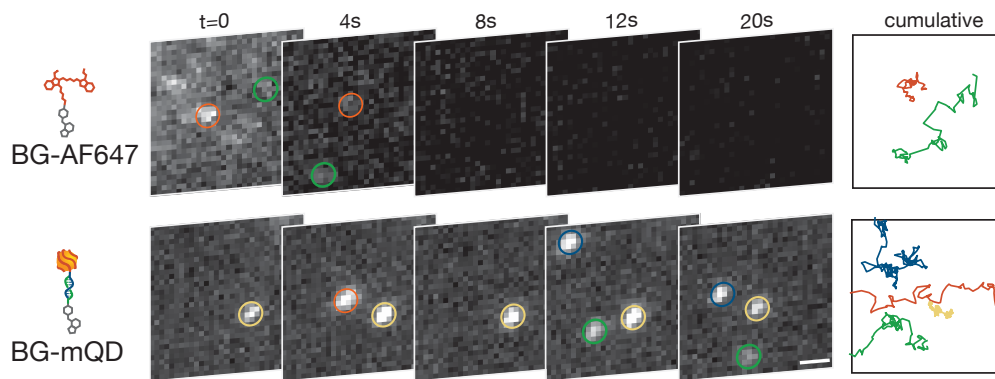


FIGURE 2.13: SINGLE PARTICLE TRACKING OF SNAP-NOTCH TAGGED WITH BG-AF647 & BG-TARGETED MQDS

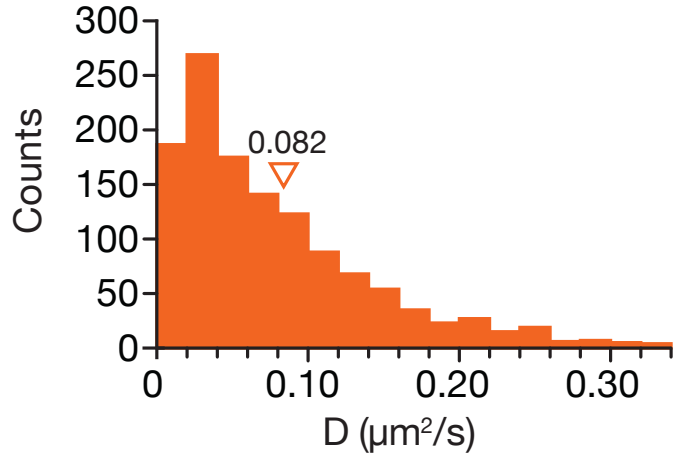
On a single U2OS cell, SNAP-hN1 receptors dyed with either BG-AF647 or BG-mQDs are imaged and then tracked over 20 seconds. The organic dye quickly photo bleaches while the mQD remains easily identifiable.

2.5 Measuring the Diffusion of Notch

The brightness of the mQDs permitted automated tracking of the Notch receptors using computational methods. However many of these methods are slow and unreliable. A number of pieces of software were tried. The Rytrack.pro script was the fastest and most effective at obtaining track data (id, x, y, z, t, i). From this data we were able to curate those tracks that were reliable, long and mobile using the program Tracker (**Chapter 5.1**). From these curated datasets parameters describing the dynamics of Notch were calculated.

The diffusion coefficient is calculated as the slope of the first few points of the mean squared displacement of a track plotted against various time-steps (τ). Traditionally it has been difficult to obtain long enough tracks to reliably extend this measurement beyond a τ of 10.⁸ With the long tracks obtained by imaging with the photostable mQDs, the minimum track length used for calculations was 40 steps, with most tracks exceeding 100 time-steps.

Full length Notch exhibited a diffusion coefficient of $0.082 \mu\text{m}^2/\text{s}^2$ (**Figure 2.14**). Additionally, by automating the tracking of the particles we are able to obtain a very large number of tracks on a large number of cells.



2.6 Analysis of Notch Dynamics

With large amounts of long track data we were able to calculate the MSD of the entire population of receptors, and subsequently calculate a confinement coefficient (α) as defined by the exponent of the curvature associated with the MSD

FIGURE 2.14: DIFFUSION OF NOTCH ON A LIVE U2OS CELL AS MEASURED WITH MQDS

SNAP-hN1 receptors labeled with mQDs are tracked over at least 2 seconds at a 0.05ms frame rate. From those tracks the mean diffusion coefficient was calculated to be $0.082\mu\text{m}^2/\text{s}$

plot. Where motion is Brownian, $\alpha = 1$; $\alpha > 1$ for directed motion, and $\alpha < 1$ for confined motion. The diffusion of Notch as calculated from the bulk MSD was in good accord with the average diffusion of Notch at $0.084 \mu\text{m}^2/\text{s}^2$. The exponent, $\alpha = 0.72$ indicating a significantly confined set of tracks over time (**Figure 2.15**). In other words, given its diffusion coefficient, Notch should have diffused farther from a point than it actually did, suggesting it was being confined at longer length-scales. Literature suggests that the surface of a cell should generally be considered to be crowded and an alpha value of 1 would not be expected in a biological experiment⁹, however 0.72 was lower than one might expect for a generic transmembrane protein.

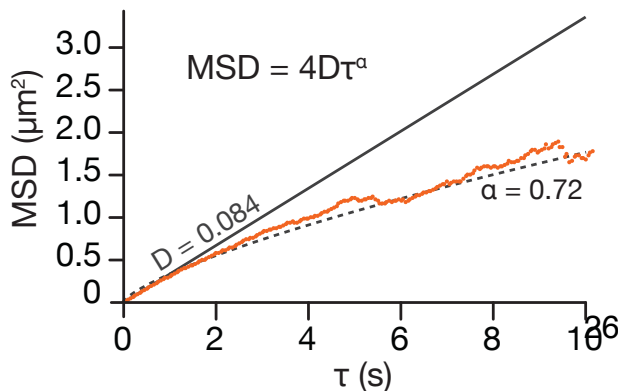


FIGURE 2.15: CONFINEMENT OF SNAP-TAGGED NOTCH ON LIVE U2OS CELLS AS MEASURED WITH MQDS

From tracks, a mean MSD for the entire population of Notch receptors was fitted to an exponential revealing a confinement of 0.72 and a population diffusion of $0.084 \mu\text{m}^2/\text{s}$, similar to the mean diffusion of each receptor.

Given our observation that Notch was begin excluded from focal adhesions we were curious if that kind of spatial exclusion could result in the kind of confinement we observed. Using images of actual cells and their focal adhesions, along with the diffusion coefficients above we set up a simulation wherein Notch could both freely diffuse over the whole cell, or would be excluded from the observed focal adhesions, focal adhesions that were significantly smaller, or focal adhesions that were significantly larger.

By simulation¹⁰ it was clear that impermeable features at the surface of a cell of the size and shape of a focal adhesion could indeed significantly alter the measurable confinement of receptors traversing across the cell at the rates observed of the Notch receptor. One of the interesting aspects of the simulation was the finding that the kind of interaction that the mobile receptor had with its boundary too could affect both local diffusion rates and confinement. Mathematically, the receptor-boundary interaction could be modeled as elastic, inelastic, or force-like.

2.8 Discussion

In requiring multiple interactions for activation, Notch has a number of means to check its regulation. As Notch activation generally leads to binary cell-fate decisions during development, checking interaction and curtailing spurious activation are critical for proper development. Additionally, the activation of Notch by force puts a different set of regulatory mechanisms in place than would be found for receptors of diffusable ligands. The uneven distribution of any of the components of the Notch signaling pathway at the cell surface is a compelling mechanism for regulation of this process. Here we set out to monitor those interactions taking place during Notch activation at the surface of live mammalian cells.

We find Notch diffusion to be slower than a generic transmembrane domain prompting inquiries into partners it may be bound to while at the surface. Additionally the receptor

showed confined diffusion demonstrating that not only was the receptor likely being bound by other features, but it was also being sequestered into or out of particular regions of the surface. We found Notch to be particularly excluded from focal adhesions as demonstrated by mutually exclusive localization of paxillin and Notch. Though focal adhesions are known to be dense other receptors similarly observed were not so exclusively localized from focal adhesions.

Knowing that Notch is spatially regulated we endeavored to determine the mechanism of regulation. To do this we made truncations of various Notch domains which hypothetically could regulate its distribution. Surprisingly the extracellular EGF repeats which make up a significant bulk of the receptor was not required to exclude notch from Focal adhesions. Additionally, the intracellular domain of Notch (NICD) was insufficient to prevent diffusion into focal adhesions. Thus it appeared that the Notch regulatory region (NRR) was playing some role in directing the distribution of the receptor.

Additional experiments are required to determine whether the NRR is sufficient to exclude Notch, whether other regions of the surface exclude Notch, and how other proteins might actually collect or aggregate Notch. STORM images often showed regions of enrichment as well as exclusion leading to questions of multimerization. Further, the exclusion of the receptor from focal adhesions appeared qualitatively stronger in the full length receptor than in the EGF-truncated receptor indicating that the EGF repeats might play some role in these interactions.

With respect to the larger picture of how Notch is regulated and to what extent that regulation is spatial in nature, future experiments would benefit from being able to similarly monitor the other components of the activation pathway: ADAM protease, gamma-secretase and the ligands - present in both *cis* and *trans*. Here we present a demonstration of the success in monitoring the receptor alone and interpret the kinds of data that can be gleaned from these investigations. Applying those same techniques to the rest of the system, simultaneously,

would certainly elucidate significant interactions that are difficult to infer from monitoring a single component. Finally, here we present a number of microscopy techniques to monitor components of a system - but a still-distant goal would be the monitoring of these components not just on the surface of a single cell, but at the point of interaction between two cells. Though technically challenging, such observation would be significant in understanding how the Notch receptor is regulated *in vivo*.

2.8 References

-
- ¹ Ploscariu, N., Kuczera, K., Malek, K. E., Wawrzyniuk, M., Dey, A., & Szoszkiewicz, R. (2014). Single molecule studies of force-induced S2 site exposure in the mammalian Notch negative regulatory domain. *The Journal of Physical Chemistry. B*, *118*(18), 4761–4770. doi:10.1021/jp5004825
 - ² Gordon, W. R., Roy, M., Vardar-Ulu, D., Garfinkel, M., Mansour, M. R., Aster, J. C., & Blacklow, S. C. (2009). Structure of the Notch1-negative regulatory region: implications for normal activation and pathogenic signaling in T-ALL. *Blood*, *113*(18), 4381–4390. doi:10.1182/blood-2008-08-174748
 - ³ Li, K., Li, Y., Wu, W., Gordon, W. R., Chang, D. W., Lu, M., et al. (2008). Modulation of Notch signaling by antibodies specific for the extracellular negative regulatory region of NOTCH3. *The Journal of Biological Chemistry*, *283*(12), 8046–8054. doi:10.1074/jbc.M800170200
 - ⁴ Furriols, M., & Bray, S. (2001). A model Notch response element detects Suppressor of Hairless-dependent molecular switch. *Current Biology : CB*, *11*(1), 60–64.
 - ⁵ Gordon, W. R., Arnett, K. L., & Blacklow, S. C. (2008). The molecular logic of Notch signaling--a structural and biochemical perspective. *Journal of Cell Science*, *121*(Pt 19), 3109–3119. doi:10.1242/jcs.035683

-
- ⁶ Huang, B., Jones, S. A., Brandenburg, B., & Zhuang, X. (2008). Whole-cell 3D STORM reveals interactions between cellular structures with nanometer-scale resolution. *Nature Methods*, *5*(12), 1047–1052. doi:10.1038/nmeth.1274
- ⁷ Paszek, M. J., DuFort, C. C., Rossier, O., Bainer, R., Mouw, J. K., Godula, K., et al. (2014). The cancer glycoalyx mechanically primes integrin-mediated growth and survival. *Nature*, *511*(7509), 319–325. doi:10.1038/nature13535
- ⁸ Saxton, M. J. (2001). Anomalous subdiffusion in fluorescence photobleaching recovery: a Monte Carlo study. *Biophysical Journal*, *81*(4), 2226–2240. doi:10.1016/S0006-3495(01)75870-5
- ⁹ Saxton, M. J. (2012). Wanted: a positive control for anomalous subdiffusion. *Biophysical Journal*, *103*(12), 2411–2422. doi:10.1016/j.bpj.2012.10.038
- ¹⁰ Saxton, M. J. (2007). Modeling 2D and 3D diffusion. *Methods in Molecular Biology (Clifton, N.J.)*, *400*(Chapter 20), 295–321. doi:10.1007/978-1-59745-519-0_20

Production & Targeting of Monovalent Quantum Dots

Precise control over interfacial chemistry between nanoparticles and other materials remains a significant challenge limiting the broad application of nanotechnology in biology. To address this challenge, we use 'steric exclusion' to completely convert commercial quantum dots (QDs) into monovalent imaging probes by wrapping the QD with a functionalized oligonucleotide. We demonstrate the utility of these QDs as modular and non-perturbing imaging probes by tracking individual Notch receptors on live cells.

Quantum dots provide advantages over other fluorescent probes such as organic dyes or fluorescent proteins in that they are bright, stable, and have very precise spectral properties, however they are often difficult to interface with biological materials - and generally the targeting mechanism is polyvalent (**Table 3.1**). As a result, commercial quantum dots are quite large compared to other fluorescent probes and are a non-starter in applications where affecting the valency of one's target would upset experimental assumptions. ptDNA-wrapped mQDs overcome these challenges by reliably producing a bright, photostable quantum dot that is monovalent, modular, and because of its monovalency, smaller than most biologically targeted quantum dots.

	Commercial QDs	Organic Dyes	Fluorescent Proteins
Brightness (extinction coefficient)	intense (10^{6-7})	moderate (10^{4-5})	moderate (10^{6-7})
Photostability (# photons before bleaching)	stable (>10)	low (~ 10)	low ($<5 \times 10$)
Spectral Monodispersity (FWHM)	narrow, symmetric ($<30\text{nm}$)	broad, asymmetric ($40-60\text{nm}$)	broad, asymmetric ($40-60\text{nm}$)
Targeting Valency	mixed (undefined)	monovalent (defined & controllable)	monovalent (defined & controllable)
Hydrodynamic Size	large ($15-30\text{nm}$)	small ($1-2\text{nm}$)	medium ($5-10\text{nm}$)
Functional Modularity	low	easily controllable	genetic fusions

TABLE 3.1 COMPARISON OF QDS WITH OTHER FLUORESCENT PROBES

3.1 mQDs Produced by Steric Exclusion

Common strategies for chemically linking materials to nanoparticles generate products with valencies that follow a Poisson distribution due to the presence of multiple reactive sites at the particle surface.¹ For example, titration of QDs with increasing concentrations of a trithiolated DNA (ttDNA) generates an underdispersed Poissonian distribution of product valencies², where the desired monovalent QDs are always obtained alongside unconjugated and multivalent QD byproducts. Multivalent nanoparticles present in these mixtures complicate their use for biological imaging because of their potential for perturbing their target's function by oligomerization, leading to receptor activation, internalization, or redistribution on the cell surface.^{3 4 5} These confounding properties of multivalent nanoparticles have motivated the development of methods for purifying monovalent QDs from more complex mixtures.^{6 7} However, the low synthetic yield of these strategies, along with the multiple steps necessary to isolate pure monovalent QDs, have slowed their broad application in the biomedical sciences. More recent efforts have aimed to synthesize QDs of controlled valency without the need for

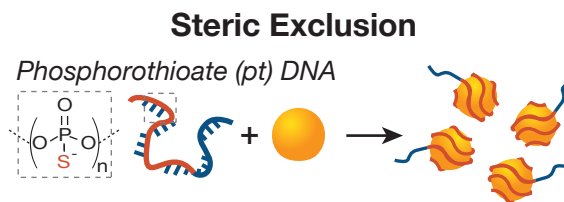


FIGURE 3.1 MONOVALENT QDS PRODUCED BY STERIC EXCLUSION

A strand of phosphorothioate DNA wraps a quantum dot to produce a single species of mQD by sterically excluding another strand

purification.⁸ These methods remain technically challenging for the typical researcher, generate products with low overall yield, or lack the necessary modularity to be broadly useful.

By nature of their large size, macromolecules or nanoparticles conjugated to QDs limit the maximum valency of products by sterically excluding a large fraction of the QD surface from additional reactions.⁹ We envisioned using this concept to synthesize monovalent QDs, in quantitative yield, by using a polymer having only a modest per-monomer affinity for the nanoparticle surface to wrap the QD in a single synthetic step, irreversibly forming a monovalent product and simultaneously preventing the binding of a second polymer molecule by ‘steric exclusion’ (**Figure 3.1**). Ideally, this approach would produce monovalent QDs that retain their excellent photophysical properties, not add significantly to their size, work efficiently under homogeneous reaction conditions, form a stable colloidal product, use commercially available reagents as starting materials, and allow for modular conjugation to a variety of targeting molecules.

To implement this steric exclusion strategy, we used phosphorothioate DNA (ptDNA) as a polymer due to 1) the demonstrated affinity of phosphorothioates for semiconductor surfaces¹⁰, 2) the ease of synthesizing ptDNA of precisely defined sequence and length, and 3) its availability to any researcher from most oligonucleotide synthesis companies. After transfer of commercial CdSe:ZnS QDs from the organic to the aqueous phase, we treated the QDs with ptDNA of various sequences and lengths. DNA-functionalization produced QDs with an ionic

character that were easily distinguishable from unfunctionalized QDs by agarose gel electrophoresis.¹¹ We titrated 605 nm emitting QDs (605-QDs) with increasing concentrations of an oligonucleotide comprising a 50 adenosine ptDNA domain ($A^{S_{50}}$) and a 20 nucleotide ssDNA targeting tail. The modularity of the quantum dot was demonstrated by the production of mQDs of various sizes and emission spectra (**Figure 3.2**).

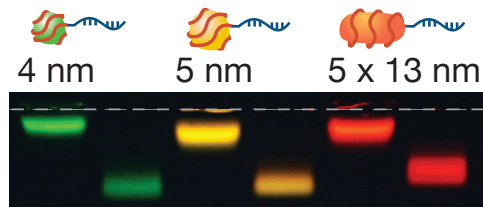


FIGURE 3.2: MQDS PRODUCED WITH VARIOUS SIZED/COLORED QDS

A band of un-conjugated and conjugated QDs of various sizes run on an agarose gel.

3.2 Targeting mQDs by Hybridization

The 5' end of a DNA strand complementary to the mQDs can be modified to enable targeting of a number of different biomolecules. There are a number of established techniques available to covalently modify proteins, lipids & sugars with single stranded DNA (ssDNA) (**Figure 3.3**).

So long as the ssDNA is presented extracellularly, it is accessible to soluble mQDs. mQDs with the above sequences will rapidly hybridize with their complementary DNA strand under cell

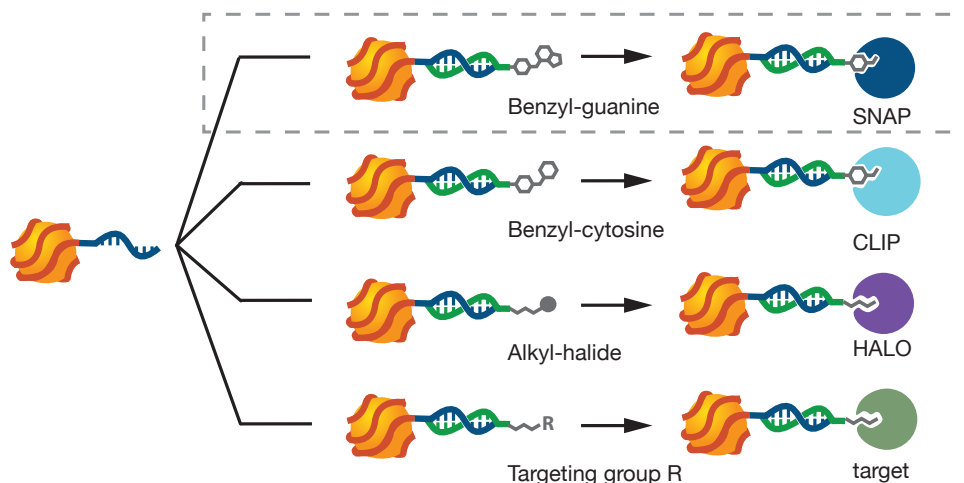


FIGURE 3.3: SCHEMATIC OF THE MODULARITY OF MQDS TARGETED BY HYBRIDIZATION

culture conditions. A 10-20X poly-(CT) spacer between the ptDNA and the targeting sequence may be required for efficient targeting so as to elevate the binding sequence above the thick and negatively charged glycocalyx of the cell. For this protocol we chose to produce a BG-DNA with a complementary sequence of (CAGT)₅ that will both hybridized to the mQDs and covalently link itself to a SNAP-tag protein for rapid and specific labeling. A similar protocol functions well for coupling other NHS-esters to amino-modified oligonucleotides.

The modularity of the mQD design enables an increased degree of experimental flexibility. For example, a variety of mQDs can be quickly prepared in unique colors allowing for the simultaneous imaging of multiple targets. The ssDNA targeting sequence can direct mQDs to proteins, sugars¹², lipids and surfaces¹³. **Figure 3.4** demonstrates the targeting of mQDs to the surface of live Jurkat cells by means of complementary strand of DNA bound to lipid. Cells exposed to lipid conjugated to DNA which was non-complementary to the mQDs were not labeled. Labeling was imaged using confocal microscopy where a cross-section showed a bright ring of surface-

labeling.

A number of enzymatic tags are available with orthogonal reactivities, allowing multiple targets to be imaged simultaneously with differentially targeted

mQDs. In addition to targeting with the SNAP tag, labeling of target proteins with mQDs using the CLIP tag, the HALO tag, and biotinylated proteins

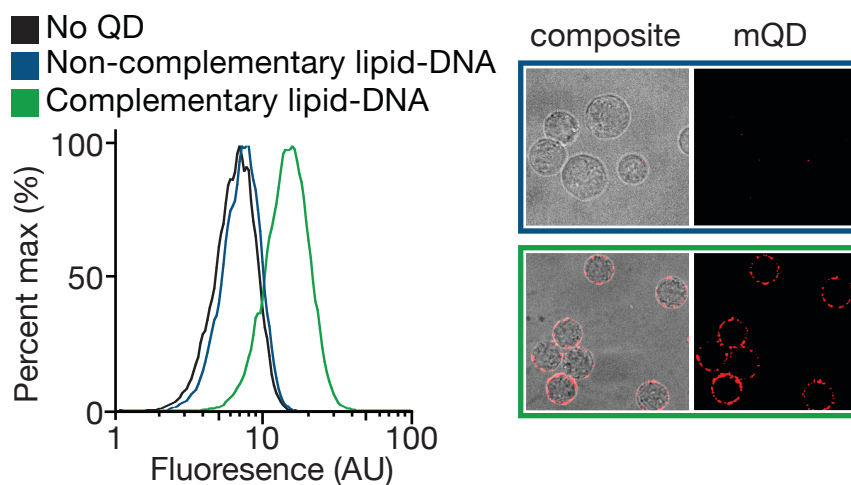


FIGURE 3.4: MQDS TARGETED TO THE SURFACE OF LIVE JURKAT CELLS USING LIPID-DNA

Cells incubated with lipid-DNA complementary or non-complementary to mQDs were detected via FACS and subsequently imaged via confocal microscopy. Only those cells with complementary DNA show a significant increase in fluorescence upon incubation with mQDs.

was also successful. This protocol demonstrates the specific labeling of a surface receptor on live cells with these mQDs, but the protocol could easily be adapted to a number of different contexts. **Figure 3.5** demonstrates a gel-shift in mQD mass only when targeted specifically to the SNAP or CLIP proteins by their respective DNA-conjugates.

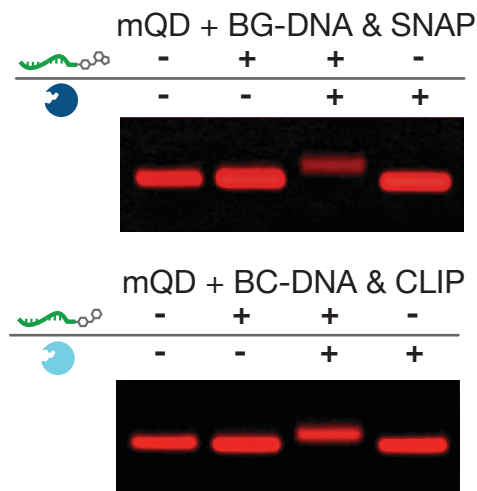


FIGURE 3.5: MQDS TARGETED TO SNAP & CLIP TAGS BY BG- & BC-DNA, RESPECTIVELY

Agarose gels run with each component, separately and together of a protein-targeted mQD. Only when all targeting components are present (Protein, BG-DNA, mQD) is there a shift in molecular weight of the visualized mQD.

We further investigated whether mQDs could be modularly and efficiently targeted to protein or lipid tags used frequently for live cell imaging. Targeting was achieved by 3'-modification of the ptDNA or by hybridization of mQDs with complementary DNA bearing a 5'-modification. We used these strategies to conjugate mQDs with biotin, benzylguanine (BG), benzylcytosine (BC), and lipids, thereby targeting them to streptavidin, SNAP, CLIP, and cell membranes, respectively.

3.3 Production of Benzylguanine-DNA

We targeted mQDs to SNAP-tagged extracellular constructs using benzylguanine linked to the terminus of a complementary strand of DNA. This molecule was produced by reacting NHS-BG with amine-terminated DNA in dry DMSO buffered with pH 8.5 HEPES for 1 hour at room temperature while being sonicated. Once desalted, the BG-DNA was purified from unreacted DNA by reversed-phase HPLC using a C18 column. As the DNA linked to the targeting moiety can be composed of any sequence, sequences capable of scaffolding multiple binding partners, sequences containing a ratcheting effect for more efficient binding, or sequences containing spacer strands can all be made to facilitate efficient utilization of the mQDs. BG-DNA composition was confirmed by MALDI and found to be stable at 4 °C for over one year.

3.4 Confirming Monovalency

Agarose gel electrophoresis revealed a single band with increased mobility relative to starting

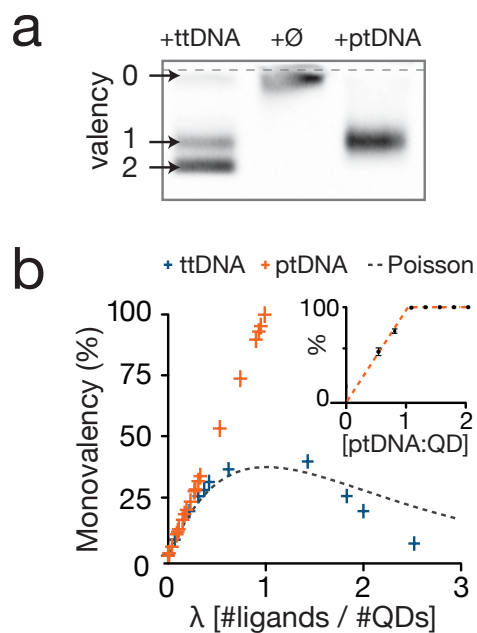


FIGURE 3.6:
CHARACTERIZING
THE MONOVALENCY
OF mQDs

a gel (a) comparing unfunctionalized QDs, mQDs and QDs produced by exposure to ttDNA shows the exclusive production of mQDs when produced with ptDNA. (b) Average number of molecules bound per QD (λ) versus percentage of monovalent products using

ttDNA and ptDNA. Dashed curve is fit with a Poisson distribution. Inset, reaction stoichiometry (ptDNA:QD) versus percentage of monovalent products.

materials indicating production

of a single species (Fig. 3.6b).

At stoichiometric or higher ratios of ptDNA and QD, no sign of unfunctionalized or multiply functionalized products were observed, consistent with the quantitative formation of a monovalent product (mQDs).

QD-DNA conjugation was most efficient with oligonucleotides having a phosphorothioate backbone and adenosine bases. The ptDNA-wrapped mQDs had excellent colloidal

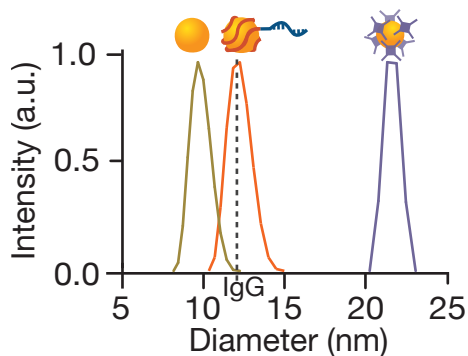


FIGURE 3.7: CHARACTERIZING THE SIZE OF MQDS

Hydrodynamic radius of unfunctionalized, monovalent and streptavidin QDs as measured by DLS and in comparison to an IgG protein.

To provide more direct evidence for monovalency, we hybridized mQDs to gold nanocrystals bearing a single complementary sequence of ssDNA. We observed the formation of a single higher molecular weight band by gel electrophoresis, consistent with the exclusive formation of heterodimers. Analysis of this band by transmission electron microscopy (TEM) revealed nearly exclusive formation of mQD-Au

heterodimers ($n = 545$, **Figures 3.7a, b**).

We rarely observed higher order structures, such as trimers (2%) and tetramers (<0.2%) by TEM. In contrast, a reaction of multivalent Streptavidin QDots

and photophysical properties in physiologically relevant buffers such as phosphate buffered salines (PBS) and culture media when passivated with commercially available polyethyleneglycol (PEG) ligands. The hydrodynamic diameter of 605-mQDs was narrowly distributed around 12 nm as measured by dynamic light scattering (DLS) – only 2 nm greater than bare particles

(**Figure 3.6a**).

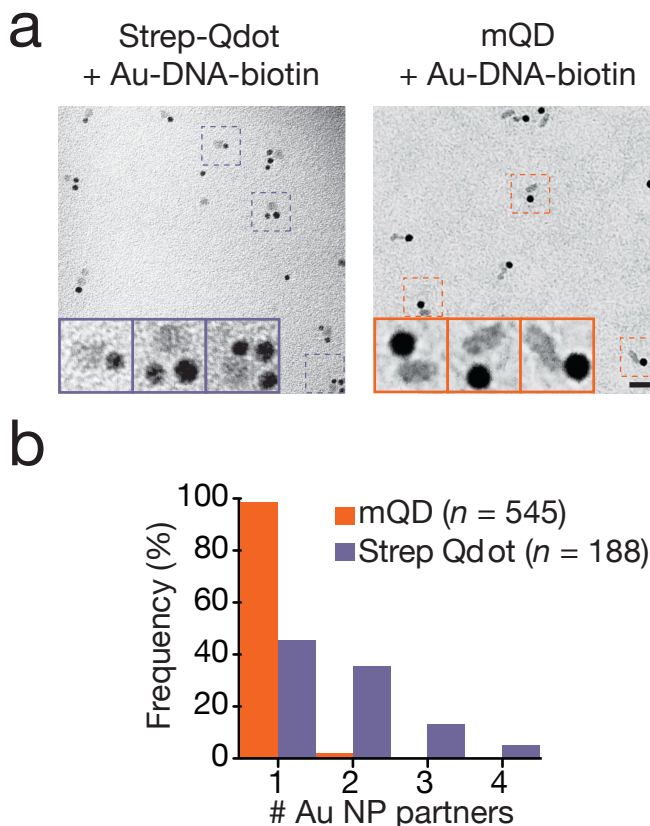


FIGURE 3.8: EM MICROGRAPHS CHARACTERIZING THE VALENCY OF MQDS AND STREPTAVIDIN QDS LINKED VIA HYBRIDIZATION TO AU-NANOPARTICLES

Representative TEM images (**a**) of commercial streptavidin-conjugated QDots or mQDS hybridized with gold nanoparticles and the frequency (**b**) of QD valences measured from a number of micrographs.

with similar DNA-linked monovalent gold nanocrystals conjugated to biotin resulted in multivalent products such as trimers and tetramers along with QD-Au heterodimers (**Figure 3.7a**).

Previous studies reported that multivalent QDs generate imaging artifacts by triggering receptor clustering and endocytosis³⁻⁵. QD-mediated receptor clustering can also perturb the receptors' diffusion. To investigate whether mQDs crosslink protein targets, we prepared supported lipid bilayers (SLBs) incorporating His-tagged SNAP protein via a small fraction of NTA-linked lipid (**Figure 3.8a**). We imaged the diffusion of the membrane-bound SNAP using a small organic dye, commercially available Streptavidin QDots, or mQDs and analyzed several hundred single molecule trajectories for each probe. The diffusion coefficient measured using the Streptavidin QDots was significantly lower than using the dye ($p = 0.001$). The diffusion further slowed at higher SNAP protein density (**Figure 3.8b**), consistent with the notion that

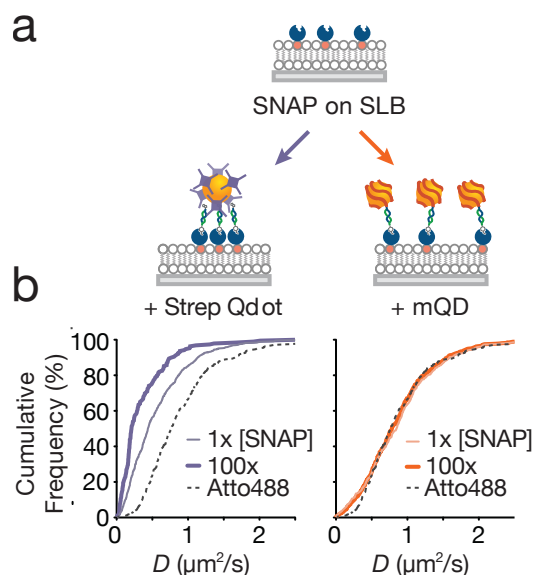


FIGURE 3.9: DIFFUSION OF VARIOUS CONCENTRATIONS OF STREPTAVIDIN QDS & MQDS ACROSS A SUPPORTED LIPID BILAYER

Streptavidin-QDs or mQDs were targeted to a lipid bilayer via a His-tagged SNAP-tag (**a**). An increase in SNAP-density on the bilayer resulted in a decreased diffusion rate for Streptavidin-QDs but not mQDs demonstrating the increased cross-linking from the polyvalent streptavidin QDs.

multivalent Streptavidin QDots crosslink the target. In contrast, we observed a nearly identical distribution of diffusion coefficients for mQDs and the dye, independent of protein density (**Figure 3.8b**). These data indicate that mQDs behave as *bona fide* and non-perturbing single molecule imaging agents in model cell membranes.

3.5 Passivation for *in vivo* imaging

Passivation of the ptDNA-wrapped QDs is usually required in order to improve colloidal stability of QDs and reduce background binding for most experimental applications. The protocol uses a PEG-layer to passivate the QDs (**Figure 3.9**). Carboxy PEG alkane thiol with additional PEG units ((CO₂H)CH₂O(CH₂CH₂O)₁₂C₁₁H₂₃SH, carboxy-PEG12 alkane thiol) provides significantly reduced background, though the longer PEGs are both larger, and generally more expensive. mQDs coated with carboxy PEG alkane thiol ligands are highly stable in physiological buffers such as phosphate buffered salines and culture media. Long-term storage (> 8 months) of mQDs at 4 °C showed no significant aggregation or ptDNA detachment¹¹. Depending upon the experiment, PEG passivation of the QDs alone does not always sufficiently reduce non-specific binding of the mQDs. Incubating both cells and mQDs in phosphate buffered saline (PBS) containing 3% BSA for 20 min prior to use substantially reduces non-specific binding to cells, though it does increase the apparent hydrodynamic radius of the mQDs by ~50%. Passivation with 0.5% casein reduces the non-specific binding even further but it increases the apparent size to a greater extent than BSA.

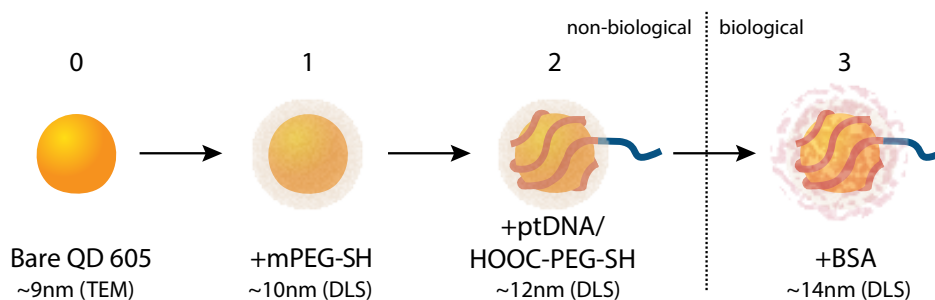


FIGURE 3.10: VARIOUS PASSIVATION STEPS IN THE PRODUCTION OF

3.6 Discussion

We next applied these small, modular, and monovalent QDs to track individual Notch receptors on live cells. Notch activation plays a central role in cell fate decisions during development, normal tissue maintenance and cancer.¹⁴ Despite its importance in these biological processes, little is known about the dynamics of Notch receptors at the cell surface. We aimed to measure the diffusion coefficient of single Notch receptors in order to reveal whether their diffusion is dominated by interactions with the viscous lipid bilayer or by surrounding proteins and glycans on the cell surface and cortex. To track Notch, we inserted a SNAP tag onto the N-terminus of a previously reported human Notch1 construct and expressed the resulting protein (SNAP-Notch) in U2OS cells.¹⁵ The BG-mQDs labeled the cells expressing SNAP-Notch (red fluorescent cells) with high specificity. Negligible binding was observed to cells expressing a control GFP-Notch construct lacking the SNAP tag.

To confirm that the mQDs did not alter the mobility of Notch on live cells, we tracked SNAP-Notch labeled with mQDs and compared their average diffusion coefficients to receptors labeled with BG-Alexafluor-647 on the same cell (**Figure 3.10**). Analysis of mean-square-displacement (MSD) versus time revealed mean diffusion coefficients (D) of 0.081 and 0.076 $\mu\text{m}^2/\text{s}$ ($p = 0.7255$) for Notch imaged with Alexa-647 and mQDs, respectively. The measured diffusion constant of Notch deviates from other freely diffusing single pass transmembrane proteins tracked by fluorescence microscopy (0.17-0.5 $\mu\text{m}^2/\text{s}$).^{16 17} The observed differences are not a consequence of cell type or imaging conditions, as a minimal protein based

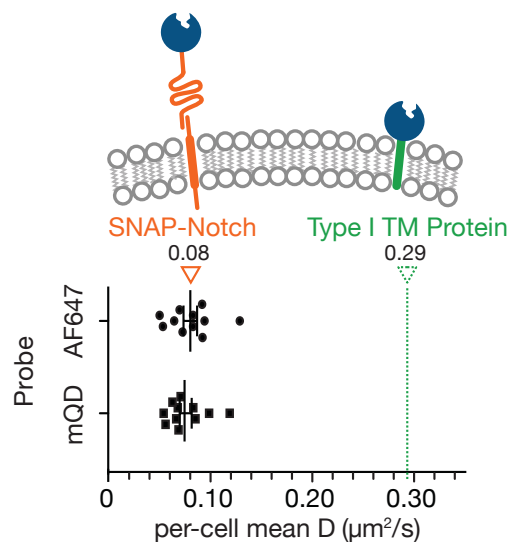


FIGURE 3.11: DIFFUSION OF NOTCH MEASURED EITHER BY DYE OR MQDS IS SIMILAR

Each point is the average of >15 receptors on a cell to give a per-cell average diffusion. Diffusion on each cell was calculated with both a mQD and an organic dye.

on the type I transmembrane domain from CD86 in U2OS cells also yielded an apparent diffusion coefficient ($0.29 \mu\text{m}^2/\text{s}$) several fold higher than Notch (**Figure 3.10**). In contrast, measured diffusion coefficients for Notch are consistent with reported values of single pass transmembrane proteins known to interact with components of the cell surface or cell cortex.¹⁸ Although the physical source of the slow diffusion remains to be determined, our measurements suggest that the diffusion of Notch is dominated by interactions with proteins or glycans, rather than the viscous lipid bilayer.

In conclusion, we report a potentially general method for preparing nanoparticles of fixed targeting valency using the principle of steric exclusion. The method is likely applicable to other nanoparticle materials using either modified nucleic acids or other polymers of low dispersity and controlled chemical functionality. We apply this simple method to prepare ptDNA-wrapped mQDs in quantitative yield and from commercially available starting materials. mQDs prepared by steric exclusion retain their small size and excellent photophysical properties, and incorporate a single, modular targeting functionality. As a consequence of their monovalency, they do not perturb the diffusion of biomolecules in model membranes or live cells. The facile preparation of these small, bright, monovalent, and modular imaging probes make them accessible to any researcher with basic molecular biology tools and reagents. Therefore mQDs should find broad utility in biophysical and cell biological studies requiring single molecule imaging, either *in vitro* or in live cells.

3.7 References

¹ Pons, T., Medintz, I. L., Wang, X., English, D. S., & Mattoussi, H. (2006). Solution-phase single quantum dot fluorescence resonance energy transfer. *Journal of the American Chemical Society*, *128*(47), 15324–15331. doi:10.1021/ja0657253

-
- ² Kadane, J. B., Borle, S., & Boatwright, P. (2005). A useful distribution for fitting discrete data: revival of the Conway–Maxwell–Poisson distribution. *Journal of the Royal*
- ³ Saxton, M. J., & Jacobson, K. (1997). Single-particle tracking: applications to membrane dynamics. *Annual Review of Biophysics and Biomolecular Structure*, 26(1), 373–399. doi:10.1146/annurev.biophys.26.1.373
- ⁴ Banerjee, D., Liu, A. P., Voss, N. R., Schmid, S. L., & Finn, M. G. (2010). Multivalent display and receptor-mediated endocytosis of transferrin on virus-like particles. *Chembiochem : a European Journal of Chemical Biology*, 11(9), 1273–1279. doi:10.1002/cbic.201000125
- ⁵ Saxton, M. J., & Jacobson, K. (1997). Single-particle tracking: applications to membrane dynamics. *Annual Review of Biophysics and Biomolecular Structure*, 26(1), 373–399. doi:10.1146/annurev.biophys.26.1.373
- ⁶ Clarke, S., Pinaud, F., Beutel, O., You, C., Piehler, J., & Dahan, M. (2010). Covalent monofunctionalization of peptide-coated quantum dots for single-molecule assays. *Nano Letters*, 10(6), 2147–2154. doi:10.1021/nl100825n
- ⁷ Carstairs, H. M. J., Lympelopoulou, K., Kapanidis, A. N., Bath, J., & Turberfield, A. J. (2009). DNA monofunctionalization of quantum dots. *Chembiochem : a European Journal of Chemical Biology*, 10(11), 1781–1783. doi:10.1002/cbic.200900300
- ⁸ You, C., Wilmes, S., Richter, C. P., Beutel, O., Liße, D., & Piehler, J. (2013). Electrostatically controlled quantum dot monofunctionalization for interrogating the dynamics of protein complexes in living cells. *ACS Chemical Biology*, 8(2), 320–326. doi:10.1021/cb300543t
- ⁹ Tikhomirov, G., Hoogland, S., Lee, P. E., Fischer, A., Sargent, E. H., & Kelley, S. O. (2011). DNA-based programming of quantum dot valency, self-assembly and luminescence. *Nature Nanotechnology*, 6(8), 485–490. doi:10.1038/nnano.2011.100
- ¹⁰ Jiang, L., Yang, B. Q., Ma, Y. D., Liu, Y. C., Yang, W. S., & Li, T. J. (2003). The binding of phosphorothioate oligonucleotides to CdS nanoparticles. *Chemical Physics*
- ¹¹ Claridge, S. A., Liang, H. W., Basu, S. R., & Fréchet, J. (2008). Isolation of Discrete Nanoparticle–DNA Conjugates for Plasmonic Applications. *Nano*

-
- ¹² Wilson, J. J., & Kovall, R. A. (2006). Crystal structure of the CSL-Notch-Mastermind ternary complex bound to DNA. *Cell*, *124*(5), 985–996. doi:10.1016/j.cell.2006.01.035
- ¹³ Montenegro, J.-M., Grazu, V., Sukhanova, A., Agarwal, S., la Fuente, de, J. M., Nabiev, I., et al. (2013). Controlled antibody/(bio-) conjugation of inorganic nanoparticles for targeted delivery. *Advanced Drug Delivery Reviews*, *65*(5), 677–688. doi:10.1016/j.addr.2012.12.003
- ¹⁴ Bray, S. J. (2006). Notch signalling: a simple pathway becomes complex. *Nature Reviews Molecular Cell Biology*.
- ¹⁵ Gordon, W. R., Roy, M., Vardar-Ulu, D., Garfinkel, M., Mansour, M. R., Aster, J. C., & Blacklow, S. C. (2009). Structure of the Notch1-negative regulatory region: implications for normal activation and pathogenic signaling in T-ALL. *Blood*, *113*(18), 4381–4390. doi:10.1182/blood-2008-08-174748
- ¹⁶ Douglass, A. D., & Vale, R. D. (2005). Single-molecule microscopy reveals plasma membrane microdomains created by protein-protein networks that exclude or trap signaling molecules in T cells. *Cell*.
- ¹⁷ Triantafilou, M., Morath, S., Mackie, A., & Hartung, T. (2004). Lateral diffusion of Toll-like receptors reveals that they are transiently confined within lipid rafts on the plasma membrane. *Journal of Cell*
- ¹⁸ Cairo, C. W., Das, R., Albohy, A., & Baca, Q. J. (2010). Dynamic regulation of CD45 lateral mobility by the spectrin-ankyrin cytoskeleton of T cells. *Journal of Biological*

Multicellular Interactions

Here separate projects assembled with different goals, but either utilizing similar concepts or similar tools to achieve those goals are brought together. Part of my work has been in the support of a laboratory rather than in pursuit of an individual project, and in that effort I have contributed to my labmates' success and grown in those collaborations. In collaboration with Jennifer Liu, I helped quantify and analyze some of the emergent behaviors she was able to elicit from a heterogeneous microtissue consisting of nominally 'healthy' human epithelial cells brought into proximity with a 'cancerous', Ras-over-expressing cell. Here I reproduce with modification the portion of that work to which I had significant contribution.

In collaboration with Sam Liang, Kyle Broaders & Michael Todhunter, we brought together a number of the tools, experience and expertise to evaluate the capability of building a synthetic platform to mimic what we believed to be a mechanism by which microtissues might sense or send communication regarding their local microenvironment. Though the techniques themselves worked quite well together, no significant biological results were obtained. The pleasant success of the integrating of these multiple experimental techniques into a tractable synthetic system, however, necessitates their recording.

Finally, in working with a number of others, a theme emerged of image-analysis, object identification, and subsequent mathematical analysis. I put together a number of small, but significant Mathematica scripts to help others quantify and process their microscope imagery into statistical or at least actionable data. Here I very briefly give an overview of those scripts and their associated code.

4.1 Emergent Behaviors in Communicative Microtissues

Variability in signaling pathway activation between neighboring epithelial cells can arise from local differences in microenvironment, noisy gene expression, or acquired genetic changes. To investigate the consequences of this cell-to-cell variability in signaling pathway activation on coordinated multicellular processes such as morphogenesis, we use DNA-programmed assembly to construct three-dimensional MCF10A microtissues that are mosaic for low-level expression of activated H-Ras. We find two emergent behaviors in mosaic microtissues: cells with activated H-Ras are basally extruded or lead motile multicellular protrusions that direct the collective motility of their wild-type (WT) neighbors. Remarkably, these behaviors are not observed in homogeneous microtissues where all cells expressed the activated Ras protein, indicating that heterogeneity in Ras activity, rather than the total amount of Ras activity, is critical for these processes. Our results directly demonstrate that cell-to-cell variability in pathway activation within local populations of epithelial cells can drive emergent behaviors during epithelial morphogenesis.

4.1.1 Variable Ras activation as a trigger for cell-to-cell variability in epithelial microtissues

The behavior of an epithelial cell is strongly influenced by signals from the microenvironment. Many of these signals activate pathways downstream of the small GTPase Ras that affect behaviors including cell motility, survival, and proliferation. However, neighboring epithelial cells in the same tissue may differ substantially in their levels of Ras pathway activation as a consequence of local fluctuations in the microenvironment, stochastic events, or acquired genetic and epigenetic changes. The resulting cell-to-cell variability may lie dormant or trigger regulatory pathways that act at the level of cell communities to direct collective cell behaviors¹, remove cellular defects from a tissue^{2 3}, or drive malignancy^{4 5 6}.

In vitro culture of epithelial cells can facilitate the study of cell-to-cell variability by providing tight control of the cellular microenvironment. However, three-dimensional culture (3D) in

laminin-rich extracellular matrix (lrECM) is required to reveal the consequences of cell-to-cell variability on collective cell behaviors such as epithelial morphogenesis. Under these 3D culture conditions, single MCF10A breast epithelial cells proliferate to form polarized microtissues that ultimately growth-arrest as multicellular acini. These small tissues recapitulate important structural and functional features of the organ from which they were derived⁷ and even exhibit cell-to-cell variability in the activation level of kinases downstream of Ras, such as Akt, Erk and MLCK^{8 9 10}. Unfortunately, directly analyzing the consequences of such cell-to-cell variability in Ras pathway activation within 3D cultured tissues is challenging, due in part to the difficulty of efficiently and selectively altering this signaling node in specific cells, within a growing microtissue, with both high temporal and spatial precision.

4.1.2 Development of reproducible 3D epithelial microtissues using chemically programmed assembly

Several methods are suitable for preparing tissues mosaic for activated proteins such as Ras. Optogenetic techniques offer exceptional precision but are generally low throughput and require significant engineering of the protein or process of interest.¹¹ Currently, the best general solutions involve mixing two or more cell populations¹² or infection of tissues by low titer virus¹³. However, the resulting mosaic tissues span a distribution of compositions, where only a fraction of the microtissues possess the desired numbers of each cell type for subsequent analysis. These configurational inconsistencies complicate the quantification of rare events and processes that occur rapidly upon the initiation of cell-cell interactions. We therefore sought an alternative method for preparing epithelial microtissues mosaic for H-Ras activity that provides additional control over initial aggregate composition and cell-to-cell connectivity, thereby facilitating quantitative analysis and increasing the time resolution of experiments involving dynamic cellular interactions during the early stages of epithelial morphogenesis.

Here, we report DNA-programmed assembly as a new approach for building mosaic epithelial microtissues with defined cell-to-cell variability for 3D culture. We demonstrate that cell

aggregates of wild-type (WT) MCF10A epithelial cells prepared by programmed assembly rapidly condense into polarized microtissues in 3D culture (**Figure 4.1**). We then use this method to analyze interactions between neighboring cells with subtle differences in Ras activation during the early stages of morphogenesis. We find that while low-level and chronic activation of H-Ras is insufficient to disrupt morphogenesis in microtissues homogeneously expressing a constitutively active form of the gene, the same level of Ras activation in only subsets of cells leads to the emergence of distinct phenotypes specifically in mosaic microtissues. Our results directly demonstrate that slight biochemical or genetic differences between neighboring cells can give rise to unique and emergent behaviors in epithelial tissues.

4.1.3 Observation of emergent behaviors in heterogeneous microtissues

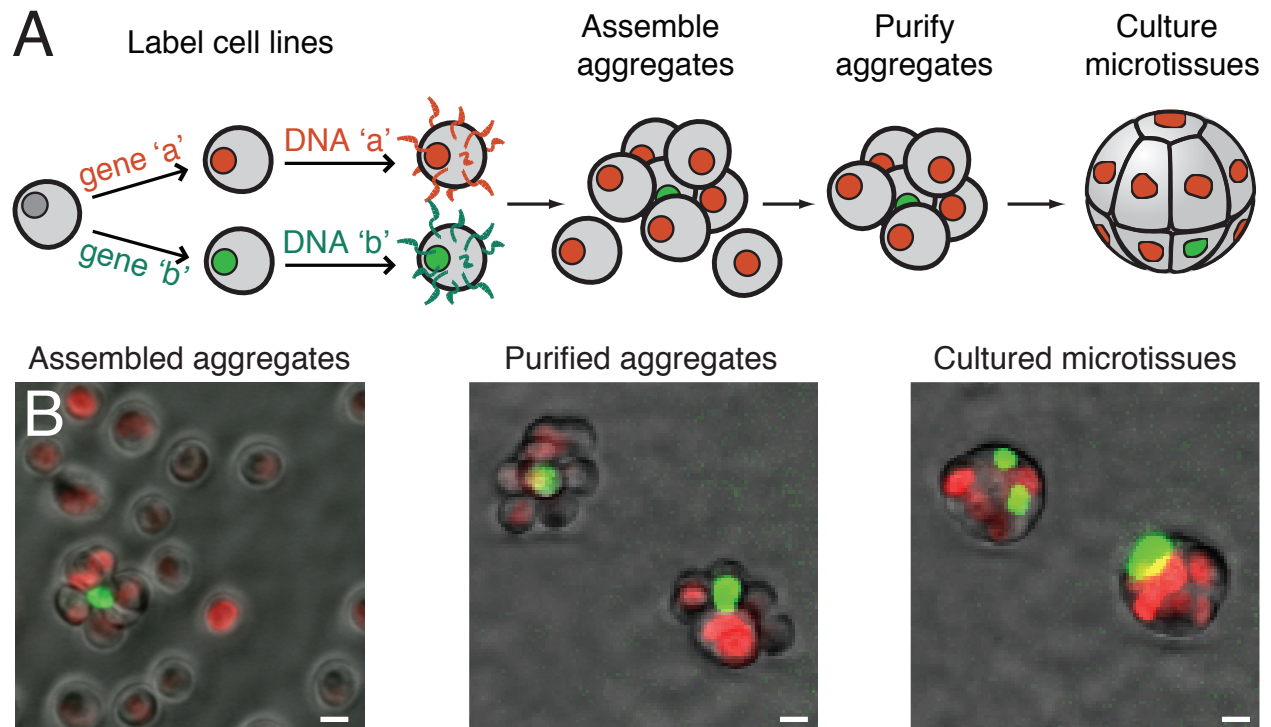


FIGURE 4.1: PROGRAMMED ASSEMBLY OF MOSAIC EPITHELIAL AGGREGATES

(a) Scheme for chemically programmed assembly. (b) Microscopy of cells after assembly, after being purified by FACS, and then after being cultured 8.5 hr in IrECM.

Using programmed assembly, we prepared mosaic aggregates comprising a single MCF10A^{Ras} cell surrounded by WT cells. While homogeneous aggregates of MCF10A^{Ras} cells were phenotypically similar to WT aggregates with respect to polarity and morphology over 24 hours, we unexpectedly observed emergent phenotypes in heterogeneous microtissues. In some cases, multicellular protrusions tipped by a single, motile MCF10A^{Ras} cell seemed to direct the motion of the surrounding WT microtissue across the IrECM over several hours (**Figure 4.2**).

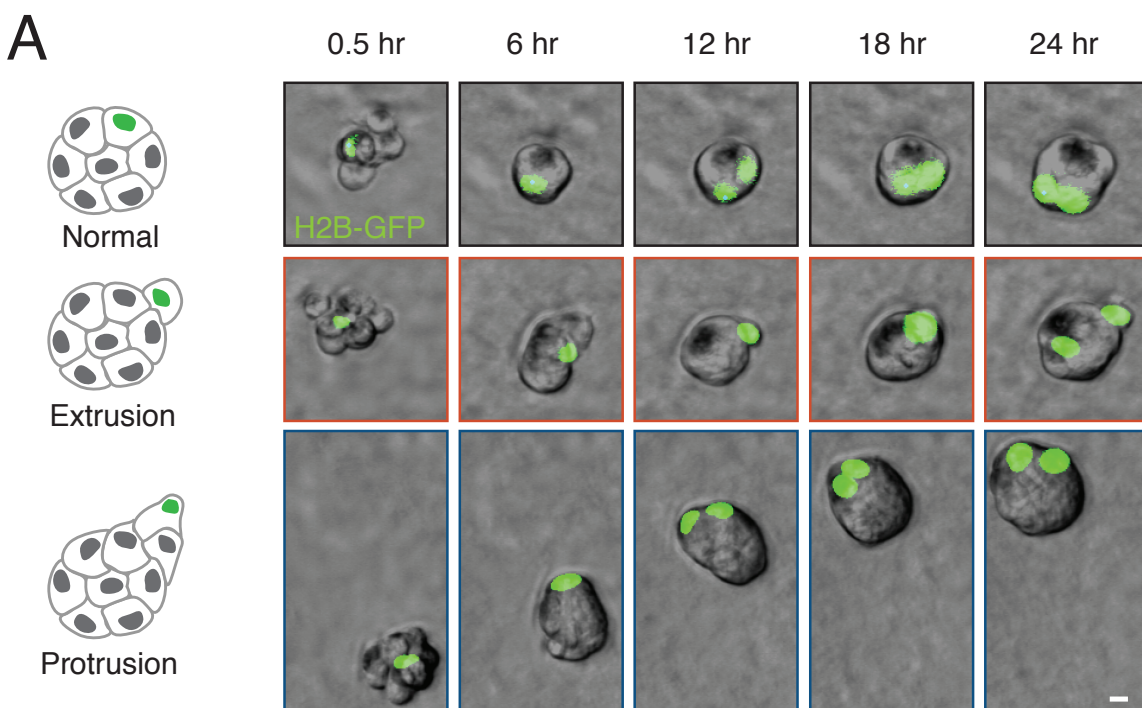


FIGURE 4.2: EXAMPLES OF BEHAVIORS EXHIBITED BY MICROTISSUES OF MAMMARY EPITHELIAL CELLS

Representative time-lapse images showing normal and emergent phenotypes in the mosaic MCF10A^{Ras}/MCF10A^{WT} microtissues (green/colorless respectively).

Multicellular protrusions occurred in 20-30% of the mosaic microtissues. In an additional 20-30% of mosaic aggregates, we observed cell extrusion where the single MCF10A^{Ras} cell exited at the basal surface but remained loosely associated with the microtissue. Significantly, the multicellular protrusion and basal extrusion phenotypes were rarely observed for single

MCF10A^{Ras} cells grown within homogeneous MCF10A^{Ras} microtissues. Additionally, in 4-6% of the mosaic aggregates, the MCF10A^{Ras} cell was highly motile and broke away from the surrounding WT microtissue, occasionally traversing over 100 μm .

4.1.4 Quantitation of observed emergent behaviors in heterogeneous microtissues

To further characterize the emergent behaviors resulting from heterogeneous Ras activity between cells during MCF10A morphogenesis, we tracked the positions of individual MCF10A^{WT} or MCF10A^{Ras} cells in microtissues over 24 hours. MCF10A^{WT} and MCF10A^{Ras} cells did not differ significantly in maximum displacement from their initial positions when grown within homogeneous microtissues containing only cells of the same type (Figure 5A and 5B). This is consistent with the qualitative observation that homogeneous microtissues have a normal morphology over this time period. In contrast, the maximum displacement of single MCF10A^{Ras} cells in heterogeneous aggregates with surrounding WT cells was increased relative to the same cells in homogeneous MCF10A^{Ras} aggregates (Figure 5A and 5B) without a significant increase in average speed (Figure 5C).

The increase in mean displacement of MCF10A^{Ras} cells when grown among MCF10A^{WT} cells was almost entirely attributable to microtissues with the multicellular protrusion phenotype (Figure 5D); when MCF10A^{Ras} cell tracks were segregated into normal, extruding, and protruding phenotypes, we found average displacements (\pm 95% CI) of 26 (\pm 3), 31 (\pm 5), and 61 (\pm 9) μm , respectively. While the displacement of MCF10A^{Ras} cells in normal and extruding microtissues typically remained within the average diameter of heterogeneous microtissues (43.7 ± 8.47 μm , average diameter of 50 microtissues after 24 hours), the displacement of protruding cells generally exceeded the size of microtissues, sometimes significantly.

To quantify the extent to which single, protruding MCF10A^{Ras} cells affected the motility of the surrounding WT microtissue, we compared the trajectories of the MCF10A^{Ras} cell to the

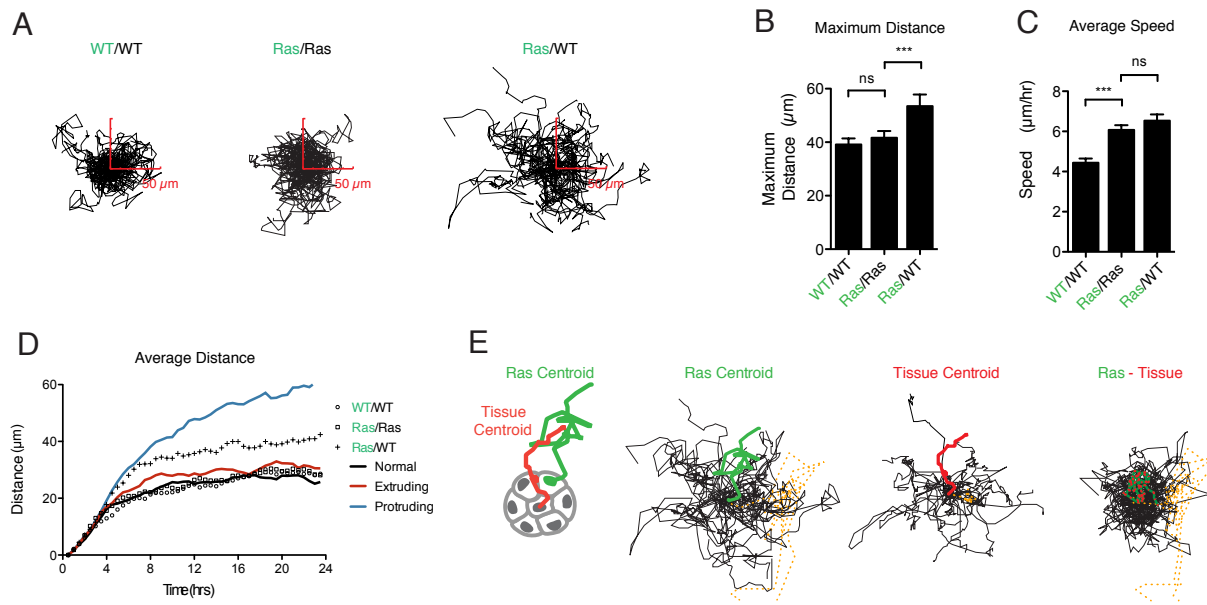


FIGURE 4.3: QUANTITATIVE ANALYSIS OF CELL MOTILITY DURING EMERGENT BEHAVIORS

(A) Representative 30 superimposed 24 hr trajectories for cells expressing H2B-GFP growing in homogeneous and heterogeneous microtissues. (B) Average maximum distance traveled and (C) speed of the H2B-GFP-expressing cell. (D) Average distance traveled as a function of time for H2B-GFP-expressing cell. (E) Trajectories of H2B-GFP-expressing MCF10A^{Ras} cells and the centroid surrounding the tissue. Subtracting the Ras centroid from the tissue centroid results in the final, collapsed, trajectories. A representative MCF10A^{Ras} cell (green), associated microtissue (red), and residual trajectory (hatched green and red) are highlighted. Trajectory of a hypermotile cell leaves a large residual (dashed orange lines).

trajectories of the overall microtissue. Overall, the trajectories for single MCF10A^{Ras} cells and the surrounding WT microtissues were correlated for all three phenotypes (Figure 4.3).

Interestingly, the large displacements observed for single MCF10A^{Ras} cells participating in motile multicellular protrusions were also observed for their associated WT microtissues, indicating that the single MCF10A^{Ras} cell does indeed direct the motion of the entire microtissue. Moreover, subtracting the coordinates of the microtissue centroid from the coordinates of the protruding MCF10A^{Ras} cell generated residual trajectories (Figure 4.3E) that were qualitatively similar to those of single cells in homogeneous MCF10A^{Ras} and WT microtissues (Figure 4.3A). This analysis occasionally revealed residual trajectories with large

total displacements, which always corresponded to the rare, hypermotile cells (**Figure 4.3E**, dashed orange track).

4.1.5 Conclusion

In conclusion, we have used a chemical programmed assembly strategy to directly probe the consequences of cell-to-cell variability in Ras activation during the morphogenesis of MCF10A mammary epithelial cells in 3D culture. We find several emergent behaviors that occur as a consequence of modest differences in Ras activation between neighboring cells, rather than due to the absolute levels of Ras activation in the microtissue. Remarkably, the microtissues exhibiting the most unusual behaviors, (including basal cell extrusions, motile multicellular protrusions, and hypermotile invasive cell) actually had lower total levels of activated Ras across the cell population than homogeneous MCF10A^{Ras} microtissues that only rarely manifested these phenotypes. Our results demonstrate that heterogeneity in pathway activation between neighboring cells is sufficient to drive emergent behaviors at the population level and highlight the need to control for the identity of surrounding cells when studying the effect of genetic, physical or chemical perturbations applied at the single cell level. More importantly, our results suggest that the regulation of cell-to-cell variability in Ras activation, particularly in developmental contexts, is important for controlling the global behavior of a tissue.

4.2 Synthetically programmed Polarization

Many of the protein domains used to enable analysis of the biological systems identified for basic scientific study were robust enough to be used in isolation, on their own, in synthetic systems aimed at better understanding biological principles without regard to a particular, identifiable biological mechanism. In cooperation with my labmates who were each working on different, but technologically bridgeable projects, we came together to use our ‘scrap materials’ in designing a synthetic platform for creating and evaluating the interface between a cell and another cell or a surface. The extracellular SNAP tag enabled conjugation of the expressed protein to a single strand of targetable DNA. The SNAP tag would cross the membrane via a generic transmembrane domain.

Our hypothesis was that by using as a scaffold the intracellular portion of our synthetic molecule with various biologically functional intracellular domains, we could affect the signaling of the cell upon clustering of the ICDs by means of a cell-cell or cell-surface interaction.

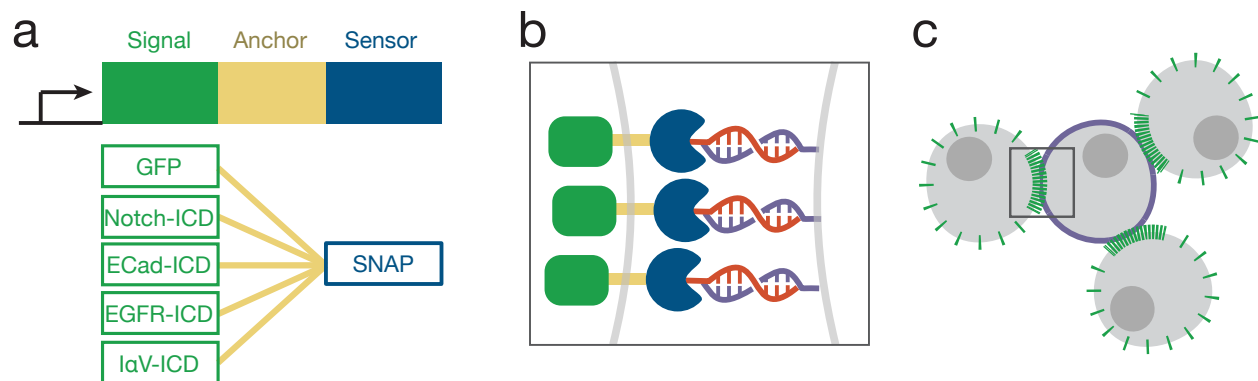


FIGURE 4.4 SCHEMATIC OF A SYNTHETIC ADHESION COMPLEX

(a) Schematic of the synthetic adhesion proteins created - each consisting of a signal, anchor and sensor domain. (b) Illustration showing how cells expressing the synthetic adhesions protein bind to cells displaying ssDNA via hybridization after being exposed to BG-DNA. (c) Zoomed out view of (b) demonstrating the formation of a high-density ‘synapse’ at the junction between two cells formed by the synthetic adhesion proteins.

To this end we produced a number of clones containing an extracellular SNAP tag and a variety of intracellular domains tagged with GFP: Integrin α -V-ICD, EGFR-ICD, Notch1-ICD & E-Cadherin-ICD (**Figure 4.4**). We were successfully able to clone EGFR, Notch1, and integrin α -V Intracellular domains into our scaffolding.

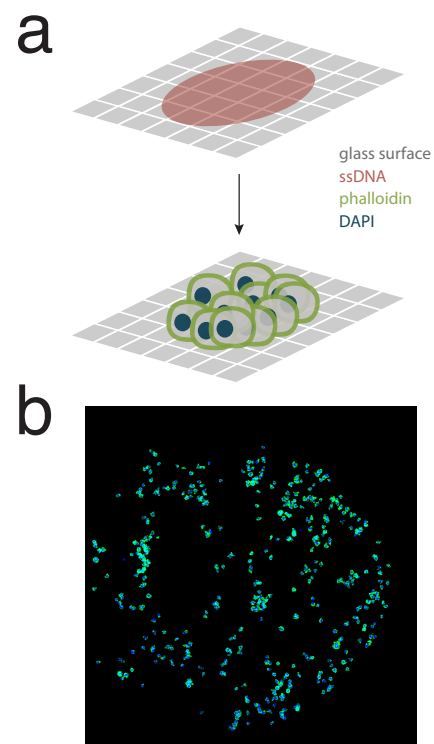
Constructs were transfected into cell lines prior to experimentation, treated with BG-DNA for 25 min at 37 °C, and allowed to hybridize with their complement.

4.2.1 Surface adhesion of cells via a synthetic protein via a DNA-mediated linkage

To determine if the SNAP tagged constructs were capable producing adhesive properties, cover slips were functionalized with DNA by first coating with an aldehyde-containing silane. Reductive amination with amine-functionalized DNA followed by hydrophobic passivation yielded usable surfaces onto which cells could be assembled. TM-GFP expressing Jurkat cells were incubated with BG-T₄₀(CAGT)₅ for 15 min at 37 °C then introduced onto the functionalized cover glass through a PDMS flow cell at 10⁶ cells / mL. After waiting 5 min, unbound cells were washed away using PBS through the flow cell. Confocal microscopy revealed efficient adhesion of cells onto a millimeter-sized spot of DNA (**Figure 4.5**).

FIGURE 4.5: ADHESION OF JURKAT CELLS TO A SURFACE BY HYBRIDIZATION TO A SYNTHETIC ADHESION PROTEIN

A glass surface treated with ssDNA is exposed to cells displaying the complementary strand of DNA off of its synthetic adhesion protein (**a**). After washing, tiled microscopy of the glass shows cells remaining only in regions containing the surface-bound DNA (**b**).



4.2.2 Cell-cell mediated adhesion enriches junctions with the synthetic adhesion protein

While performing the prior experiments, it was noticed that the BG-GFP protein concentrated at points of contact with both cells and surfaces. To investigate the clustering of proteins at a cell-cell junction we mixed two cells together in solution to enable clusters to form. Jurkat cells expressing TM-GFP were labeled with BG-CAGT DNA, while standard Jurkat cells were labeled with lipid-ACTG DNA. The two cells were mixed at a 1:25 ratio respectively, spun into a pellet, plated on a coverslip, and covered in an immobilizing (low-melt) agarose gel. The cell clusters were then stained for actin with AF647-phalloidin and then imaged using confocal microscopy (**Figure 4.5**).

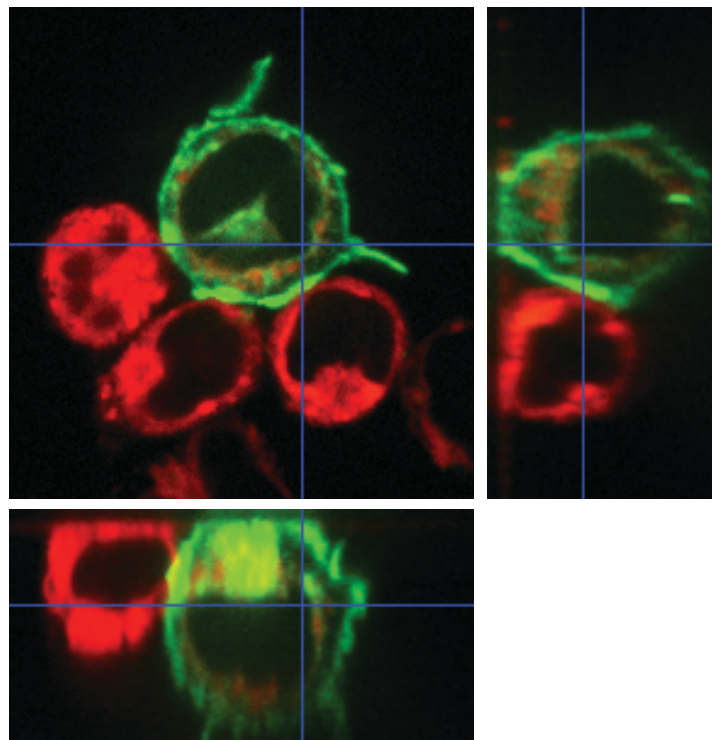


FIGURE 4.6: CONFOCAL SECTIONING OF A HETEROGENEOUS CLUSTER OF CELLS ADHERED BY THE SYNTHETIC ADHESION PROTEIN

Slight enrichment of GFP can be seen at points of intersection between the adhesion-protein expressing cell (green) and the lipid-dna-displaying cells (not-green). Red is phalloidin staining of the actin cytoskeleton.

4.2.3 Attempt to activate a synthetic EGFR-like receptor via clustering at cell-cell junctions

The EGF Receptor is a natural receptor that is activated upon clustering of the protein. In an effort to build a synthetic receptor that responded to clustering we took our synthetic receptor scaffolding and inserted the EGF intracellular domain between the transmembrane domain and GFP. CHO cells expressing this construct were incubated with BG-DNA and then briefly brought into contact with cells displaying the lipid-DNA complementary to the BG-DNA, and stained with cell-tracker dyes. The cells were let incubate for 5 minutes, spun down, and then fixed, permeabilized, and embedded under an agarose gel on a coverslip. These cells were then immunostained with an anti-phospho-EGFR antibody in order to detect the phosphorylation of the intracellular domain of our construct. Hypothetically, only in the case were the cells brought into contact with cells capable of clustering the receptor would the receptor be phosphorylated. In the absence of cells displaying the complement, or displaying a non-complementary strand, or those cells expressing the receptor brought in contact with other cells *not* by means of the receptor, the receptor should not have been phosphorylated. However, when imaged by confocal microscopy the signal to noise of the anti-phosph-EGFR immunostaining was low, thus preventing strong conclusions about the relative amounts or location of the phosphorylated receptor upon exposure to cells displaying the activating ligand (complementary DNA).

4.2.4 SENSYR - a synthetic protein sensor based on the Notch regulatory region

The Notch receptor is a natural receptor that is activated upon the contact between the receptor and its surface-bound ligand. In an effort to build a synthetic receptor that could send an arbitrary signal to a mammalian system based upon contact with a synthetic ligand we built SENSYR - a Specific, Engineered Notch as a Synthetic Receptor. More accurately, we built a BG-SENSYR and an EGFR-SENSYR. The BG-SENSYR consists of a SNAP tag fused to the notch regulatory region, through the Notch transmembrane region, with the NICD replaced by a nuclear localized Gal4. The EGFR-SENSYR is similarly built upon the NRR-Gal4 construct, but

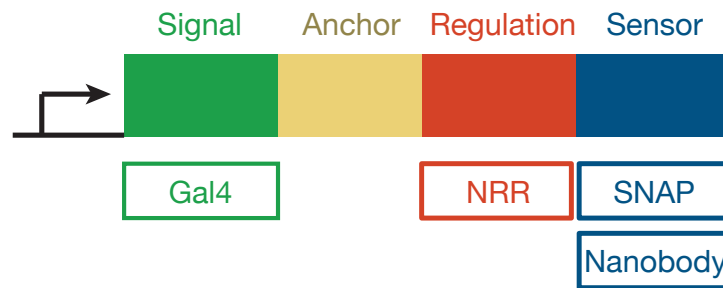


FIGURE 4.7: GENETIC SCHEMATIC OF SENSYR

Fusion of various domains comprising the SENSYR: a signal, anchor, regulatory & sensor domains.

with an EGFR-nanobody fused to its N-terminus instead of a SNAP tag (**Figure 4.6**).

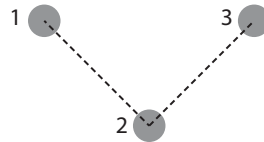
Unfortunately none of these constructs were successfully cloned into mammalian vectors by the time of graduation and so could not be tested.

4.2.5 Conclusion

In conclusion, we developed a protein scaffolding capable of adhering cells to surfaces and to other cell by a specific, synthetic protein. In an effort to confer a biological signaling capability to the adhesion, we added intracellular signaling domains to our protein scaffold. The tools we chose to sense an output for the clustering of these synthetic signaling platforms did not have the resolution to determine whether we were able to cause a biological signalling event by means of clustering cells using the synthetic proteins. We planned to further create a force sensor (SENSYR) as opposed to a clustering-sensor by adding the Notch Regulatory Region to the extracellular domain of the scaffold. These constructs were cloned but were never put into a mammalian expression system.

4.3 Statistical Spatial Analysis

A common theme encountered throughout my research was the need for quantitative analysis of the spatial distribution of various features obtained with various imaging techniques. My own projects dealt with quantifying the spatial distribution of particular receptor or cell trajectories in time. However other projects in the Gartner lab requiring similar analyses were able to benefit from the lessons learned. Specifically four different circumstances required a very similar quantitation: 1) quantitation of the distances between scaffolded proteins imaged by electron microscopy, 2) quantitation of the intensity of a reporter on a particular fluorescent bead, 3) quantitation of the number of ‘non-activated’ partners of an ER-positive cell within a specified distance, and 4) quantitation of the ‘spatial error’ introduced into a high-precision 3D culture system when transferred off of a surface and into a gel.



ID	x	y	z	t	Intensity	Distance (1)	Distance (2)	Distance (3)	...
1									
2									
3									
...									

FIGURE 4.8: GENERAL FORMAT OF OBSERVED & CALCULATED DATA USED FOR SPATIAL ANALYSIS

4.3.1 Evaluating the uniformity of nucleic-acid scaffolding between proteins

Sam Liang, in the Gartner lab, successfully linked various DNA-conjugated proteins with various scaffolding strands.¹⁴ In order to verify the geometry of the scaffolding she imaged her conjugations using electron microscopy. In an effort to quantify the uniformity of her

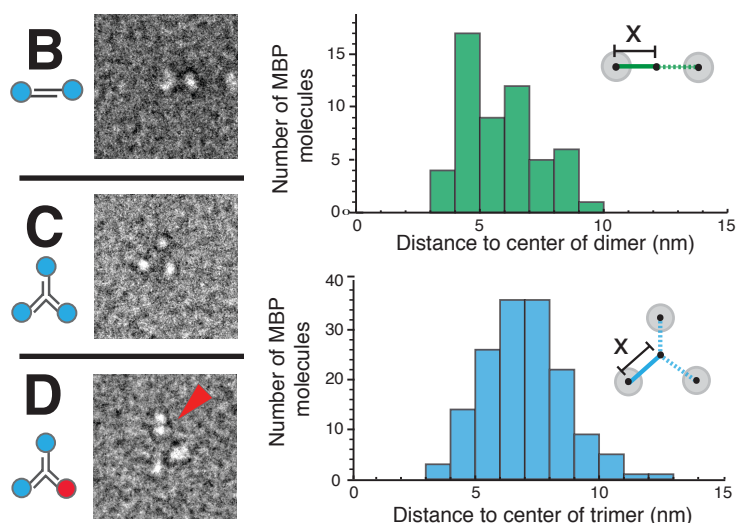


FIGURE 4.9: QUANTITATIVE ANALYSIS OF THE DISTRIBUTION OF DISTANCES BETWEEN PROTEINS IN SCAFFOLDED COMPLEXES

scaffolded constructs we used image-processing to identify the centroids of each protein. From these centroids we calculated the mean distances between them. Specifically in the case of a trimer, we calculated the mean distance between each centroid and the ‘center of mass’ of the trimer. This calculation not only enabled a measurement of the average distance of separation between the protein domains provided by the DNA-scaffolding, but also enabled a quantification of the flexibility, or geometric distribution, of the scaffolding.

4.3.2 Measuring the intensity of a fluorescent reporter at the surface of a bead

Julia Rumpf, in the Taunton lab, designed a kinase reporter assay using fluorescent beads that would fluoresce in a separate channel upon activation. Though able to image this assay, quantitation of the collected images required careful alignment, selection, and determination of background for each separable bead. This proved tedious and difficult to do by hand for the amounts of data required to obtain a quantitative perspective from this assay. Using the image

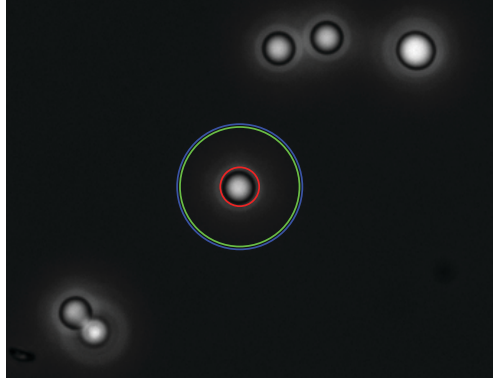


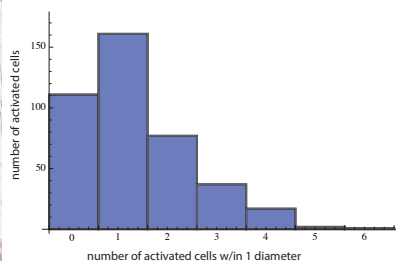
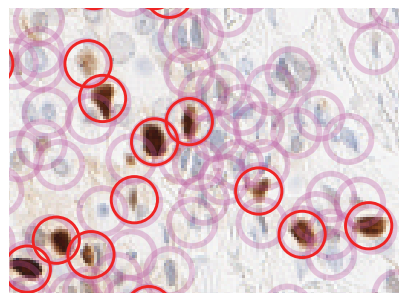
FIGURE 4.10: COMPUTATIONALLY DEFINED RINGS OUTLINING A BEAD AND ITS LOCAL BACKGROUND USED TO MEASURE INTENSITY VALUES

processing capabilities of Mathematica, we developed a script that would, in an automated fashion, detect the fluorescent beads, isolate isolatable particles, align them with the second channel, and then quantify both the signal and background for each of these isolated objects. From this data we could rapidly and quantitatively determine the relative signal intensity produced during a given assay. By processing the images in an automated way we were able to more efficiently collect and analyze these data.

4.3.3 Quantifying spatial distribution of ER-active cells in mammary tissue

Rob Webber, in the Gartner Lab, is interested in how a structured tissue like the mammary gland is able to maintain a particularized heterogeneity, for example, in the expression of estrogen-receptor-positive cells. Literature reports suggest ~20% of epithelial cells in normal human mammary tissue are ER-positive. In order to quantify not only the proportion of cells that are ER-positive, but also their spatial distribution relative to one another, we chose to quantify the distribution of ER-stained cells in a histology section. We again used the image processing capabilities of Mathematica to isolate all nuclei in the histology section, and all ER-positive nuclei in the histology section. We were then able to ask quantitative questions of these cells such as the average distance between two ER-positive cells, the number of ER-positive neighbors an ER-negative cell has, and the number of ER-positive neighbors an ER-

positive cell has. With very large histology sections we can produce statistical inferences using this software to test hypotheses regarding the spatial



distribution of ER-positive cells.

4.3.4 Determining the 'spatial error' introduced during the gel transfer step of Chemically Programmed Assembly

Michael Todhunter & Noel Jee, in the Gartner Lab, established a technique for the high-

FIGURE 4.11: THE CENTROIDS ER-POSITIVE AND ER-NEGATIVE CELLS, AND QUANTITATION OF THE NUMBER OF POSITIVE CELLS WITHIN 1 CELL DIAMETER

precision transfer of cells from a surface into a gel.¹⁵ In order to quantify the accuracy of this technique they required a means of monitoring the difference in placement prior to, and then after the gel-transfer. We were able to determine the centroids of each cell before and after the

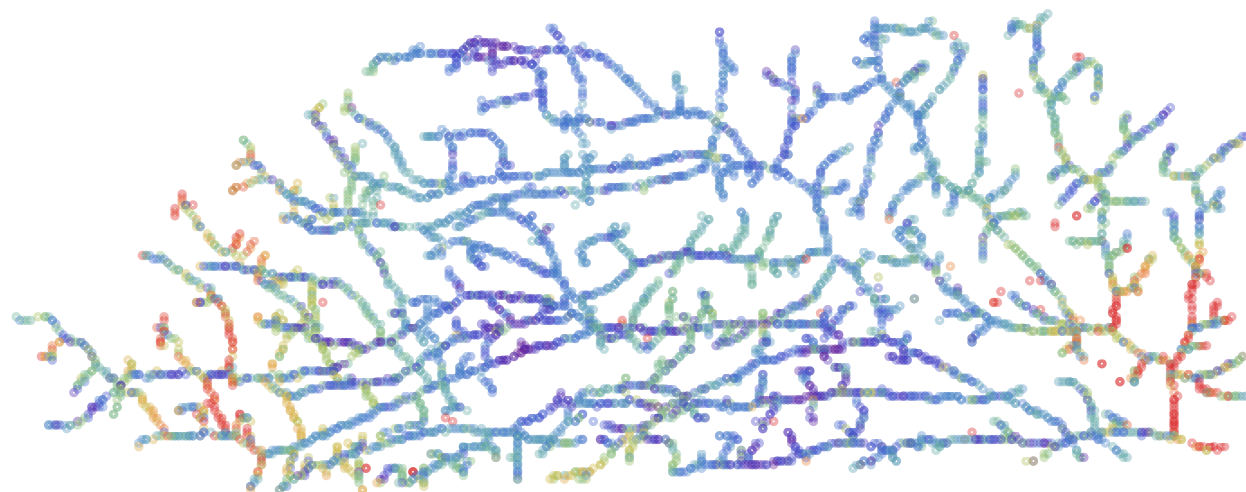


FIGURE 4.12: HEATMAP SHOWING DISTANCE BETWEEN A CELL BEFORE & AFTER LIFTING INTO A GEL

transfer step, and then calculate the cross-wise distance between its old and new position. We were also able to calculate these differences with respect to various anchor points. After

evaluating a number of different ways to represent the accuracy of the transfer, we found a representation wherein the average change in distance between any given cell and its known neighbors provided a clear way to communicate the accuracy of this gel-transfer step.

4.5 References

-
- ¹ Vitorino, P., & Meyer, T. (2008). Modular control of endothelial sheet migration. *Genes & Development*.
- ² Eisenhoffer, G. T., Loftus, P. D., Yoshigi, M., & Otsuna, H. (2012). Crowding induces live cell extrusion to maintain homeostatic cell numbers in epithelia. *Nature*.
- ³ Takemura, M., & Yamada, T. A. (2011). Repair responses to abnormalities in morphogen activity gradient. *Development (Cambridge, England)*.
- ⁴ Hogan, C., Dupré-Crochet, S., Norman, M., & Kajita, M. (2009). Characterization of the interface between normal and transformed epithelial cells. *Nature Cell ...*
- ⁵ Leung, C. T., & Brugge, J. S. (2012). Outgrowth of single oncogene-expressing cells from suppressive epithelial environments. *Nature*.
- ⁶ Marusyk, A., Almendro, V., & Polyak, K. (2012). Intra-tumour heterogeneity: a looking glass for cancer? *Nature Reviews Cancer*.
- ⁷ Streuli, C. H., Bailey, N., & Bissell, M. J. (1991). Control of mammary epithelial differentiation: basement membrane induces tissue-specific gene expression in the absence of cell-cell interaction and morphological *The Journal of Cell Biology*.
- ⁸ Debnath, J., Mills, K. R., Collins, N. L., & Reginato, M. J. (2002). The role of apoptosis in creating and maintaining luminal space within normal and oncogene-expressing mammary acini. *Cell*.
- ⁹ Pearson, G. W., & Hunter, T. (2009). PI-3 kinase activity is necessary for ERK1/2-induced disruption of mammary epithelial architecture. *Breast Cancer Res*.
- ¹⁰ Yuan, T. L., Wulf, G., Burga, L., & Cantley, L. C. (2011). Cell-to-cell variability in PI3K protein level regulates PI3K-AKT pathway activity in cell populations. *Current Biology*.

¹¹ Wang, X., He, L., Wu, Y. I., Hahn, K. M., & Montell, D. J. (2010). Light-mediated activation reveals a key role for Rac in collective guidance of cell movement in vivo. *Nature Cell Biology*.

¹² Mori, H., Gjorevski, N., & Inman, J. L. (2009). Self-organization of engineered epithelial tubules by differential cellular motility. Presented at the Proceedings of the

¹³ Lu, P., Ewald, A. J., Martin, G. R., & Werb, Z. (2008). Genetic mosaic analysis reveals FGF receptor 2 function in terminal end buds during mammary gland branching morphogenesis. *Developmental Biology*.

¹⁴ Liang, S. I., McFarland, J. M., Rabuka, D., & Gartner, Z. J. (2014). A modular approach for assembling aldehyde-tagged proteins on DNA scaffolds. *Journal of the American Chemical Society*, 136(31), 10850–10853. doi:10.1021/ja504711n

¹⁵ Todhunter ME, Jee NY, Cerchiari A, Hughes AJ, Farlow J, Garbe JC, LaBarge MA, Desai TA, Gartner ZJ. "Rapid Synthesis of 3D Tissues by Chemically Programmed Assembly." (submitted 2014)

Software

The ImageJ¹ plugin, Trackmate², successfully identifies and links tracks and even has a reasonable mechanism for curation of the tracks, however it is extraordinarily CPU and memory intensive. From image to track data can take 10 minutes or more and often failed when presented with large images, many images, or images with many tracks. For these reasons it was not useful to me, however it is under current development and is worth revisiting in the future.

The particle tracking software written by Crocker, Spalding & Losert, and given a GUI by Ryan Smith, called RyTrack³ is written in the much more efficient, IDL, a Fortran derivative. It can process a stack of images as quickly as they can be read to memory. It however has two major drawbacks - it is written for a very particular coding environment and so is not portable, and it only is capable of the first two steps required to analyze the particles, identification and track-formation. Its output is a CSV file containing uncurated, but fairly well-discovered tracks.

In order to process the data that is found in either Trackmate or RyTrack, I wrote a number of scripts in Mathematica to help me visualize and calculate properties of the tracked particles. However I quickly realized that such scripts were not only prone to personal error for being so flexible, but also entirely inaccessible to others. Knowing that others would want to utilize the mQDs we had designed to extract quantitative dynamics, a more robust software was required.

5.1 Track Analysis - Tracker

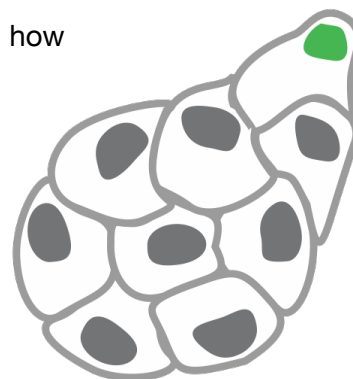
To overcome the limitations of the RyTrack software and the impenetrable nature of personal Mathematica scripts, I wrote a program in Cocoa called Tracker that would accept track data as an input and allow the user to quickly and sort well-identified tracks from poorly identified tracks, or non-relevant tracks. The program also calculates basic diffusion data for individual tracks and for sets of tracks which can be exported for further analysis. When paired with RyTrack, a user can go from a TIFF stack to an average diffusion coefficient in just a few minutes. This ability to do analysis in near-experimental-realtime allows one to quickly design experiments, quickly see results, and spend time, instead of on computational processing, on more physical experiments. In addition to enabling more effective use of experimental time, rapid analysis allows one to comfortably collect more data. As such, the number of tracks used as input to various statistical methodologies can increase in order to build a greater confidence in one's results.



Source-code can be found at <https://github.com/jfarlow/Tracker>

5.2 Time-lapse Annotation - NEP

Time-lapse imaging of multicellular aggregates as they become microtissues allows us to monitor a critical phase of communication between cells and how that communication can result in various behaviors. I developed a program to more easily and reliably annotate those videos and return to those annotations at a later time. The program allows one to mark a particular location and time with a phenotype. It collects and organizes those marks to rapidly quantitate the behavior of microtissues across many replicates and conditions.



Source-code can be found at <https://github.com/jfarlow/NEP>

5.3 References

- ¹ Johannes Schindelin, Ignacio Arganda-Carreras, Erwin Frise, Verena Kaynig, Mark Longair, Tobias Pietzsch, Stephan Preibisch, Curtis Rueden, Stephan Saalfeld, Benjamin Schmid, Jean-Yves Tinevez, Daniel James White, Volker Hartenstein, Kevin Eliceiri, Pavel Tomancak and Albert Cardona (2012) Fiji: an open-source platform for biological-image analysis, *Nature Methods* 9(7): 676-682
- ² Tinevez, Jean-Yves. Trackmate, (2014) <https://github.com/fiji/TrackMate/>
- ³ Smith, Ryan (2005) RyTrack.pro, <http://sun.iwu.edu/~gspaldin/rytrack.html>

Appendices

A.1 Genetic Constructs

A.1.1 *flag-hNotch1-Gal4*

atgccgcgctcctggcggccctgctctgctggcgtgctgcccgcgctcggcgacagggctccgggtattacaaggatgacgacgataagggtgta
cctgctcccagcccggtgagacctgacctgaatggcgggaagtgtgaaagcgccaatggcacggaggcctgctctgtggcggggccttctgaggcc
gcgatgccaggaccccaacctgctcctcagcacccttgaagaacgcccgggacatgcccacgtggggaccgagaggcgtggcagactatgctg
agctgtgcccgggcttcttggggcccttctgctgacaccctggacaatgctgctcaccacccctgcccgaacggggggcactgacactg
tcacgctgacggagtacaagtgcgctgcccggcggctggcagggaaatcgtgcccagcaggctgacccgtgcccctccaacccctgcccacgg
tggccagtgctgcccctcagggcctctacatctgcccactgcccaccagcttccatggccccaccctgcccggcaggatgtcaacgagtgaggccag
aagcccgggcttggcggccaggggacactgcccacaacgaggtggctcctaccgctgctgcccggcaccacactggccccaaactgcgagc
ggccctacgtgacctgacggccctgcccctgcccagaacggggggcactgcccggcggggcagctcaccacgagtgctgctgctgcccaggctt
caccggccagaactgtgagggaaaatcgcagattgtccaggaaacaactgcaagaacgggggtgcttgtgtggacggcgtgaacacctacaactg
cgtgcccggcagagtgaggacagtgactgtaccgaggatgtggacgagtgccagctgatgccaatgctgcccagaacggcgggacactgcccaca
acaccacgggtggctacaactgctgtgtgtcaacggctggactggtaggactgcagcgagaacattgatgactgtgcccagcggcctgctcca
cggcggcaccctgcatgacctgtggcctccttactgcgagtgccccatggccgcacaggtctgctgtgcccaccctcaacgacgcatgcatcagc
aaccctgtaacgagggctccaactgacacccaacccctgtaatggcaaggccatctgacctgcccctcggggtagacggggccggcctgacgg
aggacgtggatgagtgctgctgggtgccaacccctgcccagcatgcccggcaagtgtcaaacacgctgggctccttggagtgccagtgctgtaggg
ctacacggggcccccgatgagagatcgagctcaacgagtgctgctcgaacccctgcccagaacgacgccacctgcccggaccagattggggagttccag
tgcatctgcatgcccggctacgaggggtgctgactgaggggtcaacacagacgagtggtgcccagcagcccctgctgcaaatggccgctgctggaca
agatcaatgagttccagtgagtgcccacgggcttactgggcatctgtgcccagtagatgtggacgagtggtgcccagcaccctgcaagaatgg
tgccaagtgcctggacggaccacaacttacacctgtgtgtgacggaagggttacacggggacgactgagggggacatgatgagtgaccccc
gaccctgcccactacggctcctgcaaggacggcgtgcccacttaccctgcttgcggcccaggctacacggggcaccactgagagaccaacatca
acgagtgctccagccagccctgcccggcggggcactgcccaggacgcgacaacccctacccttctgcttctgcccgaaggggaccacaggacc
ctgcgagatcaacctggatgactgtgcccagcagccccctgacactgcccggcaccctgtctggacaagatggctacagagtgctgcccggggc
tacacagggagcatgtgtaacatcaacatcgatgagtggtgcccggcaacccctgtcacaacggggggcactgcccaggacggcatcaatggcttccact
ggcgtgccccgaggggtaccacgaccaccctgctgtctgagggtcaatgagtgcaaacgcaacccctgctgcccaggggctgcccgggacagcct
caacgggtacaagtgcgactgtgacctgggtggagtgggaccaactgtgacatcaacaacaacgagtgatgaaatcaaccccttgtgtcaacggcggc
acctgcaaaagacatgaccagtggtactgtgacactgcccgggagggcttccaggggtcccaactgcccagaccaacatcaacgagtgctgctccaacc
catgtctgaaccagggcagctgtattgacgactgtgcccgggtacaagtgtgcccactgctgcccacacagtgcccagctgtgaggtgggtgctgagg
cccgtgctgccccccctgcccagcagccccctgcccagggagtgagggcaatccaggactatgagagcttctcctgtgtgctgccccacggcctggcaaggg
cagactgtgaggtgacatcaacgagtgcttctgagcccgtgcccggcagggcgcacccctgcccagaacaccacggcggctaccgctgcccactg
aggccggctacagtgggcgcaactgagagaccgacatcgacgactgcccggccaacccctgtgcaaacgggggctcctgacagacggcatcaacac
ggccttctgagactgctgcccggcttccggggcacttctgtgaggaggacatcaacgagtggtgcccagtgacccctgcccgaacggggcacaactg
acggactgctgagcagctacacgtgacactgcccggcaggcttccaggggtccactgtgagaacaacacgctgactgacagagagctcctgct
tcaacgggtggcactgctgagggcactcaactgcttccactgctgctgctgcccagggcagctactgcccagcagatgtcaatgagtg
cgactcacagccctgctgagggcagcactgctgagggcctgcccggctcctacaggtgacactgcccagggcactgcccagggcacaactgcccag
aaccttgtgactggtgtgactcctgcccctgcaagaacggcggcaaatgctggcagaccacaccagtgaccgctgcccagtgcccagggcctgga
ccggccttactgagactgcccagcgtgctctgtgaggtggctgcccagcagcaagtggtgacgttggcccctgtgcccagcatggagggtctg
tgtggacggggcaacacgacccactgcccgtgcccagggcctacacagggcagctactgtgaggacctggggagagtgctcaccagccctg
cagaacggggcaccctgacggactactgggggctactcctgcaagtgcgtggccggctaccacgggggtgaactgctctgaggagatcgacgag
gctctcccaccctgcccagaacggggcaccctgcccagcctcccaacacactacaagtgtcctgcccagggggcactcaggggtgtgactgtga
gatcaactggcagactgcaatcagaacggcggggagtgagggcaatccaggactgtcttaacaacggcactgctgaggaccaggtggggggcctac
agctgacactgcccggggctctgagggtgagcgtgtgagggggatgtcaacgagtgctgtccaatccctgagcggcctggaaccagaact
gctgagcggcgtcaatgacttccactgagagtgccgtgctggtcacaccggcgcccctgagtgctcctcaatggctgcaaaaggcaagccctg
caagaatgggggacactgcccgtggcctccaacaccggccggttcatctgcaagtgcctgcccggcttccagggcggcagctgtgagaatgac
gctcgtacctgcccagcctgctgctcacaacggcggcactgacatcctggcccgcagccccaccctgctgtgctggggccttccagggc
ccgaatggcagttcccggcagccctgctgaggcggcaacccctgtcaaacagggggacctgtgagccacatccgagagcccttctaccg
ttgctgtgccccgcaaatcaacgggctcttgtgcccacatcctggactacagcttccgggggtggggccgggacatccccccgctgac
gaggaggcgtgagctgcccagtgcccaggaggacgcccggcaacaaggctctgagcctgagtgcaacaaccacgctgcccggctgggacggcgggtg
actgctccctcaacttcaatgacccctggaagaactgcacgagctctctgagtgctggaagtactcagtgacggcactgtgacagccagtgcaa
ctcagccggctgcttctgacggcttggactgccagcgtgcccgaaggccagtgcaacccctgtacgaccagtgactcaaggaccacttccagc
gggactgcccagggctgcaacagcggagtgagtgaggacgggctggactgtgcccagcatgtaccgagaggctggcggccggcagcgtgg
tgggtgggtgctgagcccgggagcagctgcccgaacagctcctcacttccacttctgcccgggagctcagccgctgactgcaacacaactggtctcaa
ggctgacgacacggcagagatgatcttcccactactggccggcggaggagctgcccgaagcaccatcaagctgcccgggagggcggcc
gcactgacgcccctgctggggcagggtgaaggcctgctgctcctggtggcagcaggggtggcggcggcgggagctggaccatggacgtcc
gcccctccatgcttactggagattgacaaccggcagtggtgacggcctcctgagtgcttccagagtgcccaccgatgtggccgcatctctggg
agcgtcgcctgctgggagcctcaacatccccctacaagatcgaggccgtgagagtgagaccgtggagcccccggcggcagctgacttcc
atgtacgtggcggcggcgccttctgtcttcttctctgagggtgcccgggtgctgctgctcccgaagcggcggcggcagcatggccagctctggt
tccctgaggtgaagctactgtcttctatcgaacaagcatgcatatgtgcccacttaaaaagctcaagtgctccaaagaaaaaccgaagtgcacca

APPENDICES

gtgtctgaagaacaactgggagtgctgctactctcccaaaacaaaagggtctccgctgacttagggcacatctgacagaagtggatcaaggctagaa
agactggaacagctatttttactgatttttctcctcgagaagaccttgacatgattttgaaaatggattctttacaggatataaaagcattgttaacag
gattattttgtacaagataatgtgaataaagatgccgtcacagatagattggctttagtgagactgatatgctcctaaccattgagacagcatagaat
aagtgcgacatcatcatcggaaagagtagtaacaaagggtcaaaagacagttgactgtatcgccccatggctacctgtcagacgtggcctcgccgcca
ctgctgcccctcccgttccagcagctcctcgtgcccctcaaccacctgacctgggatgcccagaccccacctgggcatcgggacactgaacgtgg
cggccaagcccagatggcggcctgggtggggggcggcggctggcctttgagactggcccacctgctctctcccacctgctgtggcctctggcac
cagcaccgtcctgggctccagcagcggaggggccctgaatttactgtgggggggtccaccagtttgatggtaaatgagtgaggctgtcccggctg
cagagcggcatggtgccgaaccaatacaacctctgctgggggagtggtgaccaggccccctgagcacacaggccccctccctgcagcatggcatgg
tagggcccgtgcacagtagccttctgctgcccagcggcctgctccagatgatgagctaccagggctgcccagcaccggctggccaccagcctcacct
ggtgcagaccagcaggtgcagccacaaaacttacagatgcagcagcagaacctgcagccagcaaacatccagcagcagcaaaagcctgcagccgcca
ccaccaccacacagccgaccttggcgtgagctcagcagccagcggccacctgggcccggagcttctctgagtgagagccgagccaggcagacgtgc
agccactgggccccagcagcctggcgggtgcacactattctgccccaggagagccccgcccctgcccacgtcgtgcccattctcgtggtcccaccctg
gaccgcagcccagttcctgacgccccctcgcagcacagctactcctcgtctgtggacaacacccccagccaccagctacaggtgctgagcaccct
ttcctcaccctgctcccctgagctcccctgaccagtggtccagctcgtccccgattccaacgctcctgactgggtccgagggcgtctccagccctccca
ccagcatgcagctcccagatcgcccgcattccggaggccttcaagtaa

MPLLAPLLCLALLPALAARSGDYKDDDDKGTCSQPGETCLNGGKCEAANGTEACVCGGAFVGPQRCDPNPCLSTPCKNAGTCHVVDRRGVADYAC
SCALGFSGPLCLTPLDNACLTNP CRNGGTC DLLTLTEYKCRCPGWSGKSCQQADPCASNPCANGGQLPFEASYICHCPPSFHGPTCRQDVNECGQ
KPLGLCRHGGTCHNEVGSYRVCVRATHTGPN CERPYVPCSPSPCQNGGTCRPTGDVTHECACLPGFTGQNCENIDDCPGNNCKNGGACVDGVMNTYNC
RCPPEWTGQYCTEDVDEQCLMPNACQNGGTC HNTHGGYNCVVCVNGWTGEDCSENIIDDCASAAFCFHGATCHDRVASFYCECPHGRTGLLCHLNDACIS
NPCNEGSCDTPNVNGKAICTCPSGYTGPA CSQDVDECSLGNPCEHAGKCINTLGSFECQLQGYTGPRCEIDVNECVSNPCQNDATCLDQIGEFQ
CICMPGYEGVHCEVNTDECACTCLHNGRCLDKINEFQCEACTGTGHLCLQYDVDECASTPCKNGAKCLDGNPTYCTVCTEGYTGTHEVDIDECDP
DPCHYGSCKDGVATFTCLCRPGYTGHCETNINECSSQPCRHHGGTCQDRDNAYLCFLKGTTPNCEINLDDCASSPCDSGTCLDKIDGYEACCEPG
YTGSMCNINIDECAGNPCHNGGTCEDGINGFTCRCEGYHDPTCLSEVNECNSNPCVHGACRDSLNGYKDCDPGWSGTNCDINNNECESNPCVNGG
TCKDMTSGYVCTCREGFSGPNQTNINECASNPCLNQGTCIDDVAGYKCNCLLPYTGATCEVVLAPCAPSPCRNGGECRQSEDIYESFCVCPGTGWQG
QTCEVDINECVLSPCRHGASCQNTGGYRCHCQAGYSGRNCETDIDDCRPNPCHNGGSDTDGINTAFCDCLPGFRGTFCCEEDINECASDPCRNGANC
TDCVDSYCTCPAGFSIHCENNTPDCTESSFNNGTCVDGINSFTCLCPPGFTGSYQHDVNECDSQPCLHGGTCQDGGCSYRCTCPQGYTGPNQC
NLVHWCDSPCKNGGKCAQHTHTYRCECPSGWTGLYCDVPSVSEVAARQGV DVARLCQHGGLCVDAGNTHHCRCQAGYTGSYCEDLVDECSPPC
QNGATCTDYLGYSCKCVAGYHGVNCS EIDECLSHPCQNGGTCLDL PNTYKCS CPRGTQGVHCEINVD DCPVPDPSRSPKCFNNGTCVDQVGGY
SCTCPPGFVGERCEGDVNECLSNPCDARGTQNCVQRVNDFHCECRAGHTGRRCESVINGCKGKPKKNGGTC AVASNTARGFICKPAGFEGATCEND
ARTCGSLRCLNGGTCISGPRSPCTCLCLGPFTGPECQFPASSPLCGNPNYQGTCEPTSESPFYRCLCPAKFNGLLCHILDYSFGGGAGRIDPPPLI
EEACELPECQEDAGNKVCSLQCNHACGWDGGDCSLNFNDPWKNCTQSLQCKWYFSDGHDCSQCSAGCLFDGFDCQRAEQCNPLVDQYCKDHFSD
GHCDQGCNSAECEDGLDCAEHVPERLAAGTLVVVLMPEQLRNSSFHFLRELSRVLHTNVVFKRDAHQQMIFPYGREEELRKHPIKRAAEGWA
APDALLGQVKASLLPGGSEGGRRRRELDPMDVRGSIVYLEIDNRQCVQASSQCFQSATDVA AFLGALASLGNLIPYKIEAVQSETVEPPPAQLHF
MYVAAA FVLLFFVCGVLLSRKRRRQHGLWLFPEVKLLSSIEQACDICRLKLLKCSKEKPKCAKCLKNNWECRYSPTKRSPLTRAHLTEVESRLE
RLEQLFLLIFPRELDMLKMDSLQDIKALLTGLFVQDNVNDKDAVTDRLASVETDMP LTRQHRISATSSSESSNKGQRQLTVSPHYLSDVASPP
LLPSPFQQSPSVPLNHLPGMPDTHLGIHNLVAAKPEMAALGGGRLAFETGPPRLSHLPV ASGTSTVLGSSSGGALNFTVGGSTSLNGQCEWLSRL
QSGMVPNQYNPLRGSVAPGPLSTQAPSLQHGMVGPLHSSLAASALSQMMSYQLPSTRLATQPHLVQTQQVQPQNLQMQQNLQPANIQQQSLQPP
PPPPPHLGVSSAASGHLGRSFLSGEPSQADVQPLGPSLAVHTILPQESPALPTSLPSSLVPPVTA AQLTPPSQHSYSSPVDNTPSHQLQVPEHP
FLTPSPESPDQWSSSSPHSNVSDWSEGVSSPPTSMQSIARIFEAFK*

A.1.3 flag-hNotch1-HALO-mCherry

atgccgccctctctggcggccctgctctgctggcgtgctgcccgcctcgcgcgacagggctccggtgattacaaggatgacgacgataagggta
cctgctccagaccggtagacctgctgaatggcgggaagtgtgaagcggcaatggcacggaggcctgctctgtggcggggccttctgaggggcc
gcgatgccaggaccccaaccctgctcagcacccttgaagaacgcccggacatgccacgtggtagaccgagaggcgtggcagactatgctctgc
agctgtgcccctgggcttctctgggcccctctgctgacaccctggacaatgctgctcaccacccctgcccgaacggggggcacctgagcactgc
tcacgtgacggagtacaagtgcgctgcccggcctggctcagggaaatgctgcccagcagctgacccgtgctcctcaaccctgcccgaacgg
tggccagtgcctgcccctcgaggcctctacatctgccactgcccaccagcttccatggccccacctgcccggcaggtatgcaacgagtggtggccag
aagccccgggcttggcggccaggggacactgcccacaacagaggtcggctcctaccgctgctgctgcccggcaccacccacactgcccgaacggc
ggcccctagctgcccctgacccccctgcccctgcagaacggggggcacctgcccggcggcagctcaccacagagtggtgctgcccagggctt
caccggccagaactgtgaggaaaatctgacgattgtccaggaacaactgcaagaacgggggtgctgtgtggagcggcgtgaacacctacaactgc
cgctgcccggcagagtgagcaggtcagctactgtaccaggatgtggacagtgccagctgatgcaaatgctgcccagaacggcgggacctgcccaca
acaccacgggtggctacaactgcgtgtgtgtcaacggctggactggtgaggactgcagcgagaacattgatgactgtgccagcggcggcctgctcca
ggcggccacctgcatgaccgtgtggctcctctactgagtggtccccatggccgcacaggtctgctgtgccacctcaacgacgcatgcatcagc
aaccctgtaacagagggctccaactgcgacaccaacctgtcaatggcaaggccatctgcacctgcccctcgggggtacacgggcccggcctgcagcc
aggacgtggatgagtgctcgtgggtgccaaccctgcgagatgcggcgaagtgcataaacacgctgggctcctcagtgagtgccagtgctcaggg
ctacacgggccccgatcgagatgcagctcaacgagtgctctgaaccctgcccagaacgacgccacctgctggaccagattggggagttccag
tgcatctgcatgcccggctacgaggggtgctcactgcgaggtcaacacagacagtggtccagcagccccctgctgcaaatggcggctgctggaca
agatcaatgagttccagtgagtgccccacgggcttccactgggcatctgtgccagtagatgtggacagagtggtccagcaccctgcaagaatgg

APPENDICES

tgccaagtgcctggacggaccaacacttacacctgtgtgtgacacggaagggtacacggggacgcactgagaggtggacatc gatgagtgcgacccc
gaccctgccactacggctcctgcaaggacggcgctcgccaccttaccctgcctctgcccggcaggctacacggggccaccactgagagaccaatca
acgagtgctccagccagccctgcccggcggggacacctgcccaggaccgagcaacgcttacctctgcttctgcttgaaggggaccacaggacccaa
ctgagatcaacctggatgactgtgacgacgccccctgacactgggcaacctgtctggacaagatc gatggctacgagtgctgtgagccgggc
tacacagggagcatgtgtaacatcaacatc gatgagtgctggggcaacctgtgacaaacgggggcaacctgagggagggcatcaatggcttccact
gcccgtgccccgagggctaccacgacccccacctgacctgtctgaggtcaatgagtgcaacagcaacccccgctccacggggcctgcccgggacagcct
caacgggtacaagtgcgactgtgacctgggtggagtgggaccaactgtgacatcaacaacaacgagtgtaatcaaaccttgtgtcaacggcggc
acctgcaagacatgaccagtggttacgtgtgacactgcccgggagggcttcagcgggtcccaactgcccagaccaatcaacgagtgctgctcaacc
catgtctgaaccagggcacgtgtattgacgactgtgcccgggtacaagtgaactgctgctgcccctacacaggtgcccacgtgtgaggtgggtgctggc
cccgtgtgccccagccccgcaagaacggcggggagtgcaggcaatccgaggactatgagagcttctctgtgtctgccccacgggctggcaaggg
cagacctgtgaggtcgacatcaacgagtgcttctgagccccctgcccggcagccatccctgcccagaacccccagggcctaccgctgccactgccc
aggccggctacagtgggcgcaactgagagaccgacatcgacgactgcccggcccaacccgtgtcacaacgggggctcctgacagagggcatcaacac
ggccttctgagctgctgcccggcttccggggcacttctgtgaggaggacatcaacgagtggtgcccagtgacccccctgcccgaacggggccaactgc
acggactgctgagacagctacacgtgacactgccccgagggcttcagcgggatccactgtgagaacaacacgctgactgacagagagctcctgct
tcaacgggtggcactgctgagcggcatcaactcgttccactgctgtgtccaccggcttcacgggcagctactgcccagcagatgtcaatgagtg
cgactcacagccccctgctgacggggcactgtcaggacggctgcccgtcttacaggtgacactgccccagggctacactggccccactgcccag
aacctgtgacactgggtgacctctgcccctgcaagaacggcgggcaaatgctggcagacccccacccagtgctgaggtgcccagcggctggga
ccggccttactgacgactgcccagcgtgctctgtgaggtgctgagcagcaaggtgtgacgttggcccctgtgcccagcatggagggtctgtg
tgtggacgcccgaacacgacccactgcccgtgcccagggcggctacacaggcagctactgtgaggacctgggtggacgagtgctcaccagccccctgc
cagaacggggccacctgacggactacctgggcccgtactcctgcaagtgcctggccggctaccacgggggtaactgctctgagggagatcgacgagtg
gctctccccaccctgcccagaacgggggcaacctgcccctgacctccccaacctacaagtgctcctgcccacggggcactcaggggtgtgactgtga
gatcaactgagcagctgcaatccccctgtgacccccgttccgggagcccccaagtgctttaacaacggcactgctggcagggctggggcggcact
agctgacactgcccggcctctgagggtgagcgtctgtgaggggagctgcaacgagtgcttcaactccccctgcccagccccggcagcccaact
gctgagcagcgtcaatgacttccactgagtgccgtgctggttccacagggcgccgctgagtgccgtatcaatggctgcaaaaggcaagccccg
caagaatgggggcaactgcccgtggcctcaaacaccgcccggggttcaatgcaagtgcctgcccggcttccagggcgccacgtgtgagaatgac
gctcgtacctgcccagcctgcccgtgctcaacggcggcagatgacatcctggcccgcagccccacctgctgtgctgggcccccttccagggcc
ccgaatgcccagttccccggccagcagccccctgctggcggcgaacccccctgtacaaccaggggacactgtgagccccatccgagagcccccttaccg
ttgctgtgccccgcaaatcaaacgggctctgtgcccacatctggactacagcttccgggggtggggcggggcggcagatccccccgcccgtgac
gaggagcgtgagctgcccagtgccagtgccagggagcggcgggcaacaagctctgagcctgcaagtgcaagaacccagcagctggagcggcggg
actgctcccccaactcaatgacccccgggaagaactgacagcagctctctgagtgctggaagtacttcaagtgacggccactgtgacagccagtga
ctcagccggctgctctctgacggcttctgactgccagcgtgcccgaaggccagtgcaacccccctgtacgaccagctactgcaaggaccacttccagc
gggactgcccagggctgcaacagcgcggagtgcaagtggggacgggctggactgtgcccggagcatgtaccgagaggctggcggccggcagcgtgg
tggtgggtgggtgctgagtgcccgggagcagctgcccgaacagctccttccacttctgcccggagctcagccgctgctgacaccaactgtgcttcaa
cgctgacgacacggcagcagatgatcttccccctactacggcccggcagggagagctgcccgaacccccatcaagcgtgcccggcgggctggggc
gcaactgacccccctgaggcaggtggaagcctgctgcttccctggcagcagcggagtgggcggcggcggagggagctggacccttccatgacgctc
gcccgtccactgcttacctggagattgacaaccggcagctgtgtgacggcctcctcgcagtgcttccagagtgccaccagatgtggccgcatctctggg
agcgtcgcctcgtgaggcagctcaacatccccctacaagatcagggcgtgacagagtgagaccgtggagccccccgcccggcagctgacactt
atgtactggcggcggccgcttctgtcttctgttctctgaggctgcccgggtgctgctgctcccgaagcggcggcggcagcagctggccagctctgg
tccctgagggatccgaatcgggtactggcttccacttccagccccattatggaagtgctggggcagcagcagctgactacgctgatgttggctccg
cgatggcaccctgtgctgttctgacggtaaccgacctcctctactgctggcgaacatcatcccgcagtggtgaccgaccatcgtctgcat
gctccagacctgctggtatgggcaaatccgacaaccagacctgggttatttctgacgaccacgtcccgttccagggactccttccatgacgccc
tgggtctggaagaggtgctcctggctattccagactggggctccgctgctgggttccactgggccaagcgaatccagagcgtcaaggtattg
atattgaggttccatccgcccctatcccagctgggacgaatggccagaatttggcccggagacctccaggccttccgaccaccgacgctggccc
aagctgatcatcagatcagaacgtttttatcaggggtacgctgcccagtggtgctgctcccggcctgactgaagtcgagatggaccattaccgagc
gcttctgaaatcctgtgaccgagccactgtggcgttcccaaacgagctgccaatcggcggtagccagcgaacatcgtcgcgctggctgaaga
atacatggactggctgacaccagctccccgtcccgaagctgctgttctggggcaccacggcgttctgatcccaccggcgaagccgctgcccggcc
aaaagcctgcccactgcaaggtggtgacatcggcccgggtcgaatctgctgcaagaagacaaccggacctgatcggcagcagatcgcgct
ggctgctactctggagatttcccgggtgctagctggtagcaagggcagggagataaacatggccatcatcaaggagttcatgcttcaaggtg
acatggagggctccgtgaacggccacgagttcagatcgaaggggcagggcgagggccgcccctacgagggcaccagaccgccaagctgaatgtga
ccaaagggtagggccccctgcccctgcccggacatcctgtcccctcagttcatgtacggctccaaggcctacgtgaagcaccgccgacatccccg
actactgaagctgctcctccccgagggcttcaagtgggagcgcgtgatgaacttcgaggacggcggcgtggtagcctgaccaggactcctcccc
gaggacggcagttcatcacaaggtgaagctgcccggcaccactccccctggcagggccccgtaatgcaagaagaccatggctgggagggc
tctccgagcggatgtacccccgagggagggccttgaagcagagatcaagcagagctgaagctgaaggacggcggccactacgacgctgaggtca
agaccacctacaaggccaagaagccccgtgagctgcccggccttacaacgtaacatcaagttggacatcactccccacaacaggagctacaccat
cgtggaacagtagaacgcccagggcggcactccaccggcggcatggacgagctgtacaagtaggctagcctggagctacccccatggctacctg
tcagactggcctcggccactgctgcccctcccgttccagcagctcctgctccgtgcccctcaaccactgctgggatgcccgacaccacctgg
gcatggggcactgaactggcggccaagcccagatggcggcgtgggtggggggcggccggctggcctttagactggcccactcgtctctccca
cctgctgtggccttggcaccagcaccgctcctgggctccagcagcggagggccccctgaatttcaactgtggcggggtccaccacttgaatggta
tgcagtggtgctcccggctgcccagggcagctggctgcccgaacatacaacccccctgcccggggagtggtggcaccagccccctgagcacaagggccc
cctcccctgacagatggtaggtaggccccgtgacagtagccttctgcccagcggcctgtcccagatgatgagctaccagggcctgcccagcaccg
gctggccaccagcctcactgggtgacagccagcaggtgacccacaaaacttacagatgacagcagcagaacctgacagcagcaaacatccagcag
cagcaaacctgacggccaccaccaccacagccgaccttggcgtgagctcagcagccagcggccacctgggcccggagcttctgagtgagg
agccgagccaggcagactgacagccactgggccccagcagcctggcgggtgacacatcttgcgccagggagccccgcccctgcccacgtcgtgccc
atcctcgtggtcccaccctgaccgacggcagcttctgacgccccctgacgacagctactcctgcccgtggacaacccccagccaccag

APPENDICES

ctacaggtgcctgagcaccctctctcaccctgccccctgagtcctccagctcgtccccgattccaacgtctccgactggtccc
aggcgctctccagccctcccaccagcatgcagtcctccagatgccccgattccggaggccttcaagtaa

MPLLAPLLCLALLPALAARSGDYKDDDDKGTCSQPGETCLNGGKCEAANGTEACVCGGAFVGPQRCDPNPCLSTPCKNAGTCHVVDVRRGVADYAC
SCALGFSGPLCLTPLDNAICTNCRNGGTDLLTLTEYKCRPPGWSGKSCQADPCASNPCANGGQCLPFEASYICHCPPSFHGPTCRQDVNECGQ
KPLCRHGGTCHNEVGSYRVCVRATHGPNCRPYVPCSPSPCQNGGTCRPTGDVTHEACALPGFTGQNCENIDDCPGNCKNGGACVDGVNTYNC
RCPPEWTGQYCTEDVDEQCLMPNACQNGGTCNTHGGYNCVVCVNGWTGEDCSENIDDCASAACFHGATCHDRVASFYCECPHGRTGLLCHLNDACIS
NPCNEGSCDNTNPNVNGKAICTCPSGYTPACSDQVDECSLGNPCEHAGKICINTLGSFECQCLQGYTGPCEIDVNECVSNPCQNDATCLDQIGEFQ
CICMPGYEGVHCEVNTDECASSPCLHNGRCLDKINEFQCECPTGFTGHLQYVDVDECASTPCKNGAKLDGPNYTCVCTEGYTGTHCEVDIDECDP
DPCHYGSCKDGVATFTCLCRPGYTGHCETNINECSSQPCRGGTCQDRDNAYLCFLKGTTPNCEINLDDCASSPCDSGTCCLKIDGVEACCEPG
YTGSMCNINIDECAGNPNCHNGGTCEDGINGFTCRCEGYHDPTCLSEVNECNSNPCVHGACRDSLNGYKDCDPCGWSGTNCDINNNECESNPCVNGG
TCKDMTSGYVCTCREGFSGPNQTNINECASNPCLNQGTICDDVAGYKCNCLLPYTGTATCEVVLAPCAPSPCRNGGECRQSEDIYESFSCVCPGTGWQG
QTCEVDINECVLSPCRHGASCQNTGGYRCHCQAGYSGRNCETDIDDCRPNPCHNGGCTDGINAFCDCLPGFRGTCEEDINECASDPCRNAGNC
TDCVDSYCTCPAGFSGIHCENNTPDCTESSFNNGTVDGINSFTCLCPPGFTGSYQHDVNECDSQPCLHGGTCQDGGCSYRCTCPQGYTPNQC
NLVHWCDSPPCKNGGKWCQHTYQYRCECPGWTGLYCDVPSVSEVAAQRQGVAVARLQHGGLCVDAGNTHHCRCQAGYTGSYCEDLVDECSPPSC
QNGATCTDYLGGYSCKVAGYHGVNCEEIDECLSHPCQNGGTCCLDLNPTYKCSRGTQGVHCEINVDDCNPPVDPVRSRSPKCFNNGTCVDQVGGY
SCTCPPGFVGERCEGDVNECLSNPCDARGTQNCVQRVNDFHCECRAGHTGRRCESVINGCKGKPKNGGTCVASNTARGFICKCPAGFEGATCEND
ARTCGSLRCLNGGTCISGPRSPCTCLLGPFTGPECQFPASSPLGNNPCYNQGTCEPTSESPFYRCLCPAKFNGLLCHILDYSFGGGAGRDIPPLI
EEACELPECQEDAGNKVCSLQCNHACGWDGGDCSLNFPDWNKCTQSLQCKWYFSDGHDCSQNSAGCLFDGFDCQRAEQCNPLYDQYCKDHFSD
GHCDQGCNSAEEWDGLDCAEHVPERLAAGTLVVVLMPEQLRNSFFHLRELRLVHTNVVFKRDAHQQMIFPYVGREELRKHPIKRAAEGWA
APDALLGQVKASLLPGGSEGGRRRRELDPMVDVRSIVYLEIDNRQCVQASSQCFQSATDVAALFALASLGSLNIPYKIEAVQSETVEPPPAQLHF
MYVAAAFFVLLFFVCGVLLSRKRRRQHGLWFPEGSEIGTFPDPHYEVVLGERMHYVDVGPDRDTPVLFHGNPTSSYVWRNIIPHVAPTHRCI
APDLIGMGKSDKPDLYGFDDHVRFMDFIEALGLEEVVLIHDWGSALGFHWAKRNPVVKGIAMFIRIPTWDEWPEFARETFQAFRTTDVGR
KLIIQNVFIEGLPMGVVRPLTEVEMDHYREPLNPDREPLWRFPNELPIAGEPANIVALVEEYMDWLHQSPVPKLLFWGTPGVLIPPAEARLA
KSLPNCKAVDIGPGLNLLQEDNPDIGSEIARWLSTLEISRC*HGEQGRGG*HGHHQGVHALQGAHGLRERPRVRDRRARARAAPTRAPRPPS*M*
PKGGPLPFAWDILSPQFMYGSKAYVKKPADIPDYLKLSFPEGFKWERVMNFEDGGVVTVDQSSLDQGEFIYKVKLRGTNFPDGPVMQKKTMGWEA
SSERMYPEDGALKGEIKQLKLDGGHYDAEVKTTYKAKKPVQLPGAYNVNIKLDITSHNEDYIVEQYERAEGRHSTGGMDELYK*ASLESHPHYL
SDVASPPLLSPFQQSPSVPLNHLPGMPDTHLIGHLNVAAPKPEMAALGGGGRALAFETGPPRLSHLPVASGTSTVLGSSSGGALNFTVGGSTSLNGQ
CEWLSRLQSGMVPNQYNPLRGSVAPGLSTQAPSLQHGVMGPLHSSLAASALSQMMSYQGLPSTRLATQPHLVQTTQVQPNLQMQQNLQPNIIQQ
QQSLQPPPPPPQPHLGVSSAASGHLGRSFLSGEPSQADVQPLGPSLAVHTILPQESPALPTSLPSSLVPPVTAQFLTPPSQHSYSYPVDNTPSHQ
LQVPEHFLTPSPESPDQWSSSSPHSNVSDWSEGVSSPPTSMQSIARPEAFK*

A.1.4 *flag-SNAP-hNotch1-Gal4*

atgccgcgctctctggcgcctctgctctgctggcgtgctgcccgcgctcgcggcagcaggctccggtgattacaaggatgacgacgataagggta
ccgacaaaagactgcgaaatgaagcgcaccaccctggatagccctctgggcaagctggaactgtctgggtgcgcaacaggccctgcacgagatcaagct
gctgggcaaaaggaacatctgccgccgacccgtggaagtgcctgccccagccgctgctggcgccgaccagagccactgatgacggccaccgctgg
ctcaacgcctactttcaccagcctgagggcatcgaggagtccctgtgccagccctgcaccacccagtggtccagcaggagagctttaccgcccagg
tgctgtgaaactgtgaaagtgggtgaagtccggagaggtcatcagctaccagcagctggccgcccaggcgaatcccgcgcccaccgcccctg
gaaaaccgcccctgagcgggaaatcccgtgcccattctgatccccctgccaccgggtggtgcttagctctggcgccgctggggggcttacgaggcgggctc
gctgaaagagtggctgctggcccacgagggccacagactgggcaagcctgggctgggtggtacctgctcccagcccggtagacctgctgaaatg
gagggaagtgtgaagcggccaatggcacggaggcctgctgctgtggcggggccttctgggcccgcgatgccaggacccaaccctgctcctcagcac
ccctgcaagaacgcccggacatgccacgtggtggaccgagaggcgtggcagactatgcctgcagctgtgcctgggcttctctgggcccctctgc
ctgacacccttgacaatgctgctcctcacaaccctgcccgaacgggggacactgcgacctgctcaagctgacggagtacaagtgcctgctcccgc
ccgctggctcagggaatctgctcagcaggctgaccctgctcccaaccctgcgcaaacgggtggccagtgctgcccctcagggcctcctacat
ctgcccactgcccaccagcttccatggccccacactgcccggcaggatgtcaacgagtggtggccagaagcccgggcttggccgacggaggcactgc
cacaacgaggctgctcctaccgctgctgctgcccgcaccacactggcccactgagagcggcctacgtgcccctgcagcccctgcccctgccc
agaacgggggacactgcccggccacggcgagctcaccacagagtgctgctgctgcccaggctcaccggccagaactgtgaggaaaaatcagacga
ttgtccaggaaacaactgcaagaacgggggtgctgctgtggagcggcgtgaacacctacaactcccgtgcccggcagagtggaaggtcagtagt
accgaggtatgtaggacgagtgccagctgatgccaatgctgcccagaacggcgggacctgcccacaaccccagggtgctacaactgctgtgtgtca
acggctggactgtaggactgcagcagaacattgatgactgtgcccagcgcgctgcttccacggcgcacctgcccagctgtgcccctctct
ctactcgagtgctccccatggccgacaggtctgctgtgcccactcaacagcagcatcagcaaccctgtaacgagggtcctcaactgcgacacc
aaccctgtcaatggcaaggccatctgcacctgcccctgggggtacacgggcccggcctgcagccaggacgtggatgagtgctgctgggtgccaacc
cctgcgagcatgcccgaagtgcatcaacacgctgggctcctctgagtgccagtgctgacgggtacacgggccccgatgagatcagctcaa
cgagtgctctgcaaccgctgcccagaacgacgcccactgctggaccagattggggagttccagtgcatctgcatgcccggctacgagggtgtgcac
tgcgaggtcaacacagacgagtgctgcccagcagcccctgctgcacaatggcccgtgctggaagaatcaatgagttccagtgccagtgccccaggg
gcttccactgggcatctgcccagctacgagtgacgagtgctgcccagcagcagcagcagcagcagcagcagcagcagcagcagcagcagcagcagc
ctgtgtgtgacggaagggtacacgggacgactgcaggtggacatcagtagtgcgaccggaccctgcccactgcccactgcccactgcccactgccc
gtcggcaccttaccctgctctgcccggcaggctacacgggcccactgcgagaccaacatcaacgagtgctccagccagccctgcccggcagggg
gcacctgcccaggaccgcaaacgctaccctgcttctgctgacggggaccacaggacccaactgcgagatcaacctggatgactgtgcccagcag
ccctgagctgcccagcctgctggaagaatcagtgctgacgagtgctgtagccgggctacacaggagcagatgtgtaacatcaacatcagat
gagtgtagggcaaccctgtcacaacgggggacactgcgaggacggcatcaatgcttaccctgcccgtgcccggaggctaccacgacccccact

APPENDICES

gcctgtctgaggatcaatgagtgcaacagcaaccctgctgccaggggctgcccgggacagcctcaacgggtacaagtgcgactgtgaccctgggtg
gagtgaggaccaactgtgacatcaacaacaacagagtgtaatcaacccttgtgtcaacggcgccacctgcaaaagacatgaccagtggtctacgtgtgc
acctgcccgggagggtctcagcgggtcccaactgcccagaccaatcaacgagtgctgctcaacccatgtctgaaccaggggcagctgtattgacgacg
ttgccgggtacaagtgaactgctgctgcccacacaggtgcccacgtgtgaggtggtgctggccccgtgtgccccagccccgcagaacggcg
ggagtgcaaggcaatccgaggactatgagagcttctcctgtgtctgccccacgggctggcaagggcagacctgtgaggtcgacatcaacgagtgctt
ctgagcccggtccggcagcgcatcctgcccagaacacccacggcgctaccgctgcccactgcccaggccggtacagtggggcgcaactgagagaccg
acatcgacgactcccggcccaaccgctgtcacaacgggggctcctgacagacggcatcaacacggccttctgagactgctgcccggcttccgggg
cacttctgtgaggaggacatcaacgagtggtgacccctgcccgaacggggccaactgcacggactgctgaggacagctacacgtgacactgc
cccagggcttcaaggggatccactgtgagaacaacacgcctgactgcacagagagctcctgcttcaacgggtggcactgctgagggcagcacaact
cgttccactgctgtgtccaccggcttcacgggcagctactgcccagcagatgtcaatgagtgagctcacagccctgctgcatggcgccacctg
tcaggagggctgcccgtctacaggtgacactgccccagggctacactggccccaaactgccaagacctgtgacactggtgactcctcgccctgc
aagaacggcggaatgctggcagaccacaccagtagcctgagtgccccagggctggaccggccttactgagcagtgcccagcgtgtcct
gtgaggtggctgagcagcgacaagggtgtgacgttgcccgcctgtgcccagcatggagggtctgtgtggagcgggcaacacgaccactgcccgtg
ccaggcgggtacacagggcagctactgtgaggacctggtggagcagtgctcaccagcccctgcccagaacggggccaactgcacggactacctgggc
ggctactcctgcaagtgcgtggcgggtaccacggggtgaactgctctgaggagatcgacgagtgcttccccacccctgcccagaacggggcactt
gctcagactccccaacactacaagtgtcctgcccacggggcactcagggtgtgactgtgagatcaactggagactgcaatccccccgttga
ccccgttccccggagccccaaagtgtcttaacaacggcactgctgaggacgggtggcgctacagctgacactgcccgggcttctggtggtgag
cgctgtgagggggtatgtaacagagtgcttcaatcctgagcggcggcagccccagaactgctgagcagcgtcaatgacttccactgagcaggt
gcccgtgtggtcacaccggcgccgctgagtgccgtatcaatggctgcaaaaggcaagccctgcaagaatgggggacactgcccgtggcctccaa
caccgcccgggttcatctgcaagtgcctgcccgggtctgagggcgcccactgtgagaatgacgctcgtacactgcccagcctgctgctgctcaac
ggcggcagatgcatctccggcccgcgacccccactgctgtgctgggcccccttcaagggccccgaatgcccagttccccggccagcagccccctgccc
tgggggcaaccctgctacaaccaggggcactgtgagcccacatccgagagcccccttaccggtgctgtgccccgcaaatcaaccgggctctt
gtgacacactcctgagcagcttccgggggtggggcgccagctgccccccccggcctgctgagggagcgtgcaagctgcccagctgcccagggag
gacggggcaacaaggtctgagcctgagcagtgcaacaaccacgctgcccggctgggagcggcgggtgactgctcccccaacttcaatgacccccggaaga
actgcacgcagctctgagtgctggaagtacttcagtgacggccactgtgacagccagtgcaactcagccggctgctcttccgagccttggactg
ccagcgtgcccgaaggccagtgcaacccccctgtacgaccagctactgcaaggaccacttcagcagcgggcaactgcccagcagggctgcaacagcgcggag
tgcgagtgaggagcgggctggactgtgcccagcagtgaccagagaggctggcggcggcagcgtgggtggtggtgctgatgcccgggagcagctgc
gcaacagctccttccacttctgcccggagctcagccgctgctgacaccaacgtggtcttcaagcgtgagcagcagcggcagcagatgatcttccc
ctactacggccgaggaagagctgcccgaagcaccctcaagcgtgcccggcagggctgggcccagcctgagccttccagccttccagccttccagcct
tcgctgctcccctggggcagcaggggtggggcggcgggagggagctggaccctggagctccgagccttccagccttccagccttccagccttccagcct
ggcagtggtgagcggcctcctcagctgcttccagagtgccaccagatgtggccgcatcttgggagcgtcgcctcgtgaggcagcctcaacatccc
ctacaagatcagggccctgcaagtgagacctggagccgccccggcggcagctgacattcatgtacgtggcgccggcccttggcttctg
ttcttctgagggtgcccgggtgctgctgtcccgaagcggcggcagcagatggccagctctgggtccccaggtgagactgtcttctatcgaac
aagcagcagatattggcagctaaaaagctcaagtgctcaaaagaaaaaccgaagtgcccgaagtgctgaaagaacactgggagtgctgctactc
tcccaaaaacaaaaggctcctcctgactagggcacatctgacagaagtggaaatcaaggctagaagaactggaacagctatttctactgatttttctt
cgagaagaccttgacatgattttgaaaaatggattctttacaggaatataaaagcattgttaacaggattattgtacaagataatgtgaaataaagatg
ccgtcacagatagattggcttccagtgagactgatgtccttcaacattgagacagcagatagaataagtgagacatcatcaggaagagagtagtaa
caaggtcaaaagacagttgactgtatgccccatggctacctgtcagacgtggcctgcccggcactgctgcccctcccgttccagcagctcctcgtcc
gtccccctcaaccacctgctgggatgcccagaccccactgggcatcgggcactgaaactgcccggcgaagcccagatggcggcgtgggtgggg
gcccggcgtggccttggagactggcccacctgctcttcccactgctgtggcctctggcaccagcaccgtcttgggctccagcagcggagggggc
cctgaatttcaactgtggcggggtccaccagtttgaatggtaaatgagtgctgctcccggctgagagcggcagatggtgcccgaacaatacaaccct
ctgcccggggagtggtgaccagggccccctgagcacacagggccccctcctgagcagatggcagtgtagggcccgtgacagtagccttctgcccagc
cctgtcccagatgatgagctaccagggcctgcccagcaccggctggccaccagcctcactgggtgagaccagcaggtgagccacaaaactt
acagatgagcagcagaaactgagccagcaaacatccagcagcagcaaacctgagccgcccaccaccaccacagccgaccttggcgtgagc
tcagcagccagcggccactggggcggagcttctgagtgagagccgagccagcagcagctgagccactgggccccagcagcctggcgggtgaca
ctattctgccccaggagagccccgcccctgcccagctgctgcaatcctgctggtcccaccctgaccgcagccagcttctgagccccctcaca
gcacagctactcctcctggtgagcaaacacccccagccacagcctacaggtgctcctgagcacccttctcaccctgctcaccctgagctcccctgaccag
tggctcagctcctcccgcattccaacgtctccgactggctccgagggcgtctccagcctcccaccagcagctgagctcccagatgcccgcattccgg
aggccttcaagtaa

MPLLAPLLCLALLPALAARGSDYKDDDDKGTDKDCMKRRTLDSPGLKLELSGCEQLHEIKLLGKGTSAADAVEVPAPAVALGGPEPLMQATAW
LNAFHHQPEAIEEFPVPAALHPVFQESFTRQVLWKLKVVKFGVEISYQLAALAGNPAATAAVKTAALSGNPVPIIPCHRUVSSSGAVGGYEGGL
AVKEWLLAHEGHRLLGKPLGGTCSQPGETCLNGGKCEAANGTEACVCGGAFVGPCCQDPNPLSTPCKNAGTCHVVDRRGVADYACSCALGFSGLC
LTPLDNACLTNPCRNGGTCDLLTLEYKCRPPGWSGKSCQADPCASNPCANGGQCLPFASYICHCPPSFHGPTCRQDVNECGQKPLCRHGGTC
HNEVGSYRVCRAHTHGPNCERPYPVPCSPSPCQNGGTCTCRPTGDVTHEACLPGFTGQNCENIDDCPGNNCKNGGACVDGVNTYNCRCPEWTGQYC
TEDVDEQQLMPNACQNGGTCHNTHGGYNCVNVNGWTGEDCSENIDDCASAACFHGATCHDRVASFYCECPHGRTGLLCHLNDACISNPCNEGSNCDT
NPVNGKAICTCPSGYTPACSQDVDECSLGNPCEHAGKCIINTLGSFECQLQVGTGPRCEIDVNECVSNPCQNDATCLDQIGEFQICMPGYEKGVH
CEVNTDECASSPCLHNGRCLDKINEFQCEPTGFTGHLQYDVDFCEASTPCKNGAKCLDGPNTYTCVCTEGYTGTHCEVDIDECDPDPCHYGSCKDG
VATFTCLCRPGYTGHEHRECLDINESSQPCRHHGTCQDRDNAYLFCCLKGTTGNPCEINLDDCASSPCDSTGTLCKIDYGEACEPEGYTGMSCNINID
ECAGNPCHNGGTCEDGINGFTCRCEGYHDPTCLSEVNECNSNPCVHAGCRDSLNGYKCDPWSGNTNCDINNECESNPCVNGGTCCKDMTSGYVC
TCREGFSGPNQTNINECASNPCLNQGTICDDVAGYKCNLLPYTGATCEVLAPCAPSPCRNGGECRQSEDIYEFSCVCPGTGWGGTCEVDINECV
LSPCRHGASCQNTHGGYRCHCQAGYSGRNCETDIDDCRPNPCHNGGCTDGINAFCDCLPGFRGTFCEDINECASDPCRNAGNCTCDVDSYCTC
PAGFSGIHCENNTPDCTESSFNNGTCDVGINFTCLCPPGFTGSYQHDVNECDSQPCLHGGTCQDGGCSYRCTCPQGYTGPNCQNLVHWCDSPP
KNGGKQWQHTQYRCEPSPGWTGLYCDVPSVSCEVAARQGVQVAVRLCQHGLCVDAGNTHHRCRCQAGYTGSYCEDLVECESPSPCQNGATCTDYL

APPENDICES

SQADVQLGPSSLAVHTILPQESPALPTSLPSSLVPPVTAQFLTPPSQHSYSSPVDNTPSHQLQVPEHPFLTPSPESPQDQWSSSSPHSNVSDWSEG
VSSPPTSMQSQIARIPEAFK*

A.1.10 SENSYR

atgccgcgctcttggcggccctgctctgccttgcgctgcttccagcgcctcggcggcgaacaggtgaagctggaagagagtggcggaggtagtgtgc
agacagggggaagcctgcgccttacctgcgcccctccggaaggaccagtaggtcatatggaatgggttgggttccgagggccccagcgaagagcg
agagttcgtctccggcatcagctggagaggggacagcaccggttacgcgactccgctcaaaggcggtttaccatctctcgggataatgcgaagaat
acagtggaactgcaaatgaattccctgaagcccgaagatactgcaatcttactgcgccgacggctggctcagcctggatgggacgctttacg
agtagattattggggtaacgaaccaggtgacagtcagttcaaccctgggagataaagactgtgagatgaagagaacagcctggacttctctct
gggtaaatgggagctgagcgggtgtgaaacagggttgcacagaaattcttttggggaaagggaacctcagctgcccgatgcccgtggaaagtgcocg
ccagcggcgtgctgggtggccagagccgctgatgacggctaccgctggctgaatgcatactttcaccaacctgaagcaatcgaggaaatccctg
tccagcactccaccacctgtttccagcaggaaatcttctcagcagcagcctctgaaacttctgaaagtctgaaatggggagggttatcag
ctactcccactggctgcccctcgggaaaccccgagcagctgcccgtgtcaagaccgcccgtcagggcaatcccgtaccaatcttgattccttgc
cacaggggtggccaaggcgatctggacgtggggcgggtatgaaggggggctggccgtgaaggagtggctcttggctcacgaggggcatcgctgggta
agcctggcttgggtatcttggactacagcttccgggtggcggcggcggcagggacatccccctcccctgatcgaagaagcatgcagcctcccagtg
ccaagaggatgctggtaacaaggatgacagcctcagtgcaataatcagcttggctgggatggcgggtgactgctcccctcaactcaatgacccc
tggagaactgcacgagctcttgcagtgctggaagtacttgcagtgccgactgtgacagccagtgcaactcagccggctgctcttgcagggct
ttgactgcccagctgcccgaaggcagtgcaacccccgtacgaccagctgcaaggaccacttcagcagcggcactgacgaccaggctgcaacag
cgcggagtgcgagtgggacggctggactgtgcggagcatgtaccgagaggctggcggcggcagcctgggtgggtgggtgcttatgctccagaa
cagcttaggaatagtagcttccacttctcgggaaacttagtaggggtgcttcacacgaacgtagtattcaaaaggagcgtcacggacagcagatga
tcttccatattacggccgagagggagctcaggaacacccaattaaagcagcagcggaaagggtgggctgcccctgacgctctgttggccaggt
gaaagctcccctgctgcccgggagggtcagaggcggccgacgcagggaggagctggatcctatggatgtgaggggctcaatagctcactggagata
gacaatagacagtggtccaagcatccagtcagtggttccaatcagccacagacgttgcagccttcttgggcgctctggcctcccctcggaaagctga
acattccgtataaaaattgaagctgtccagtcagactgtcagcggccccccgagctcagctgcattttatgtacgtggctgcccggcatttgt
gcttcttttttctgctgggtgctgctgctgggatccatggtagcaaggcggagggagataacatggcctctctcccagcagacacatgagtt
cacatcttggctccatcaacgggtgaggactttgacatggtagggctcagggcaccggcaatccaatgatggttatgaggagttaaactgaagtcca
ccaagggtagctccagttctcccctggattctggctcccctcatatgggtatggcttccatcagctaccctaccctgacgggtagctgctccctt
ccaggccagctggtagatggctccggataccaagtcacatgcacaaatgagcttggatggctcccctactgttaactaccctacacctac
gaggaagccacatcaaaaggagaggccaggtgaaggggactggtttccctgctgacggctctgtgatgaccaactcgtgaccgctcggactgg
gcaggtcgaagaagacttaccacaacgacaaaacatcatcagctacccttaagtgaggttacaccactggaatggcaagcgtaccggagcactgc
gaggaccactacaccttgcgaagccaatggcggctaacatctgaagaaccagccgatgtacgtgttccgtaagacggagctcaagcactccaag
accgagctcaactcaaggagtggcaaaaggcctttaccgatgtgatgggcatggacagctgtacaagggatccgacagccagcagcctgacttga
agttgctgctcatctatcagcagggcttgcgatataatgtcagactgaaaaaacgaagtgtcttaaggagaacctaagtgcgcaagtgtctgaagaa
caactgggaatgcccgtatagcccaaaaaccaaaggcgtctcttctgactcagcacaacctcagagaggtagagttcagacttgagagactggagcaa
ctgttctgctcatcttccgagagaagatctcgatagattctgaagatggacagctcaccaggaattaaagcattgctggaaatccccggagtg
accaggaagcactcccattggaattccagctaccgagcacagacagccgacagggatgaagaaaagcggaaagcagcacttatgagaccttaa
gtccataatgaagaagctccccttccggcccaacggaccctcagccccctccaagaagaatcggcgttcttcccgtccaagcagcactgtgccc
aaaccgctccacagccctatcttccacaagcagcttcttccactatcaattacgacaggttcccacaatgggtgttcccctagcgggcaaatttac
aagccagcggcctggcaccggctccccccaggttctcccacaagctcctgcccagccccctgcccctgcaatggatccgcccctggcgaagctcc
cgcgagctaccggctgctcctcagggccacccgagcgtgttggcccccccgaccgcaacccacagggctggggagggcaacccagcagcagcga
ctcctcagctgagcttccgatgatgaggatctggcgcctctgcttggtaatagcactgacctgctgtcttccaggtatggcctcccgtggataact
ctgaattccagcagcttcttaaccagggcatcccgggtggctccacacactacagagccatgctgatggagtaccagaggcaatcactaggctgg
aactgggtcccagcagccgcccagccagcagcctcactggcgcacccggctgccaatggactgcttagtgagatgaggacttcagctcc
attgccgatatggattttagcgcgcttctgtcagacttcttcttaatag

MPPLLAPLLCLALLPALAGEQVKLEESGGSVQTGSSLRLTCAASGRTRSRYGMGWFRRQAPGKEREFVSGISWRGDSTGYADSVKGRFTISRDNKN
TVDLQMNLSKPEDTAIYYCAAAGSAWYGLTYEYDYWGQGTQVTVSSTGGDKDCMKRTTLDSPGLKLELSGCEQLHRIIFLKGKTSAADAVEVPA
PAAVLGGPEPLMQATAWLNAYFHQPEAIEEFPVPALHHPVQQESFTRQVLWKLKVVVKGFEVISYSHLAALAGNPAATAAVKTALSGNPVPIIPC
HRVVQGDLDVGGYEGGLAVKEWLLAHEGHRLLGKPLGLDYSFGGGAGRDIPPLIEEACELPECQEDAGNKVCSLQCNNHACGWDGGDCSLNFDN
WKNCTQSLQCWYFSDGHCDSDQNSAGCLFDGFDQRAEGQCNPLDYQYCKDHFSDGHCDQGCNSAECEWDGLDCAEHVPERLAAGTLVVVLMPE
QLRNSFFHLRELSRVLHTNVVFKRDAHQQMIIPYIEGEEELRKHPIKRAEAWAAPDALLGQVKASLLPGGSEGGRRRLDPMRVRSIVYLEI
DNRQCQVQASSQCFQSATDVAAFLGALASLGSINIPYKIEAVQSEKTEVEPPPAQLHFMVAAAAFVLLFFVGGCVLLGSMVSKGEEDNMASLPATHEL
HIFGSINGVDFDMVGGTGNPNDDGYEELNLKSTKGDQLFSPWILVPHIGYGFHQYLPYPDGMSPFQAAMVDGSGYQVHRTMQFEDGASLTVNYRYTY
EGSHIKGEAQVKGTFPAGDVPMTNSLTAADWCRSKKTYPNDKTIISTFKWSYTTGNGKRYRSTARTTYTFAKPMAANYLKNQPMYVFRKTELKHSK
TELNFKWQKAFQVDMGMDLEYKGSQSDQPPDLKLLSSIEQACDICRLKLLKCSKEKPKCAKCLKNNWECRYSKTKRSPLTRAHLTEVESRLERLEQ
LFLLIIPREDLDMILKMSLDQIKALLEFPVGDQGSTPMEFQYLPDTRHRIEERKRTYETFKSIMKKSPPFSGPTDPRPPPRRIAVPSRSSASVP
KPAPQYPFTSSLSTINYDEFPMTVFPSSGQISQASALPAPPQVLPQAPAPAPAMVYVSAQAAPAPVPLAPGPPQAVAPPKPTQAGEGTLSEA
LLQLQFDDDLGALLGNSTDPVFTDLASVDNSEFQQLLNQGIQVAPHTTEPMLMEYPEAITRLVTGAQRPPDPAPAPLGNLPLNGLEDSS
IADMDFSALLSQISS**

A.2 Code & Software

A.2.1 Random Diffusion

Mathematic code to generate random walks of particles that fit physically defined parameters. The particles are confined to a 'cell' and are excluded from definable boundaries in 3 different ways: 1) by 'losing a turn' in the simulation upon trying to enter a bounds, 2) 're-rolling' upon trying to enter a bounds, 3) ignoring the bounds. From the simulated particle trajectories diffusion coefficients and confinement parameters are calculated. The simulation can be run for a given number of particles over the course of a given time in order to identify trends in how different sized, or shaped barriers, or the kinds of interactions with those barriers affect the calculated parameters. No input it required, though a 'cell' and a list of 'barriers' should be defined as an enclosed polygon.

```
Graphics`Mesh`MeshInit[];

particleNumber = 500;
RunTime = 200;
timestep = 0.03;
spacestep = 0.01;
diffusionMean = 0.085;
diffusionVariance = 0.07;
initialBoxSize = 7;
TheCell = {{4, 0}, {6, 0}, {6, 7}, {4, 6}};

Barriers = {{{1.8, 1.1}, {2.5, 1}, {3, 1}, {3.5, 1.6}, {2.6, 1.3}, {1.8,
  1.4}}, {{1.2, .4}, {4, .8}, {4.2, .8}, {1.4, .2}}, {{3.8, 1.1}, {4.5,
  1.4}, {4.6, 1.3}, {4.4, 1.1}}, {{1.7, 2}, {4.3, 2.3}, {4.1, 2.1}, {4.9,
  2.4}, {4, 2.6}, {4.3, 2.4}, {1.9, 2.1}}, {{.1, 5.9}, {1.5, 4.1}, {1.4,
  4.1}, {.1, 5.8}}, {{2.9, 3.4}, {3, 3.4}, {1.7, 4.9}, {1.5, 4.8}}, {{1.6,
  5.9}, {2.9, 4.8}, {3.2, 4.9}, {2.9, 5.0}, {1.9, 5.9}}, {{5.3, 1.9}, {6,
  2.1}, {6, 2.3}, {5.3, 2}}, {{4.9, 2.6}, {4.9, 2.55}, {5.2, 2.55}, {5.2,
  2.7}}, {{.9, 1.7}, {.9, 2}, {1, 2.1}, {.9, 2.3}, {.5, 2.1}, {.8,
  1.7}}, {{.3, 4}, {1, 3.4}, {.9, 3}, {.2, 3.6}}, {{.6, 1}, {2.2, 2}, {2,
  2}, {.6, 1.2}}, {{2.5, 5}, {3.8, 3.5}, {3.7, 3.4}, {2.4, 4.9}}};

sizeScale = 10/7;

TheCell = {{4, 0}, {4, 0}, {8, 1.5}, {7.5, 3}, {8, 6}, {6.5, 8}, {4, 7}, {4,
  8}};

pax = {{0, 0}, {1.6, 0}, {1.6, .01}, {0, .01}};
```

APPENDICES

```

Barriers = {
  Plus[{6, 2}, # ] & /@ pax,
  Plus[{5.5, 3}, # ] & /@ pax,
  Plus[{6, 4}, # ] & /@ pax,
  Plus[{6, 5}, # ] & /@ pax,
  Plus[{6, 6}, # ] & /@ pax,
  Plus[{5.4, 7}, # ] & /@ pax
};

(*Barriers = {};)

TheCell = TheCell * sizeScale;
Barriers = Barriers *sizeScale;
spaceStep = initialBoxSize = 12;

BarrierAreas = PolygonArea /@ Barriers
BarrierArea = Total[BarrierAreas];
CellArea = PolygonArea[TheCell];
PercentAreaBarrier = BarrierArea / CellArea

angle[{p1_, p2_}] := Module[{c1, c2}, {c1, c2} = #.{1, I} & /@ {p1, p2};
  Arg[c2/c1]]

PointInsidePolygonQ::usage =
  "PointInsidePolygonQ[point,polygon] will return True if the point is on the \
boundary or inside the polygon and False otherwise.";
SyntaxInformation[PointInsidePolygonQ] = {"ArgumentsPattern" -> {_, _}};
PointInsidePolygonQ[point_, polygon_] :=
  Module[{work = Join[polygon, {First[polygon]}]},
    If[¬ FreeQ[work, point], Return[True]];
    work = # - point & /@ work;
    (Total[angle /@ Partition[work, 2, 1]] // Chop) != 0];

PointInsidePolygonsQ::usage =
  "Will return True if the point is in any of the polygons";
SyntaxInformation[PointInsidePolygonsQ] = {"ArgumentsPattern" -> {_, _}};
PointInsidePolygonsQ[point_, polygonlist_] :=
  MemberQ[ MapIndexed[PointInsidePolygonQ[point, #] &, polygonlist], True];

Particles = {};
Rejected = {};
test = 0;

While[Length[Particles] < particleNumber,
  roll = {-1, -1};
  While[PointInsidePolygonQ[roll, TheCell] == False,
    roll = Round[ RandomReal[initialBoxSize, 2], spacestep];
  ];
  inAnyBarrier = {};
  Do[
    barrier = Barriers[[b]];
    insideQ = PointInsidePolygonQ[roll, barrier];
    (*Print[{roll,insideQ,barrier}];*)
    AppendTo[inAnyBarrier, insideQ];
    , {b, 1, Length[Barriers], 1}];
  If[! MemberQ[inAnyBarrier, 1],
    AppendTo[Particles, roll],

```

APPENDICES

```

AppendTo[Rejected, roll];
];

test++;
If[test > 4*particleNumber,
Print["Barriers might be too big, broke before number of desired particles \
was reached"]; Break[]];
];
Particles = {Particles};
Graphics[{{White, EdgeForm[Thin], White, Polygon[TheCell], Darker[Green],
Point /@ Particles, Red, Polygon /@ Barriers, Blue, Point /@ Rejected}}]

Do[
newPositions = {};
Do[
thisParticle = Particles[[t, n]];
instantMeanDiffusion = diffusionMean * timestep;

randomVectorMag =
RandomVariate[NormalDistribution[instantMeanDiffusion, diffusionVariance]];
RandomVectorAngle = RandomReal[2*Pi];
jumpX = randomVectorMag * Sin[RandomVectorAngle];
jumpY = randomVectorMag * Cos[RandomVectorAngle];
newPosition = thisParticle + {jumpX, jumpY};

timeout = 0;
While[PointInsidePolygonQ[newPosition, TheCell] == False ||
PointInsidePolygonsQ[newPosition, Barriers] == True,
randomVectorMag =
RandomVariate[
NormalDistribution[instantMeanDiffusion, diffusionVariance]];
RandomVectorAngle = RandomReal[2*Pi];
jumpX = randomVectorMag * Sin[RandomVectorAngle];
jumpY = randomVectorMag * Cos[RandomVectorAngle];
newPosition = thisParticle + {jumpX, jumpY};
timeout++;
If[timeout > 200,
newPosition = thisParticle;
Print["Quit because bumped into barriers too many times"];
Break[]];
];
];

newPositions = AppendTo[newPositions, newPosition];
, {n, 1, particleNumber, 1}];
Particles = AppendTo[Particles, newPosition];
, {t, 1, RunTime, 1}];
AllParticles = Transpose[Particles];
boundaryPlot =
Graphics[{{White, EdgeForm[Thick], Polygon[TheCell], White,
Polygon /@ Barriers}}];
trackplot = ListPlot[AllParticles, Joined -> True];

Show[boundaryPlot, Graphics[trackplot]]

CompleteData = {};
scale = 1;
dTs = {1, 2, 3, 4, 5, 6, 7, 8, 9, 10, 11, 12, 13, 14, 15, 16, 17, 18, 19, 20,

```

APPENDICES

21, 22, 23, 24, 25, 26, 27, 28, 29, 30, 35, 40, 45, 50, 55, 60, 65, 70, 75, 80, 85, 90, 95, 100, 120, 140, 160, 180, 200, 250};

```
AllDistances = {};

Do[
  path = AllParticles[[p]];

  MSDs = {};
  Do[
    dT = dTs[[tau]];
    dists = {};
    squaredDistances = {};

    If[(dT + 1) <= Length[path],
      Do[
        t1 = path[[t]];
        t2 = path[[t + dT]];
        d = EuclideanDistance[t1, t2];
        AppendTo[dists, d];
        AppendTo[squaredDistances, d^2];
        , {t, 1, Length[path] - dT - 1, 1}];
      ];

    If[Length[squaredDistances] != 0,
      MSD = Total[squaredDistances]/Length[squaredDistances];
      AppendTo[MSDs, {dT * timestep, MSD}];
      ];, {tau, 1, Length[dTs], 1}];

  minTau = 6;
  DCs = {};

  Do[
    MSDLF = LinearModelFit[MSDs[[1 ;; ds]], x, x];
    rsquared = MSDLF["AdjustedRSquared"];
    MSDslope = MSDLF["BestFitParameters"][[2]];
    TauDC = MSDslope/(4);

    AppendTo[DCs, {rsquared, TauDC}];
    , {ds, minTau, Length[MSDs], 1}];
    BestDCPosition = Position[DCs, Max[DCs[[All, 1]]]][[1, 1]];
    BestDC = {DCs[[BestDCPosition, 2]], (BestDCPosition + minTau - 1)*
      timestep};
    BestDCLine = Fit[MSDs[[1 ;; (BestDCPosition + minTau - 1)]], {1, x}, x];

    dataToAppend = {AllParticles[[p]], MSDs, BestDC};

    AppendTo[CompleteData, dataToAppend];

    , {p, 1, Length[AllParticles], 1}];

Diffusions = CompleteData[[All, 3, 1]];
Histogram[Diffusions]
MeanDiffusion = Mean[Diffusions]

ListPlot[CompleteData[[All, 2]], Joined -> True]
AllDCs = Transpose[CompleteData[[All, 2]]];
MeanAllDCs = Map[Mean, AllDCs];
meanDCPlot =
  ListPlot[MeanAllDCs, Joined -> True, PlotStyle -> {Thick, Blue}];
slope = MeanDiffusion * 4;
alpha = FindFit[MeanAllDCs, (slope * x^a) , a, x]
diffusionLine = Plot[slope*x, {x, 0, 10}, PlotStyle -> Black];
```

APPENDICES

```
aa = alpha[[1, 2]];
alphaPlot =
  Plot[slope * x^aa, {x, 0, 10}, PlotStyle -> Red,
  PlotRange -> {{0, 10}, {0, Automatic}}];
Show[alphaPlot, meanDCPlot, diffusionLine]
list = {{particleNumber, RunTime, MeanDiffusion, Length[Barriers], aa}};
cellImage = Show[boundaryPlot, Graphics[trackplot]];
MeanDiffusionPlot = Show[alphaPlot, meanDCPlot, diffusionLine];
exportGrid =
  Grid[{{"n", "t", "D", "Barriers", "alpha"}},
  list, {cellImage, Histogram[Diffusions]}, {MeanDiffusionPlot}}]

filepath =
  "~/Desktop/Particle List(" <> ToString[particleNumber] <> "-" <>
  ToString[RunTime] <> ") " <> DateString[{"Day"}] <> DateString[{"Hour"}] <>
  DateString[{"Minute"}] <> ".csv";
Export[filepath, AllParticles, "CSV"]
```

A.2.2 Spatial Analysis of Nuclei Distribution

Mathematic code to find the centroids of variably stained nuclei in a histological section. The input is a TIF file. Initial settings such as intensity threshold, channel, and search-radius can be adjusted in order to positively identify nuclei. Once identified as either 'positive' or 'negative' based on threshold intensities in different channels, cells can be quantitatively compared to their neighbors in order to determine the number of neighbors of a particular quality, the distance between cells of a particular quality, or the average distances between cells of a particular quality. Calculated results of these measurements are the output of the script.

```
ClearAll["Global`*"];
folderpath = "/Users/justin/Gartner/For Rob/slices/";
SetDirectory[folderpath];
files = FileNames["*.tif"];

dims = ImageDimensions[Import[files[[1]]]];

IntensityThreshold = 0.055; (*threshold for positive staining *)

NucleiThreshold = 0.2;

NucleiSize = 9;

markerRadius = 9; (* radius for circling each cell *)

everyNuclei = {};
everyOnNuclei = {};

Do[
```

APPENDICES

```

name = files[[i]];
image = Import[folderpath <> name];
coords =
ToExpression[
StringCases[
  name, {"i" ~~ x : DigitCharacter .. -> x ,
  "j" ~~ y : DigitCharacter .. -> y}]];

baseCord = {dims[[1]]*(coords[[1]] - 1), dims[[2]]*(coords[[2]] - 1)};

channels = ColorSeparate[image, "CMYK"];

cyanChannel =
MorphologicalComponents[Threshold[channels[[1]], NucleiThreshold]];
allNucleiObjects =
SelectComponents[cyanChannel, "BoundingBoxArea", # > NucleiSize & ] ;
allNucleiLong =
ComponentMeasurements[allNucleiObjects, "Centroid"][[All, 2]];
allNuclei = Map[Round, allNucleiLong, 2];
nucleiRings = Circle[#, markerRadius] & /@ allNuclei;
nucleiCircles = Graphics[{Darker[Green], Opacity[.3], Thick, nucleiRings}];

(*get every positive nuclei*)
blackChannel = channels[[4]];
onNucleiObjects =
SelectComponents[blackChannel, "MeanIntensity", # > IntensityThreshold &];
onNucleiActuals =
SelectComponents[onNucleiObjects, "BoundingBoxArea", # > NucleiSize &];
onNucleiLong =
ComponentMeasurements[onNucleiActuals, "Centroid"][[All, 2]];
onNuclei = Map[Round, onNucleiLong, 2];
onRings = Circle[#, 8] & /@ onNuclei;
onCircles = Graphics[{Red, onRings}];

final = Show[image, nucleiCircles, onCircles];

Export[folderpath <> "/data/" <> name <> " searched.tif", final];
Export[folderpath <> "/data/" <> name <>
" Data Output.csv", {{IntensityThreshold, NucleiThreshold}, {coords, dims,
  baseCord}, {onNuclei}, {allNuclei}}, "CSV"];

scaledN = baseCord + # & /@ allNuclei;
scaledO = baseCord + # & /@ onNuclei;

AppendTo[everyNuclei, scaledN];
AppendTo[everyOnNuclei, scaledO];

Print[ToString[i] <> " of " <> ToString[Length[files]] <> " (" <>
ToString[(N[i]/Length[files], 3]*100)] <> "%)" <> " [" <>

DateString[] <> "];
, {i, 1, 3(*Length[files]*), 1}];
Export[folderpath <> "/data/All Nuclei.csv", {Flatten[everyOnNuclei],
Flatten[everyNuclei]}];

```

A.2.3 Kinase Bead Assay Analysis

Mathematic code to take a two-channel TIFF stack, find isolated beads based on thresholded segmentation, define a local outline as 'background region' and then compare the signal region vs background region intensities in the second channel. Location, ID, signal intensity, background intensity and corrected intensity values are all outputted along with a graphical overlay to enable rapid spot-checking of the analysis.

```

ClearAll["Global`*"];
BaseFolder =
  SystemDialogInput["Directory", WindowTitle -> "Select a folder"];
SetDirectory[BaseFolder];
FoldersInDirectory = FileNames["*_*"];

bit = 2^16;
minArea = 1000;
maxArea =
  3200; (*these help define the 'good' objects from the 'bad', after \
thresholding*)
threshold = 0.1;
ThresholdBoundingNumber = 15;

meanRadius = 13.5;
diluteRadius = meanRadius + 28;
BGRadius = diluteRadius + 2;
BeadArea = (meanRadius^2)*3.141592653;
SeparationMin = 80;

EachReport = {};
EachImageTable = {};

PreviousExperimentName = "";

Do[
  eachFolder = FoldersInDirectory[[everyFolder]];
  thisFolder = BaseFolder <> eachFolder;
  folder = thisFolder;

  If[DirectoryQ[thisFolder],
    underscorePosition = StringPosition[eachFolder, "_"];
    ExperimentName =
    StringTake[eachFolder, {1, underscorePosition[[1, 1]] - 1 }];

    If[!(ExperimentName !=
      PreviousExperimentName) && (PreviousExperimentName != ""),
      Headings = {"Experiment", "X", "RhodAve", "RhodBGave", "RhodAve-Net",
        "GFPAve", "GFPBGave", "GFPAve-Net", "RhodTotInt", "GFPTotInt",
        "GFPBGTotInt", "RhodBGTotInt", "RhodTotInt-Net", "GFPTotInt-Net",
        "Ratio"}];
      ThisMeasurements = Join[Headings, EachReport];
      Print["Exporting..."];
      Export[BaseFolder <> PreviousExperimentName <> ".images.pdf",
        Grid[EachImageTable]];
      Export[BaseFolder <> PreviousExperimentName <> ".table.csv",
        ThisMeasurements];
      PreviousExperimentName = ExperimentName;
    ];
];

```

APPENDICES

```

Print[thisFolder];
transFile = "/img_0000000000_Trans_000.tif";
GFPFile = "/img_0000000000_GFP_000.tif";
RhodFile = "/img_0000000000_Rhodamine_000.tif";

tQ = FileExistsQ[folder <> transFile];
gQ = FileExistsQ[folder <> GFPFile];
rQ = FileExistsQ[folder <> RhodFile];

If[Nand[tQ, gQ, rQ], Print[tQ, gQ, rQ]; Abort[]];

rawTransImage = Import[folder <> transFile];
rawGFPImage = Import[folder <> GFPFile];
rawRhodImage = Import[folder <> RhodFile];
rawImages = {rawTransImage, rawGFPImage, rawRhodImage};
leveledImages = Map[ImageAdjust, rawImages];
Map[ImageHistogram, leveledImages];

(* Finding ALL objects - via 'threshold' method,
using a 'bounding disk' with a value of 'boundingnumber'*)
(*ADJUSTABLE*)

morphImage =
DeleteSmallComponents[
MorphologicalComponents[leveledImages[[1]], threshold,
Method -> "BoundingDisk" , ThresholdBoundingNumber];

(*Filter objects based on min/max Areas*)

selected =
SelectComponents[morphImage, "Area", # > minArea && # < maxArea &];
(*Grid[{{leveledImages[[1]], Colorize[morphImage], Colorize[selected]},
TableForm[ComponentMeasurements[
morphImage, {"Area"}]]}]*)
(*Now let's do some math on those selected \
objects*)

everyMeasuredTrans =
ComponentMeasurements[{selected, rawImages[[1]]}, {"Centroid",
"BoundingDiskCenter", "Area", "MeanIntensity", "Length",
"TotalIntensity", "Mean"}];

measuredTrans = {};
Do[
transDimensions = ImageDimensions[leveledImages[[1]]];
xlimits = {BGRadius, transDimensions[[1]] - BGRadius};
ylimits = {BGRadius, transDimensions[[2]] - BGRadius};

xcoord = everyMeasuredTrans[[each, 2, 1, 1]];
ycoord = everyMeasuredTrans[[each, 2, 1, 2]];

If[ (xcoord < xlimits[[1]] || xcoord > xlimits[[2]] ||
ycoord < ylimits[[1]] || ycoord > ylimits[[2]]),
(*Print["object "<>ToString[each]<>" was deleted"];*),

(*Now check to see if they're too close to any other*)

DeleteMe = 0;
Do[
xClose = everyMeasuredTrans[[closest, 2, 1, 1]];

```

APPENDICES

```

yClose = everyMeasuredTrans[[closest, 2, 1, 2]];

If[EuclideanDistance[{xcoord, ycoord}, {xClose, yClose}] <=
  SeparationMin && each != closest,
  DeleteMe = 1;
  (*Print["Deleted for being too close"];*);
  , {closest, 1, Length[everyMeasuredTrans], 1}];

If[DeleteMe == 0,
  AppendTo[measuredTrans, everyMeasuredTrans[[each]]];
  ];
, {each, 1, Length[everyMeasuredTrans], 1}];

Print["Generating images..."];
diskMeasureArray =
MapThread[
  Disk, {measuredTrans[[All, 2, 1]],
  ConstantArray[meanRadius, Length[measuredTrans]]}];
diskDilateArray =
MapThread[
  Disk, {measuredTrans[[All, 2, 1]],
  ConstantArray[dilateRadius, Length[measuredTrans]]}];
diskBGArray =
MapThread[
  Disk, {measuredTrans[[All, 2, 1]],
  ConstantArray[BGRadius,
  Length[
  measuredTrans]]}; (*makes an array of uniform 'disks' with the \
measured parameters above [location & radius]) *)

(*makes the exact same array, but 'rings' so we can nicely display them*)

  circles =
MapThread[
  Circle, {measuredTrans[[All, 2, 1]],
  ConstantArray[meanRadius, Length[measuredTrans]]}];
DilateCircle =
MapThread[
  Circle, {measuredTrans[[All, 2, 1]],
  ConstantArray[dilateRadius, Length[measuredTrans]]}];
BGcircles =
MapThread[
  Circle, {measuredTrans[[All, 2, 1]],
  ConstantArray[BGRadius, Length[measuredTrans]]}];

shownTransImage =
Show[leveledImages[[1]], Graphics[{Red, circles}],
  Graphics[{Green, DilateCircle}], Graphics[{Blue, BGcircles}],
  ImageSize -> Large];
shownGFPImage =
Show[leveledImages[[2]], Graphics[{Red, circles}],
  Graphics[{Green, DilateCircle}], Graphics[{Blue, BGcircles}],
  ImageSize -> Large];
shownRhodImage =
Show[leveledImages[[3]], Graphics[{Red, circles}],
  Graphics[{Green, DilateCircle}], Graphics[{Blue, BGcircles}],
  ImageSize -> Large];(*display the rings overlayed on the original image*)

overlaid =
ImageCompose[rawImages[[1]],
  ImageCompose[rawImages[[1]], Graphics[diskMeasureArray]]];

```

APPENDICES

```

(*in order to subtract the 'measured' rings, we make them 'background/
white'*)

whiteDisks =
Riffle[ConstantArray[White, Length[measuredTrans]], diskDilateArray];
singleImage = ImageCompose[rawImages[[1]], Graphics[diskBGArray]];
overlaidBG = ImageCompose[singleImage, Graphics[whiteDisks]];

(*overlaidBG = ImageCompose[rawImages[[1]],
singleImage]; *)
(*turns the 'display image' into a computer-
readable single image*)

inverted = ColorNegate[Colorize[MorphologicalComponents[overlaid]]];
Print["Measuring components..."];
preInvertedBG = MorphologicalComponents[overlaidBG, Method -> "Convex"];
invertedBG = ColorNegate[Colorize[preInvertedBG]];

finalMask =
DeleteSmallComponents[
MorphologicalComponents[inverted, .5]];(*to clean up the mask*)

finalBGMask =
DeleteSmallComponents[MorphologicalComponents[invertedBG, .5]];

GFPMeasurements =
ComponentMeasurements[{finalMask, rawImages[[2]]}, {"Centroid",
"MeanIntensity", "MedianIntensity", "TotalIntensity", "Area"}];
RhodMeasurements =
ComponentMeasurements[{finalMask, rawImages[[3]]}, {"Centroid",
"MeanIntensity", "MedianIntensity", "TotalIntensity", "Area"}];
GFPBGMMeasurements =
ComponentMeasurements[{finalBGMask, rawImages[[2]]}, {"Centroid",
"MeanIntensity", "MedianIntensity", "TotalIntensity", "Area"}];
RhodBGMMeasurements =
ComponentMeasurements[{finalBGMask, rawImages[[3]]}, {"Centroid",
"MeanIntensity", "MedianIntensity", "TotalIntensity", "Area"}];

offset = 20;
IDs = Map[ToString, Range[Length[GFPMeasurements]]];
IDLocations =
Partition[(GFPMeasurements[[All, 2, 1]] -
ConstantArray[{offset, -offset}, Length[GFPMeasurements]]), 1];
IDPlot = ListPlot[IDLocations, PlotMarkers -> IDs];

Print["Cleanup & data-prep..."];
TGR = GraphicsGrid[{{Show[shownTransImage, IDPlot],
Show[shownGFPImage, IDPlot], Show[shownRhodImage, IDPlot]}}];

AllMeasurements = {{GFPMeasurements[[All, 2]],
GFPBGMMeasurements[[All, 2]]}, {RhodMeasurements[[All, 2]],
RhodBGMMeasurements[[All, 2]]}};

examineProp = 3;
ExamineGFP =
AllMeasurements[[1, 1, All, examineProp]] -
AllMeasurements[[1, 2, All, examineProp]];
ExamineRhod =
AllMeasurements[[2, 1, All, examineProp]] -
AllMeasurements[[2, 2, All, examineProp]];

```

APPENDICES

```

objectIDArray = {};
Do[
objectIDArray =
Join[objectIDArray, {eachFolder <> " - " <> ToString[objectID]};
, {objectID, 1, Length[RhodMeasurements], 1}];

Measurements = {objectIDArray,
RhodMeasurements[[All, 2, 1, 1]], (2^16)*
RhodMeasurements[[All, 2, 2]], (2^16)*
RhodBGMeasurements[[All, 2,
2]], (2^16)*(RhodMeasurements[[All, 2, 2]] -
RhodBGMeasurements[[All, 2, 2]]), (2^16)*
GFPMeasurements[[All, 2, 2]], (2^16)*
GFPBGMeasurements[[All, 2,
2]], (2^16)*(GFPMeasurements[[All, 2, 2]] -
GFPBGMeasurements[[All, 2, 2]]), (2^16)*
RhodMeasurements[[All, 2, 4]], (2^16)*
GFPMeasurements[[All, 2, 4]], (2^16)*GFPBGMeasurements[[All, 2, 3]]*
BeadArea, (2^16)*RhodBGMeasurements[[All, 2, 3]]*
BeadArea, ((2^16)*
RhodMeasurements[[All, 2, 4]] - ((2^16)*
RhodBGMeasurements[[All, 2, 3]]*BeadArea)), ((2^16)*
GFPMeasurements[[All, 2, 4]] - ((2^16)*GFPBGMeasurements[[All, 2, 3]]*
BeadArea)), (((2^16)*
RhodMeasurements[[All, 2, 4]] - ((2^16)*
RhodBGMeasurements[[All, 2, 3]]*BeadArea)))/((2^16)*
GFPMeasurements[[All, 2, 4]] - ((2^16)*
GFPBGMeasurements[[All, 2, 3]]*BeadArea))});

EachReport = Join[EachReport, Transpose[Measurements]];
EachImageTable = AppendTo[EachImageTable, {{eachFolder, TGR}}];

Print[eachFolder <> " is done calculating"];

PreviousExperimentName = ExperimentName;
];, {everyFolder, 1, Length[FoldersInDirectory], 1}];

(*ThisMeasurements = AccountingForm[TableForm[EachReport,TableDirections-> \
Row, TableHeadings->{{"X","RhodAve","RhodBGAve","RhodAve-Net","GFPAve",\
"GFPBGAve","GFPAve-Net","RhodTotInt","GFPTotInt","GFPBGTotInt","RhodBGTotInt",\
"RhodTotInt-Net","GFPTotInt-Net","Ratio"},None} ]];*)

Print["Exporting..."];
Headings = {"Experiment", "X", "RhodAve", "RhodBGAve", "RhodAve-Net",
"GFPAve", "GFPBGAve", "GFPAve-Net", "RhodTotInt", "GFPTotInt",
"GFPBGTotInt", "RhodBGTotInt", "RhodTotInt-Net", "GFPTotInt-Net",
"Ratio"};
ThisMeasurements = Join[Headings, EachReport];

Export[BaseFolder <> ExperimentName <> ".images.pdf", Grid[EachImageTable]];
Export[BaseFolder <> ExperimentName <> ".table.csv", ThisMeasurements];

Print["Done!"];

```

A.2.4 Spatial Error

Mathematic code to find the initial and final centroid of an array of cells given a 'before' and 'after' image. Cells are identified in both cases by intensity thresholding, and identified by a nearest-neighbor search. Once identified, the distance between each centroid in the before image and the after image is calculated. Further calculations including the average distance between a given centroid and its neighbors can be calculated. Also, the average travel between a centroid and a fixed reference point can be calculated. Each of these calculated distance values are graphically represented either spatially or in the form of an error plot.

```

image1 = Import["~/Desktop/mths/before_small.tif"] ;
image2 = Import["~/Desktop/mths/after_small.tif"];

(*this is how it thresholds*)
threshold = 0.4;

binImage1 = Threshold[image1, threshold];
binImage2 = Threshold[image2, threshold];
binnedImages = {binImage1, binImage2};

components = MorphologicalComponents /@ binnedImages;

indexedCentroids = ComponentMeasurements[#, "Centroid"] & /@ components;
centroids = indexedCentroids[[All, All, 2]];

theLeast = Length[centroids[[1]]];
If[Length[centroids[[2]]] < theLeast, theLeast = Length[centroids[[2]]]];
Print["There will be " <> ToString[theLeast] <> " comparisons made:"];

distances = {};
zVectors = {};
vectors = {};

discardedZVectors = {};

(*set this as you like *)
discardAbove = 20;

Do[
  thePoint = centroids[[1, n]];
  theNearest = Nearest[centroids[[2]], thePoint][[1]];

  theDistance = EuclideanDistance[theNearest, thePoint];
  theZVector = theNearest - thePoint;
  theVector = {thePoint, theNearest};

  If[theDistance < discardAbove,
    AppendTo[distances, theDistance];
    AppendTo[zVectors, theZVector];
    AppendTo[vectors, theVector];
  ,
  AppendTo[discardedZVectors, theVector];
];

```

APPENDICES

```
, {n, 1, theLeast, 1}];

theVectors = {{0, 0}, #} & /@ zVectors;

blueImage1 =
  Colorize[binnedImages[[1]], ColorRules -> {0 -> White, _ -> Green}]
redImage2 = Colorize[binnedImages[[2]], ColorRules -> {0 -> White, _ -> Red}]
both = ImageCompose[blueImage1, {redImage2, .7}]

(*check out "guide/ColorSchemes" for cool color schemes *)
maxReasonable = \
10; (*what is the max distance value for 'red' color? *)
range = \
{-maxReasonable, maxReasonable}, {-maxReasonable, maxReasonable}}];
colorRange = ColorData[{"Rainbow", {0, maxReasonable}}];
distColors = colorRange /@ distances;

distPlot = ListPlot[vectors, Joined -> True, PlotStyle -> distColors]
Show[both, distPlot]

zeroPlot =
  ListPlot[theVectors, PlotRange -> range, AspectRatio -> 1,
  PlotStyle -> {{Gray, Opacity[0.4]}}, Joined -> True]
dotPlot =
  ListPlot[zVectors, PlotStyle -> {{Opacity[0.3], Blue}}, PlotRange -> range,
  AspectRatio -> 1]

Histogram[distances, {0, 20, 0.25}]

drift = Mean[zVectors];
Print["The total of all reasonable vectors is " <> ToString[drift] <>
" pixels."];

EuclideanDistance[{0, 0}, Mean[Abs[zVectors]]]
```

A.2.5 3D Nuclei Counter

Mathematic code to count the number of nuclei present in a given 3D confocal TIFF stack.

Based around a fantastic segmentation analysis published by “UDB” on Stack Overflow

(<http://mathematica.stackexchange.com/questions/31997/image-segmentation-and-object-separation-in-3d-using-mathematica>), this applies the segmentation analysis to count and

locate the centroids of nuclei in an image stack where the z-resolution is poor. Output is an array of x y, & z coordinates for each given nucleus.

```

ClearAll["Global`*"];
Basefolder =
  SystemDialogInput["Directory", WindowTitle -> "Select a folder"];
(*Basefolder = "/Users/justin/Gartner/for alex/May17Lane3ForJustin/*");

SetDirectory[Basefolder];
number = 32;
C1InFolder = FileNames["*c1_ORG.tif"];
C2InFolder = FileNames["*c2_ORG.tif"];
positions = Length[C1InFolder] / number;

croppedStacks = {};
meanImages = {};
cropBounds = {};
boundingBoxes = {};
shoulds = {};
imageNames = {};
imageIDs = {};
allCentroids = {};
allComponents = {};
allLabeledMeans = {};

distcompiledparallelized =
  Compile[{{dist, _Integer, 3}},
    Module[{dimi, dimj, dimk, disttab, i, j, k, ii}, {dimi, dimj, dimk} =
      Dimensions[dist];
    disttab = Table[(i - ii)^2, {ii, dimi}, {i, dimi}];
    Table[
      Min[disttab[[i, All]] + dist[[All, j, k]], {i, dimi}, {j, dimj}, {k,
        dimk}]],
    CompilationTarget ->
    "C",(*this should be set to "WVM" if a compiler is not installed*)
    RuntimeAttributes -> {Listable}, Parallelization -> True];

Options[EuclideanDistanceTransform3Dparallelized] = {Padding -> 1};
EuclideanDistanceTransform3Dparallelized[im3d_Image3D, OptionsPattern[]] :=
  Module[{dist3d, forwardtransposition, backwardtransposition, addmargin},
    backwardtransposition = Ordering[Reverse[ImageDimensions[im3d]]];
    forwardtransposition = Ordering[backwardtransposition];
    dist3d =
    Developer`ToPackedArray@
    Map[Round[
      ImageData[
        DistanceTransform[#, DistanceFunction -> EuclideanDistance,
          Padding -> OptionValue[Padding]]^2] &,
      Image3DSlices[
        Image3D[

```

APPENDICES

```

ArrayPad[Transpose[ImageData[im3d, "Bit"], forwardtransposition], 1,
  Padding -> OptionValue[Padding]]];
If[OptionValue[Padding] != 0,
dist3d =
  Developer`ToPackedArray@
  Map[
  If[Times @@ Dimensions[#] == Total[Flatten[#]], # + 1073741822, #] &,
  dist3d, {1}];];
addmargin =
Ceiling[#1/#2]*#2 - #1 &[Dimensions[dist3d][[3]], $ProcessorCount];
dist3d = ArrayPad[dist3d, {{0, 0}, {0, 0}, {0, addmargin}}];
dist3d =
Function[{len, procs},
  dist3d[[All, All, # ;; Min[# + Ceiling[len/procs] - 1, len]]] & /@
  Range[1, len, Ceiling[len/procs]]][
  Last[Dimensions[dist3d]], $ProcessorCount];
dist3d = Developer`ToPackedArray@distcompiledparallelized[dist3d];
dist3d = Join[Sequence @@ dist3d, 3];
dist3d = ArrayPad[dist3d, {{-1, -1}, {-1, -1}, {-1, -addmargin - 1}}];
dist3d = Transpose[dist3d, backwardtransposition];
Image3D[Sqrt@N@dist3d, "Real"];

Print["Started @ " <> DateString[]];
Do[ (*for each channel*)
  bothChannelPreview = {};
  Do[ (*for each position*)
    maxCount = n * 2;
    fractionOn = (n*2 - 2 + c)/maxCount;
    fOn = Round[fractionOn * 60];
    stars = ConstantArray["*", fOn];
    dashes = ConstantArray["-", 60 - fOn];
    Print["0%" <> StringJoin[stars, dashes] <> "100%"];

baseName = Basefolder <> "Experiment-1859-Image Export-03_s";
posNameLong = "000" <> ToString[n];
posName = StringTake[posNameLong, -3];

stackNames = {};
imageStack = {};
shouldDo = 0;

Print["Building Stack for: " <> ToString[n] <> ".c" <> ToString[c] <>
  " @ " <> DateString[]];
Do[
  stackNumberLong = "00" <> ToString[s];
  stackNumber = StringTake[stackNumberLong, -2];
  fileName =
    baseName <> posName <> "z" <> stackNumber <> "c" <> ToString[c] <>
    "_ORG.tif";
  AppendTo[stackNames, fileName];
  image = Import[fileName];
  AppendTo[imageStack, image];
  , {s, 1, number, 1}];

(*imageStack is the set of images in the same channel at a single point*)

image3DStack = Image3D[imageStack];

meanImage = ImageAdjust[ Image[Mean[ImageData /@ imageStack]]];
d = ImageDimensions[meanImage];

```

APPENDICES

```

padding = 50;
DilatedMask = Dilation[MorphologicalBinarize[meanImage], padding];
comps = MorphologicalComponents[DilatedMask];
measures = ComponentMeasurements[comps, {"Area", "BoundingBox"}];
sortedMeasures = Sort[measures, #1[[2, 1]] > #2[[2, 1]] &];

boundingBox = sortedMeasures[[1, 2, 2]];
boundingXs = {boundingBox[[1, 1]], boundingBox[[2, 1]]};
boundingYs = {boundingBox[[1, 2]], boundingBox[[2, 2]]};

area = measures[[1, 2, 1]];
If[area > 8000 && area < 90000, shouldDo = 1];

boundSquare =
Graphics[{EdgeForm[{Thick, White}], Transparent,
  Rectangle[boundingBox[[1]], boundingBox[[2]]]}];

croppedImageStack =
ImageTake[image3DStack, {0, All}, Reverse[d[[1]] - boundingYs],
  boundingXs];

If[shouldDo == 1,
smallCropped = croppedImageStack;
smallCroppedinterpolationfunction =
  ListInterpolation[ImageData[smallCropped, "Real"], Method -> "Spline"];
dims = Dimensions[ImageData[smallCropped]];

smallCroppedinterpolated =
  ParallelTable[
    smallCroppedinterpolationfunction[i, j, k], {i, 1, dims[[1]], 0.33}, {j,
    1, dims[[2]]}, {k, 1, dims[[3]]}];
smallCroppedstretched = Image3D[smallCroppedinterpolated, "Real"];

Print["Reinterpolating"];
img3d =
  Binarize[
    TotalVariationFilter[smallCroppedstretched, Method -> "Poisson",
    MaxIterations -> 10]];

Print["Finding components"];
components =
  MorphologicalComponents[
    ImageMultiply[
      Binarize[
        LaplacianGaussianFilter[(*Marr-Hildreth operator*)
        EuclideanDistanceTransform3Dparallelized[
          ColorNegate[
            Binarize[
              ImageMultiply[MaxDetect[#, #] &[
                EuclideanDistanceTransform3Dparallelized[img3d]],
                2(*allow only maxima with distance values>15*)]]],
              1(*LoG filter kernel size*)]]], img3d]];

integratedComponents = Total[Map[Total, components, 2]];

centroids = Table[
  p = N@Position[components, i];
  Mean[p],
  {i, 1, Max[components]}
];
xyCentroid = # + boundingBox[[1]] & /@ centroids[[All, 1 ;; 2]];

```

APPENDICES

```

zCentroid = centroids[[All, 3]];
universalCentroids =
  Table[
    Flatten[{xyCentroid[[i]], zCentroid[[i]]}], {i, 1, Length[zCentroid]};

meanCroppedImage =
  ImageAdjust[ Image[Mean[ImageData [croppedImageStack]]]];
dimRange = ImageDimensions[croppedImageStack][[1 ;; 2]];
dimy = dimRange[[2]];
flippedCentroids = {#[[2]], dimy - #[[1]]} & /@ centroids[[All, 2 ;; 3]];
If[c == 1, color = Red, color = Green];
centroidRings = {color, Opacity[0.3], , Circle[#, 6 ]} & /@
  flippedCentroids;
graphic = Graphics[centroidRings, PlotRange -> dimRange];
preview = Show[meanCroppedImage, graphic];

Export[
  Basefolder <> "Centroid Data " <> ToString[n] <> ".c" <> ToString[c] <>
  ".csv", {{n, c}, universalCentroids, boundingBox, centroids,
  components}, "CSV"];
Export[
  Basefolder <> "StackMean " <> ToString[n] <> ".c" <> ToString[c] <>
  ".tif", meanImage];
Export[
  Basefolder <> "Stack " <> ToString[n] <> ".c" <> ToString[c] <> ".tif",
  image3DStack];
Export[
  Basefolder <> "StackLabeledMean " <> ToString[n] <> ".c" <> ToString[c] <>
  ".tif",
  preview];

];
Print["File " <> ToString[n] <> ".c" <> ToString[c] <> "done"];

AppendTo[shoulds, shouldDo];
AppendTo[meanImages, meanImage];
AppendTo[cropBounds, boundSquare];
AppendTo[boundingBoxes, boundingBox];
AppendTo[croppedStacks, croppedImageStack];
AppendTo[imageNames, stackNames];
AppendTo[imageIDs, {n, c}];
AppendTo[
  allCentroids, {n, c, Length[universalCentroids], integratedComponents,
  universalCentroids, boundingBox}];
AppendTo[allLabeledMeans, preview];
, {c, 1, 2, 1}]; (*for each channel*)

, {n, 1, positions, 1}]; (*for each position*)

Export[Basefolder <> "All Data.csv", allCentroids, "CSV"];
Export[Basefolder <> "All Boundingboxes.csv", boundingBoxes, "CSV"];
(*Export[Basefolder<>"All Components.csv",allComponents,"CSV"];*)

Export[Basefolder <> "All Should Analyze.csv", shoulds, "CSV"];
Export[Basefolder <> "All Previews.pdf", allLabeledMeans, "PDF"];

Print["Ended @ " <> DateString[]];

i = Range[Length[imageIDs]];

```

APPENDICES

```
Show[meanImages[[#]], cropBounds[[#]] & /@ i  
croppedStacks
```

A.3 List of Publications

Farlow, J.; Seo, D.; Broaders, K.E.; Taylor, M.; Gartner, Z.J.; Jun, Y.W., 2013. Formation of Targeted Monovalent Quantum Dots by Steric Exclusion. *Nature Methods* 10, 1203-1205. <http://dx.doi.org/10.1038/nmeth.2682>

Seo D, **Farlow J**, Southard K , Jun YW, Gartner ZJ. "Production & Targeting of Monovalent Quantum Dots." JOVE (2014)

Liu, J.S.; **Farlow, J.**; Paulson, A.; LaBarge, M.A.; Gartner, Z.J., 2012. "Programmed Cell-to-Cell Variability in Ras Activity Triggers Emergent Behaviors during Mammary Epithelial Morphogenesis." *Cell Reports* 2, 1461-1470. <http://dx.doi.org/10.1016/j.celrep.2012.08.037>

Todhunter ME, Jee NY, Cerchiari A, Hughes AJ, **Farlow J**, Garbe JC, LaBarge MA, Desai TA, Gartner ZJ. "Rapid Synthesis of 3D Tissues by Chemically Programmed Assembly." (submitted 2014)

Publishing Agreement

It is the policy of the University to encourage the distribution of all theses, dissertations, and manuscripts. Copies of all UCSF theses, dissertations, and manuscripts will be routed to the library via the Graduate Division. The library will make all theses, dissertations, and manuscripts accessible to the public and will preserve these to the best of their abilities, in perpetuity.

I hereby grant permission to the Graduate Division of the University of California, San Francisco to release copies of my thesis, dissertation, or manuscript to the Campus Library to provide access and preservation, in whole or in part, in perpetuity.

Author Signature  Date 9/15/2014